科技部補助專題研究計畫成果報告
期末報告

氣體與微粒酸度對於二次衍生水溶性氣膠的大氣流佈及其光學特性的影響

計 畫 類 別 ： 個別型計畫
計 畫 編 號 ： MOST 102-2111-M-040-002-
執 行 期 間 ： 102 年 08 月 01 日至 103 年 09 月 30 日
執 行 單 位 ： 中山醫學大學公共衛生學系（所）

計 畫 主 持 人 ： 張士昱
共 同 主 持 人 ： 陳韡鼎
計畫參與人員： 博士班研究生-兼任助理人員：陳瑀婕

報 告 附 件 ： 出席國際會議研究心得報告及發表論文

處 理 方 式 ：
1.公開資訊：本計畫涉及專利或其他智慧財產權，2 年後可公開查詢
2.「本研究」是否已有嚴重損及公共利益之發現：否
3.「本報告」是否建議提供政府單位施政參考：否

中 華 民 國 103 年 12 月 31 日

中 文 摘 要 ： 本計劃在 2014 年 2 月 28 日至 4 月 6 日於恆春海生館進行大氣污染物逐時觀測，以逐時 PM2.5 水溶性陰陽離子、含碳物質與氣膠垂直分佈等數據，配合氣象因子(溫濕度、風向與風速)、氣態污染物(O3、SO2、CO 與 NO2)與粒狀污染物(PM10 與 PM2.5)濃度進行同步觀測，並使用逐時氣象因子與氣流軌跡模式(HYSPLIT)來區分不同傳輸事件。
本次觀測期間不同傳輸事件分別為高屏地區人為污染傳輸、陸風傳輸、西風傳輸、東北季風傳輸四種不同傳輸事件。首先，不同事件的氣象場特徵分別為日間海風(西北風)-夜間陸風(東北風)環流風、風速較弱的盛行西風、以及乾冷且風速大的盛行東北風。另外，本研究以來自於中南半島的生質燃燒污染物作為驗證下沖事件的指標物種，而下沖事件的辨別與驗證則以現址光達(LIDAR)的氣膠垂直分佈觀測與氣象模式的垂直風場剖面模擬判別出下沖氣流發生時間，同時在地面逐時生質燃燒指標污染濃度也可以觀測到峰值的出現。
本計畫不同大氣環境類別下氣膠污染特徵如下: 高屏地區人為污染傳輸的污染情況最嚴重的類型，由 NOR、NO3-/SO42-與 NO3-/K+當量濃度比的分析顯示污染源與西北方的高屏都會區污染排放及光化污染物有關，陸風傳輸污染物濃度迅速回復低值。在西風傳輸期間為空氣品質最佳的類型，且 Cl-/Na+質量濃度比(1.5)與海鹽比值(1.8)較為接近，顯示受到海洋氣流的影響。東北季風傳輸若氣流經大陸沿海污染地區，NH4+與 SO42-濃度則會有上升的趨勢。下沖事件地面量測結果顯示生質燃燒指標污染物(K+、EC 與 OC)與衍生性離子等濃度僅在下沖現象發生期間呈現較高趨勢，並且與鹿林山觀測結果比較顯示兩者生質燃燒污染來源相同，主要受到中南半島生質燃燒排放的影響。

中文關鍵詞： 中南半島、生質燃燒、下沖氣流、光化污染物、現址量測、大氣酸度、水溶性有機碳、二元酸、能見度、混合層高度

英 文 摘 要 ： Hourly measurements of meteorological parameters (temperature, relative humidity, wind direction and wind speed), particulate and gaseous pollutants (PM10, PM2.5, O3, SO2, CO and NO2), chemical compositions of PM2.5 (water soluble ions and carbonaceous materials), and vertical distribution of aerosols were made from February 28 to April 6 2014 at Hungchen in Taiwan. The HYSPLIT and hourly measurements of meteorological parameters were applied to distinguish the weather condition.

In this work, four types of air masses were identified as Anthropogenic emissions from Kaohsiung and Pingtung area, the land breeze, northeast monsoon and western sea wind. The four types of air masses can be directly characterized as daily variations with sea wind (northwest) in daytime and land wind (northeast) in nighttime, the prevailing northeaster with strong and cold wind, and the prevailing light breeze from west, respectively. The downwash processes were verified that the occurrence of peak in biomass burning tracer concentration was consistency with the period of downwash transport in the ground station. The vertical distribution of aerosols measured from the in situ LIDAR and the vertical wind section simulated from the meteorological model were used to define the period of the downwash transport. The biomass burning pollutants from the Indo-China Peninsula were regarded as the tracer to observe the downwash transport of the upper atmosphere.
The pollutant characteristics of each air mass were found in this study. Anthropogenic emissions from Kaohsiung and Pingtung area with primary photochemical pollutants led to the serious pollution at Hungchen. However, the concentrations of pollutants were quickly reduced when the wind was changed to the land wind. The pollution was related to the long range transport of polluted air from Asia in the prevailing northeasterly. During the westerly, the air quality was the best during the observed period. The ambient aerosols with the Cl^-/Na^+ ratio of 1.5 (similar to the ratio of 1.8 from sea salts) were characterized as the oceanic transport. The long-range transport of biomass burning from the Indo-China Peninsula affected the air quality at Hungchen through the downwash process. The aerosols were characterized as the high proportion of biomass pollutants. The comparison of Lulin station ‘s results showed that they had same biomass burning source, mainly influenced by Indo-China Peninsula ‘s biomass burning emissions.

英文關鍵詞： Indo-China Peninsula, biomass burning, downwash, photochemical pollutants, In-situ measurement, Atmospheric acidity, Water soluble organic carbon, Dicarboxylic acid, Visibility, Mixed layer height

科技部補助專題研究計畫成果報告

（□期中進度報告/■期末報告）

（計畫名稱）

氣體與微粒酸度對於二次衍生水溶性氣膠的大氣流佈及其光學特性的影響

計畫類別：□個別型計畫　□整合型計畫

計畫編號：NSC　102－2111－M－040 －002

執行期間：　102 年　8 月 1　日至 103　年 09 月　30 日

執行機構及系所：中山醫學大學 公共衛生學系

計畫主持人： 張士昱

共同主持人：陳韡鼐

計畫參與人員： 陳瑀婕 、鄭忠豪

本計畫除繳交成果報告外，另含下列出國報告，共 _1__ 份：

□執行國際合作與移地研究心得報告

■出席國際學術會議心得報告

期末報告處理方式：

1. 公開方式：

□非列管計畫亦不具下列情形，立即公開查詢

□涉及專利或其他智慧財產權，□一年■二年後可公開查詢

2.「本研究」是否已有嚴重損及公共利益之發現：■否 □是

3.「本報告」是否建議提供政府單位施政參考 ■否 □是，___（請列舉提供之單位；本部不經審議，依勾選逕予轉送）

中　華　民　國　103　年　12　月　31 日

Science of the Total Environment 497–498 (2014) 219–228

Contents lists available at ScienceDirect

Science of the Total Environment

journal homepage: www.elsevier.com/locate/scitotenv

The real-time method of assessing the contribution of individual sources on visibility degradation in Taichung

Wei-Nai Chen [a], Yu-Chieh Chen [b], Chung-Yih Kuo [b,c], Chun-Hung Chou [b], Chung-Hao Cheng [b], Chun-Chieh Huang [b], Shih-Yu Chang [b,c,*], M. Roja Raman [a], Wen-Lin Shang [d], Tzu-Yao Chuang [e], Su-Ching Liu [e]

[a] Research Center for Environmental Changes, Academia Sinica, Taipei 115, Taiwan
[b] School of Public Health, Chung Shan Medical University, Taichung 402, Taiwan
[c] Department of Family and Community Medicine, Chung Shan Medical University Hospital, Taichung 402, Taiwan
[d] Bureau of Environmental Protection, Taichung City, Taiwan
[e] Department of Pediatrics, Children's Hospital, China Medical University and Hospitals, Taichung, Taiwan

HIGHLIGHTS

- Hourly measurements of soluble ions, OC, EC and visibility were analyzed.
- Six factors of $PM_{2.5}$ were identified by PMF according to the hourly measurements.
- Reconstructed $PM_{2.5}$ of each pollutant source was estimated by PMF.
- Source apportionment of visibility degradation was discussed by reconstructed $PM_{2.5}$.
- Real-time b_{ext} contributions of each pollutant source.

ARTICLE INFO

Article history:
Received 22 April 2014
Received in revised form 30 July 2014
Accepted 31 July 2014
Available online xxxx

Editor: Xuexi Tie

Keywords:
Visual range
Soluble ion
Pollutant source
In situ measurement
Light extinction
PMF

ABSTRACT

Visibility degradation caused by air pollution has become a serious environmental problem in megacities in Northeast Asia. In general, aerosol chemical compositions are measured by a conventional method of time integrated filter sampling for off-line analysis, which cannot represent temporal and spatial variations in the real atmosphere. The in situ air composition measuring equipment, OCEC carbon aerosol analyzer and a long-path visibility transmissometer-3 were used to collect hourly measurements of the soluble ions, organic/elemental carbon, and ambient visibility, respectively. During the observation, two types of weather conditions were identified: transport and stagnant. Because $PM_{2.5}$ was identified as the predominant species of light extinction, the sources of $PM_{2.5}$ were determined and investigated using a positive matrix factorization (PMF) analysis. The PMF outputs characterized the six main emission sources (marine/crustal aerosols, secondary nitrate, secondary sulfate, direct vehicle exhaust, coal/incinerator combustion, and local sewage emission) and reconstructed the $PM_{2.5}$ mass concentrations of each pollutant source in two weather conditions. In addition, the light extinction (b_{ext}) was reconstructed using a multivariate linear regression analysis with hourly-reconstructed $PM_{2.5}$ mass concentrations to determine the contributions of each source to b_{ext}. The primary results showed that the extinction coefficient was proportional to the $PM_{2.5}$ with high value in stagnant weather conditions. The secondary sulfate was the most abundant source of b_{ext} contribution during the sampling period. In addition, the b_{ext} contributions of direct vehicle exhaust and coal/incinerator combustion significantly increased in the stagnant weather condition. According to the results of hourly measurements, this work further emphasized that the sources of direct vehicle exhaust and coal/incinerator combustion in $PM_{2.5}$ were the important sources of visibility degradation in the stagnant weather conditions, which suggests that the pollutants derived from direct vehicle exhaust and coal/incinerator combustion should be controlled first to improve visibility in Taichung.

1. Introduction

Visibility is also known as visual range, wherein an object in the horizontal direction of a naked-eye observation can be identified by observing the contrast between the object and background. The contrast between the object and background decreases as the distance

* Corresponding author at: No. 110, Sec. 1, Jianguo N. Rd., South Dist., Taichung City 402, Taiwan. Tel.: +886 4 24730022x12184; fax: +886 4 23248179.
E-mail address: sychang@csmu.edu.tw (S.-Y. Chang).

http://dx.doi.org/10.1016/j.scitotenv.2014.07.120
0048-9697/

between the object and the observer increases (World Meteorological Organization, 1992, 2003). Watson (2002) indicated that visibility reduction, other than on foggy days, is always associated with poor air quality caused by intensive emissions of air pollutants. Seinfeld and Pandis (2006) indicated that visibility degradation is likely the most readily perceived impact of air pollution.

The relationship between air quality and visibility is complex because of the temporal and spatial variations of air pollutants, visibility and weather conditions. At present, the visibility observation modes include naked eye observations, digital image processing (Bäumer et al., 2008; Huang et al., 2009; Liaw et al., 2010), nephelometers, aethalometers (Deng et al., 2008), and short/long optical path transmissometer measurements (Kim et al., 2006). The naked eye observation and digital image processing measurement methods lack objective direct and continuous measurements of atmospheric visibility and cannot provide objective observation data at night. Long-term filter-based aerosol sampling is still a common method of measuring the chemical composition of atmospheric aerosols in which the collected aerosols interact with the in-coming gas, environmental factors and each other. However, sampling artifacts of acidity, ammonium, nitrate, chloride and sulfate can occur and thus change the composition of the collected aerosols (Pathak and Chan, 2005). The uncertainties of aerosol optical characteristics contribute substantially to uncertainties in climate forcing and the regulatory efforts designed to improve visibility (IPCC, 2007). Thus, continuous measurements of air quality and ambient visibility with accurate time resolution are required to decrease the uncertainty when evaluating the relationship between ambient visibility and pollutant sources.

Visibility degradation caused by atmospheric pollution is a global problem in many densely populated areas that have experienced population growth and the spread of industrialization, especially in the East Asia. Several studies have reported that a significant decline of visibility in Chinese megacities was closely related to meteorological conditions and air pollution (Wang et al., 2006, 2012; Sun et al., 2006; Tan et al., 2009; Chen et al., 2014). Taiwan is situated in the western Pacific off the southeastern coast of mainland China. The atmospheric environment has been intensively influenced by monsoons, which cause rapid variations in ambient pollutants. Most of the previous studies of aerosol compositions and ambient visibility have been based on batch measurements and naked eye observations, respectively; however, such measurements are usually insufficient to explain the complex temporal characteristics between air pollution and ambient visibility under various meteorological conditions. For developing strategies of improving visual air quality, Yuan et al. (2002) have used the receptor models, based on chemical mass balance and principal component factor analysis, to establish multiple regression models for atmospheric visibility. Eatough and Farber (2009) illustrated a novel approach that coupled a positive matrix factorization (PMF) model with added extinction to identify each source contributor to extinction.

This study integrated a long-path visibility transmissometer 3 (LPV-3) into in situ air composition measuring equipment (ACME) and OCEC carbon aerosol analyzer to avoid the artifacts of naked-eye observations and long-term filter sampling. An additional investigation was conducted of the visibility related to particle size, meteorological conditions, and soluble ions in the Taichung urban area. A PMF analysis was conducted to evaluate the pollution types influencing visibility in the Taichung urban area.

2. Experimental methods

2.1. Sampling time and site

Air pollutants and ambient visibility were observed from December 9–29, 2010. During the sampling period, the atmospheric environment was mainly affected by the winter monsoon, which produced cold and dry weather conditions. The aerosol soluble ions and atmospheric visibility were observed hourly. The aerosol mass concentration, gas concentration and meteorological parameters were derived from average measurements of two neighboring environmental protection administration (EPA) site (Xitun (upwind site) and Dali (downwind site) in Fig. 1).

The sampling sites were located in the Taichung urban area in central Taiwan (Fig. 1). In this study, the hourly measurements of atmospheric visibility, $PM_{2.5}$ soluble ions and organic/elemental carbon were obtained by LPV-3, ACME, and OCEC carbon aerosol analyzer, respectively. The LPV-3 consisted of a transmitter and receiver that were installed on the campus of Chung Shan Medical University (CSMU) and the Wurih site, respectively. Two sampling sites with a distance of 2.5 km were on the top floors at 12 m above ground level. The optical path was northeast–southwest, and there were no high buildings between the two sites. The ACME monitor and OCEC carbon aerosol analyzer were placed at the Wurih site, which was located in a residential zone. Two coal-fired power plants are located to the northwest of the Taichung urban area and western coastal area. The power plants are windward of the Taichung urban area during the northwester and sea wind periods.

2.2. Instruments

2.2.1. In situ air composition measuring equipment

The in situ air composition measuring equipment (ACME) system was developed from an in situ IC system (Chang et al., 2007) and consists of a denuder, filter collector unit, aerosol growth capture unit, and ion analysis unit. This system can collect $PM_{2.5}$ and PM_{10} aerosols according to the size selective inlet. In this study, the ACME system was operated at a total flow rate of 16.7 lpm for a $PM_{2.5}$ sampling inlet. After leaving the pre-impactor, the sampling flow is split into a 10 lpm main flow and 6.7 lpm filter flow. The filter flow is passed through the filter pack, where a collection filter of the proper material can be selected according to the chemical composition of the aerosol to be analyzed. The ambient sample from the main flow is drawn through the multiple parallel-plate wet denuder with a constantly regenerated deionized (DI) water surface to remove acidic (NO_2, SO_2, HNO_2, HNO_3 and H_2SO_4) and basic gases (NH_3), then the aerosol is passed through a growth chamber where large droplets form in the supersaturated condition. After leaving the growth chamber, the aerosol is removed from the air by inertial impact onto a flat quartz plate, and highly purified and DI carrier water is used to wash the aerosol off the impact plate. The final liquid sample, which contains the soluble ions of the collected aerosol and air bubbles, is introduced into the debubbler to remove the air bubbles. The syringe pump was used to withdraw the liquid sample from the debubbler with flow rate of 0.25 ml min^{-1}. Then a sample of 3 ml was injected into each IC (ion chromatography, ICS-90, Dionex Corp., California, USA) with flow rate of 1.5 ml min^{-1}. In this work, the water-soluble inorganic ions were measured at intervals of 15 min. The filtering head for the sample drips of the ACME system is changed once every two days, and the air flow rate of the instrument is calibrated every day. Each IC consists of a 500 μl sample loop. The columns used in the anion and cation ion chromatographs are AS12A and CS12A, respectively. The retention time is 2.4, 2.7, 4.5, 8.5, 4.0, 4.5, 5.7, and 11.2 min for Cl^-, NO_2^-, NO_3^-, SO_4^{2-}, Na^+, NH_4^+, K^+, Mg^{2+}, and Ca^{2+}, respectively. Each soluble species can be clearly separated and analyzed. The mass concentrations of soluble ions in the atmosphere are obtained by calculating the analytic results of the ICs. The detection limits calculated as the three times standard deviations of seven replicate blank samples were lower than 0.5 μg m^{-3} for the various ambient ionic components. The results of blank samples were measured from DI water in the same way as normal samples. The system contamination in the blank sample can be ignored, because it is much less than the measurement of sample. To render the sampled data and other analytical results consistently representative of time, all of the measured data are converted into hourly average values before analysis. The ACME

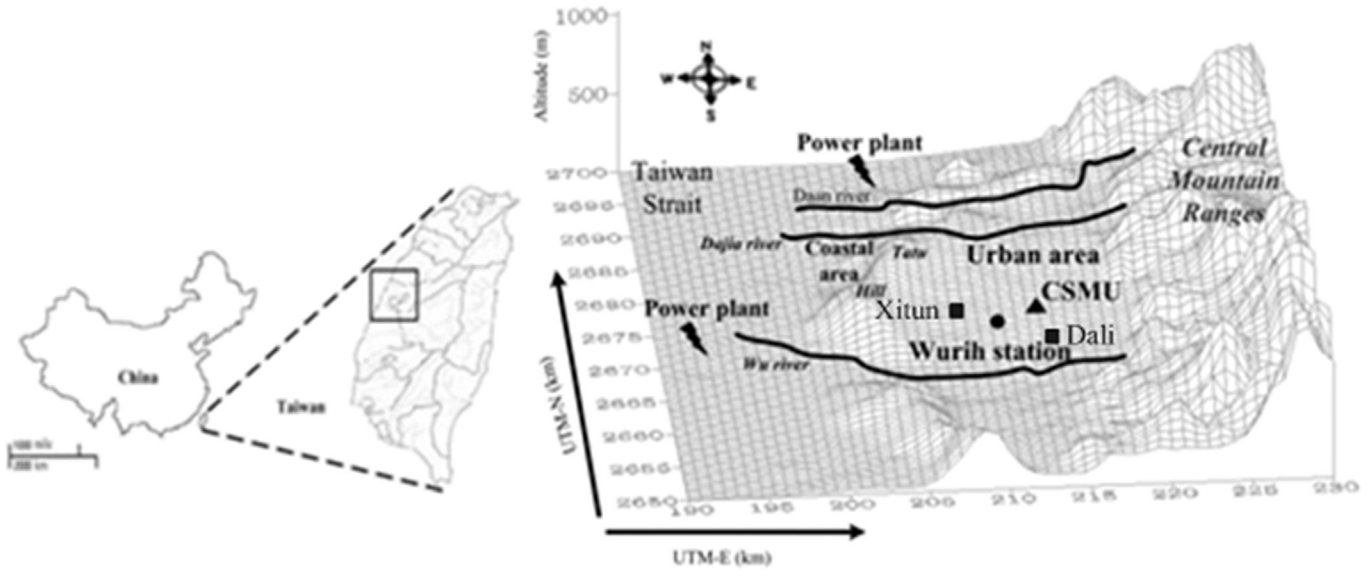

Fig. 1. Geographical location of Taichung City and sampling sites. The LPV-3 light path is between Wurih station (round) and CSMU (triangular).

system is advantageous in comparison to filter-based samples to be analyzed by IC, in the sense that it eliminates volatilization artifacts observed in the latter (unless backup filters are used).

2.2.2. OCEC carbon aerosol analyzer

The measurements of the EC and OC were made by a field semi-online OC/EC analyzer (Bae et al., 2004) from Sunset Laboratory Inc. with a $PM_{2.5}$ cyclone inlet (BGI; flow rate: 8 l min^{-1}). The device was equipped with a carbon parallel-plate diffusion denuder (from Sunset Lab.) to remove volatile organic compounds that may cause a positive bias in the OC concentrations measured. The samples were taken at 45 min intervals of which the thermal–optical analysis takes about 15 min using NIOSH protocol (NIOSH, 1998). The collected EC and OC were oxidized to carbon dioxide and analyzed by a non-dispersive infrared (NDIR) detector. The detection limits calculated as the three times standard deviations of seven replicate blank samples were lower than 0.5 μg m^{-3}.

2.2.3. Long-path visibility transmissometer 3

The long-path visibility transmissometer 3 (LPV-3, Optec, Inc., Lowell, USA) consists of a constant-output light-source transmitter (light source) and a computer-controlled photometer receiver (detector). The transmissometer directly measures the irradiance of a light source at 550 nm wavelength after the light has traveled over a finite atmospheric path. The transmittance of the path is calculated by dividing the measured irradiance at the end of the path with the calibrated initial intensity of the light source. Using Bouger's law, the average light extinction (b_{ext}) of the path is calculated from the transmittance and length of the path. Transmissometers produce a completely ambient measurement of the light extinction coefficient, which is converted into visibility using the following equation:

$$\text{Visibility(VIS)} = K/b_{ext} \quad (1)$$

where: K = the Koschmieder coefficient, which is the logarithm of the contrast threshold limit value of the human eye (3.9 in this study). The calibration was conducted using the differential path method (OPTEC, 1996; EPA, 1999) and performed by measuring the uncertainties in the path range and atmospheric transmittance of the lamp intensity over the calibration path.

2.3. Positive matrix factorization (PMF) model

PMF (PMF v3.0; USEPA, 2008) based on multilinear engine 2 program was used to identify the possible pollutant sources of $PM_{2.5}$ and estimate the contribution of each source to $PM_{2.5}$ mass. Further description of the model can be found in Paatero and Tapper (1994) and Paatero (1997). In this study, PMF was performed on the two data matrices of concentrations and uncertainties for hourly samples (over 440 (1 h) data points). Concentration value below the method detection limit (MDL) is replaced by half of MDL value and the uncertainty is calculated using the following equation (Polissar et al., 1998).

$$\text{Unc} = \frac{5}{6} \times \text{MDL}.$$

If the concentration is greater than the MDL provided, the calculation is

$$\text{Unc} = \sqrt{(\text{Error Fraction} \times \text{concentration})^2 + (\text{MDL})^2}.$$

Missing data was preliminarily replaced by the median value of the measured concentrations and their uncertainties were replaced by two times the median value. Table 1 lists the species quantified during this work along with their median concentration, uncertainty, and prevalence of missing and BDL observations. Interpretability of the resulting factor profiles and contributions was ultimately used as the primary tool for selecting the optimum number of factors. The six factor model and a

Table 1
Summary statistics and concentrations of 9 species measured for PMF analysis.

Species	Median (μg m^{-3})	Mean uncertainty (μg m^{-3})	Missing (%)	BDL (%)
Cl^-	3.3	0.8	4.6	0.0
NO_3^-	8.4	7.2	5.6	34.5
SO_4^{2-}	11.9	2.7	8.1	0.0
Na^+	0.6	0.6	11.5	0.2
NH_4^+	0.9	1.1	11.5	31.2
K^+	0.5	0.5	11.5	1.0
Ca^{2+}	0.4	0.5	12.5	1.0
OC	11.9	2.0	5.0	0.4
EC	2.4	0.7	5.0	0.4

value of FPEAK = 0.01 provided the most physically reasonable factor profiles. A total of 100 bootstrap runs were performed with a minimum R^2 of 0.6 to examine the stability and to estimate the uncertainty of the base run solution. All of the bootstrapped factors were uniquely mapped to a factor from the base solution, and no factors were unmapped.

3. Results and discussion

3.1. Classification of weather conditions

Fig. 2 exhibits the hourly variations of the meteorological parameters of wind speed (WS), wind direction (WD), temperature (T) and relative humidity (RH) in the sampling period. As mentioned by Lin et al. (2004), the dominant weather condition of each experiment day can be classified as stagnant and transport condition. The period and characteristics of each weather condition are detailed below.

During the effect of the winter monsoon, stagnant weather conditions are typical prior to a frontal passage over Taiwan. Winds before the frontal passage tend to be weak with a sea–land circulation. Ambient temperature and relative humidity show a clear diurnal cycle. Under this condition, local emissions can dominate the distribution of air pollutants. Stagnant weather conditions occurred in the periods December 9–14, 17–24 and 27–29. In contrast, as the cold front passed over Taichung, a diurnal cycle of meteorological parameters disappeared. Ambient temperature drop rapidly, and relatively strong northwesterly–northeasterly winds prevail which can carry long-range transport air masses. Therefore, these weather conditions were classified as the transport condition. Transport weather conditions occurred in the periods December 14–17 and 24–27.

3.2. Explained variations of NO_2 and PM to visibility degradation

Environmental studies have found that the relative humidity, NO_2 concentrations, and particulate matter in the atmosphere can influence the visibility (Appel et al., 1985; IMPROVE, 2006, 2010; Kuo et al., 2013). The b_{ext} is inverse proportional to visibility. Hence, higher value of b_{ext} demonstrates poorer visibility. Fig. 3 shows the hourly variations of b_{ext}, $PM_{2.5}$, $PM_{2.5-10}$ and NO_2 in the sampling period. The trend of b_{ext} is similar to that of NO_2, $PM_{2.5-10}$ and $PM_{2.5}$. On the whole, the b_{ext} was higher during the stagnant weather conditions than that during the transport weather conditions. Compared with the hourly value of b_{ext} on the stagnant days, the hourly b_{ext} was higher in the nighttime and the relatively higher b_{ext} occurred at the frontal passage. It suggested that more serious air pollution resulted in poorer visibility.

Cass (1976) indicated that the RH-correction factor [1 / (1 − RH)] was required to improve the total variation explained for b_{ext}. Lai and Sequeira (2001) applied the RH-correction factor to increase the explained variation of b_{ext} from 28% to almost 70% in Hung Kung. The explained variations of NO_2, $PM_{2.5-10}$, and $PM_{2.5}$ with and without RH-correction to b_{ext} between the stagnant and transport weather conditions were compared by the simple regression model in Fig. 4. The results indicated that the RH-correction increased the variation of $PM_{2.5-10}$ and $PM_{2.5}$ to b_{ext}. The R^2 of $PM_{2.5}$ with the RH-correction was higher than that of $PM_{2.5-10}$ and NO_2 during the transport and stagnant weather conditions. In addition, the explained variations of NO_2, $PM_{2.5}$ and $PM_{2.5-10}$ are estimated from a linear multivariate regression model as follows:

$$b_{ext} = b_1[NO_2] + b_2[PM_{2.5}]\,Cf_{RH} + b_3[PM_{2.5-10}]Cf_{RH}, \quad (2)$$

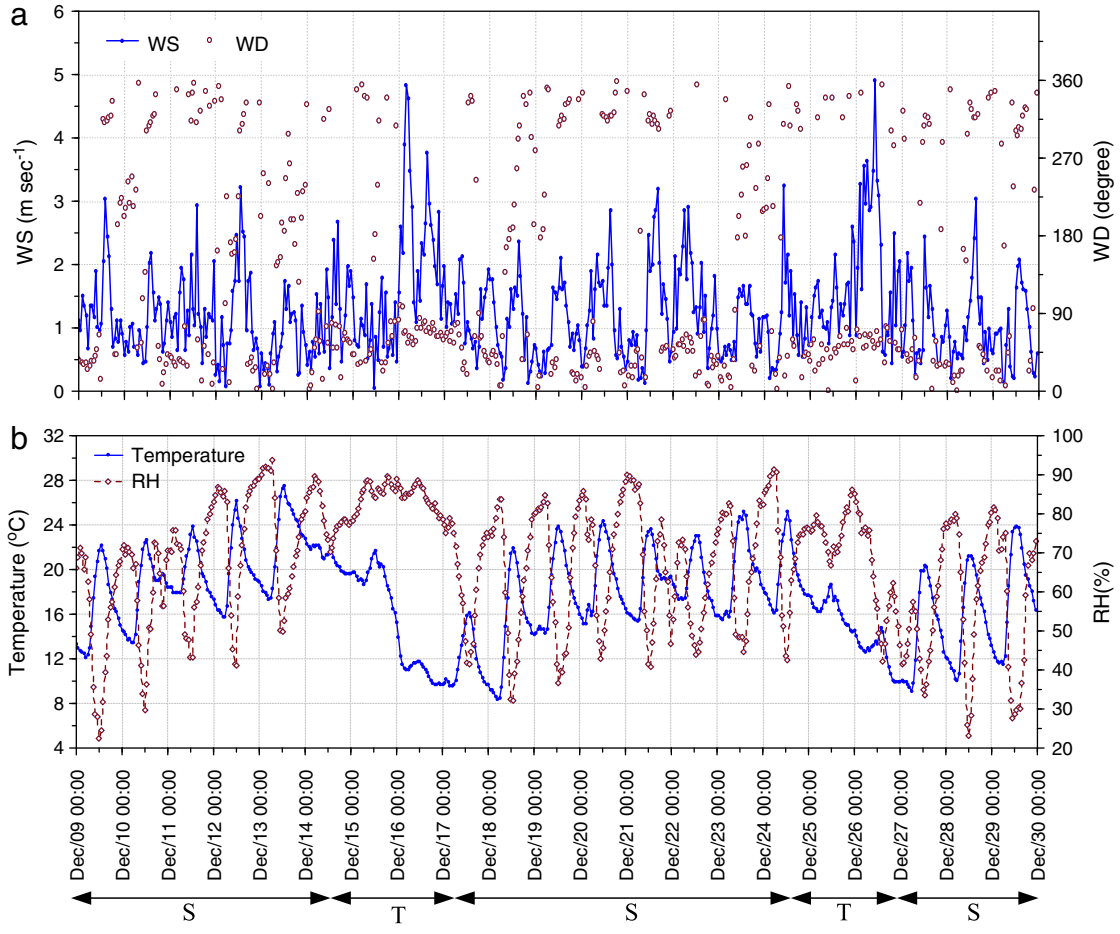

Fig. 2. The hourly variation of the meteorological parameters during the sampling period. S: Stagnant weather condition; T: Transport weather condition.

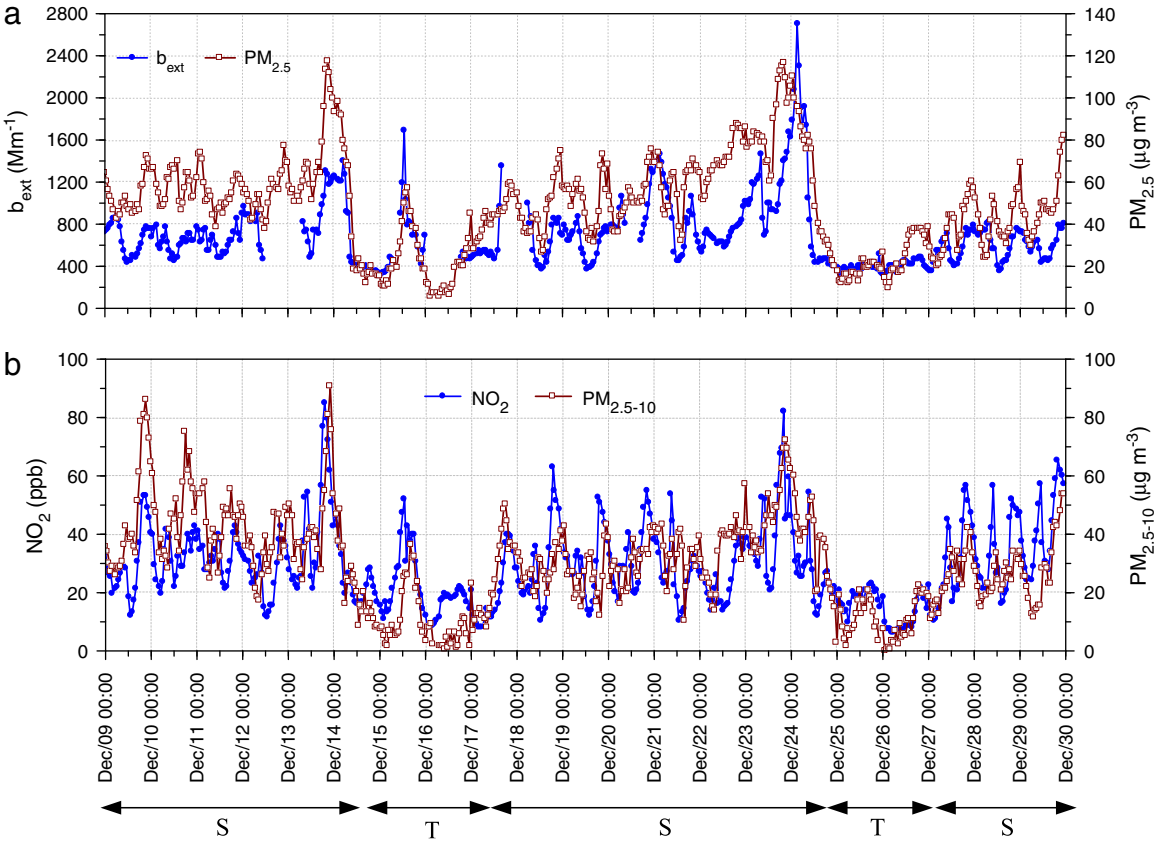

Fig. 3. The hourly measurements of b_{ext}, $PM_{2.5}$, $PM_{2.5-10}$, and NO_2 during the sampling period. S: Stagnant weather condition; T: Transport weather condition.

where b_1, b_2, and b_3 are the regression parameters; and Cf_{RH} is an RH-correction factor. Table 2 shows the calculated total variation and fractional variation with and without the RH-correction. The total variance explanation of b_{ext} in the two weather conditions improved from a range of 43–65% without the RH-correction to a range of 67–76% with the RH-correction. The fractional variation of $PM_{2.5}$ to b_{ext} was the highest compared to the NO_2 and $PM_{2.5-10}$ variations for both weather conditions. It indicated that $PM_{2.5}$ is the most important pollutant for visibility degradation. The $PM_{2.5}$ variation to b_{ext} in the transport weather conditions was slightly lower than that in the stagnant weather conditions, which might have been caused by the differences in aerosol compositions between two conditions.

3.3. Source apportioning of $PM_{2.5}$

PMF has been demonstrated as a useful statistical technique for data reduction and source interpretation. The hourly $PM_{2.5}$ composition dataset was used to apply PMF techniques to determine the sources and their contributions to the total $PM_{2.5}$ mass. The six source factor profiles that were obtained are reported in Fig. 5. Fig. 6 illustrates a time series of the estimated hourly $PM_{2.5}$ mass concentrations of each source. In a seven-factor model, the regression produces a negative constant indicating too many factors have been used. In a five-factor model, the secondary sulfate and coal/incinerator combustion factors were not separated.

The first source factor contained a higher contribution of Cl^-, Na^+, and K^+, which indicated the possible source of aged sea salt. Ca^{2+} has shown the potential source from crustal origin. The presence of SO_4^{2-} may also originate from soil particles and the possible mechanism could be the aqueous-phase oxidation of SO_2 in cloud droplets (Pandis et al., 1992). A combination of the four elements (Na^+, K^+, Cl^-, and Mg^{2+}) should provide a reliable signature of marine/crustal sources (Sharma et al., in press).

The second factor was characterized by NO_3^-, Na^+, K^+, OC, and EC. The highest contribution percentage (94.4%) of NO_3^- to total nitrate is presented in this factor. The major source of nitrate is the conversion of nitrogen oxides emitted from high temperature combustion sources making this factor predominantly secondary aerosol. OC and EC have been widely used as tracers of vehicle pollution, which also indicated that a portion of $PM_{2.5}$ in this factor was transformed from the vehicle exhaust. In addition, it is possible that the NO_3^- ions bonded with cations such as Na^+ and K^+, forming nitrate particles (Kang et al., 2008). Many studies have reported that formation of nitrate depends on the temperature, atmospheric levels of NOx and NH_3, and relative humidity (Seinfeld and Pandis, 2006; Heo et al., 2009). This factor was characterized as the secondary nitrate aerosols.

The third source factor was primarily characterized by SO_4^{2-}, which has been identified in most source apportionment work. Sulfate was formed by the oxidation of SO_2 and assigned to the secondary aerosol. As the conversion rate from SO_2 to sulfate is normally slow, this factor was most likely from long range transport, rather than from local emission. This factor was identified as the secondary sulfate from the long-range transport.

The fourth source factor was dominated by OC and EC. EC is considered to be the main tracer for vehicle emissions (Kim et al., 2002; Sardar et al., 2005). The sampling site was located in the urban area that was influenced by vehicle emissions. 72.9% of total EC is present in this factor. The hourly mass concentration of this factor illustrated the daily variation with high values occurring at rush-hours. This factor was characterized as the direct emission of vehicle exhaust.

The fifth source factor was characterized by Cl^-, OC and a small loading of Ca^{2+}. Cl^- has often been associated with sea salts, coal combustion, and municipal waste combustion. In this work, sea salt

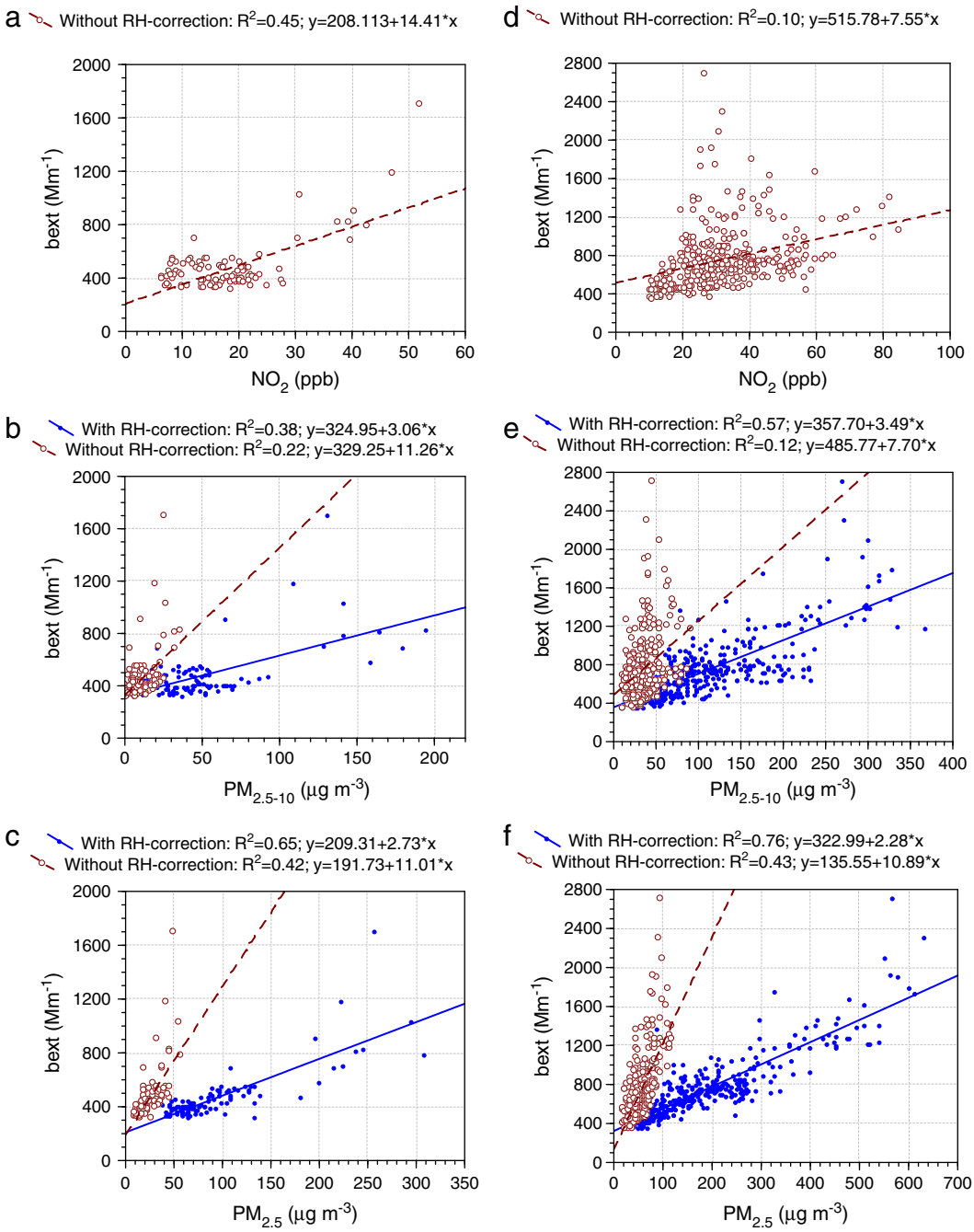

Fig. 4. The explained variations of NO_2, $PM_{2.5-10}$, and $PM_{2.5}$ with and without RH-correction to b_{ext} between the stagnant weather conditions ((a)–(c)) and transport weather conditions ((d)–(f)).

was not the main source of Cl^- because the ratio of Cl^- to Na^+ was significantly higher than that in sea salts. Marmur et al. (2005) reported that Cl^-, Ca, and OC were the tracer species of the coal combustion.

Table 2
The explained variations of major NO_2 and particulate matter with and without the RH-correction to the light extinction.

Weather condition	RH-correction	Number	Total variation	Fractional variation		
				NO_2	$PM_{2.5}$	$PM_{2.5-10}$
Transport	Without	104	0.65	0.17.	0.45	0.03
	With	104	0.67	0.02.	0.65	N.S.
Stagnant	Without	339	0.43	N.S.	0.43	N.S.
	With	339	0.76	N.S.	0.76	N.S.

N.S.: Non-significant.

Raja et al. (2010) also indicated that unlike sulfates existing as potassium sulfate, sulfates from coal combustion are expected to be incorporated in the secondary aerosol factor. A coal-fired power plant and refuse incineration plant were located in proximity to the Taichung urban area; therefore, their contributions to this factor were assumed to be coal/incinerator combustion.

The sixth factor consisted of a large fraction of NH_4^+, which is formed from its gaseous precursor (NH_3) through gas and aqueous phase reactions with acidic species. In 2010, Taichung City covered an area of 2215 km^2 and had more than 2.5 million people. However, the percentage of the population served by waste water treatment plants was approximately 35%. The NH_4^+ aerosol was most likely related to the contribution from local sewage emissions. The conversion efficiency of NH_3 to NH_4^+ aerosol depends on the level of ambient acids, temperature,

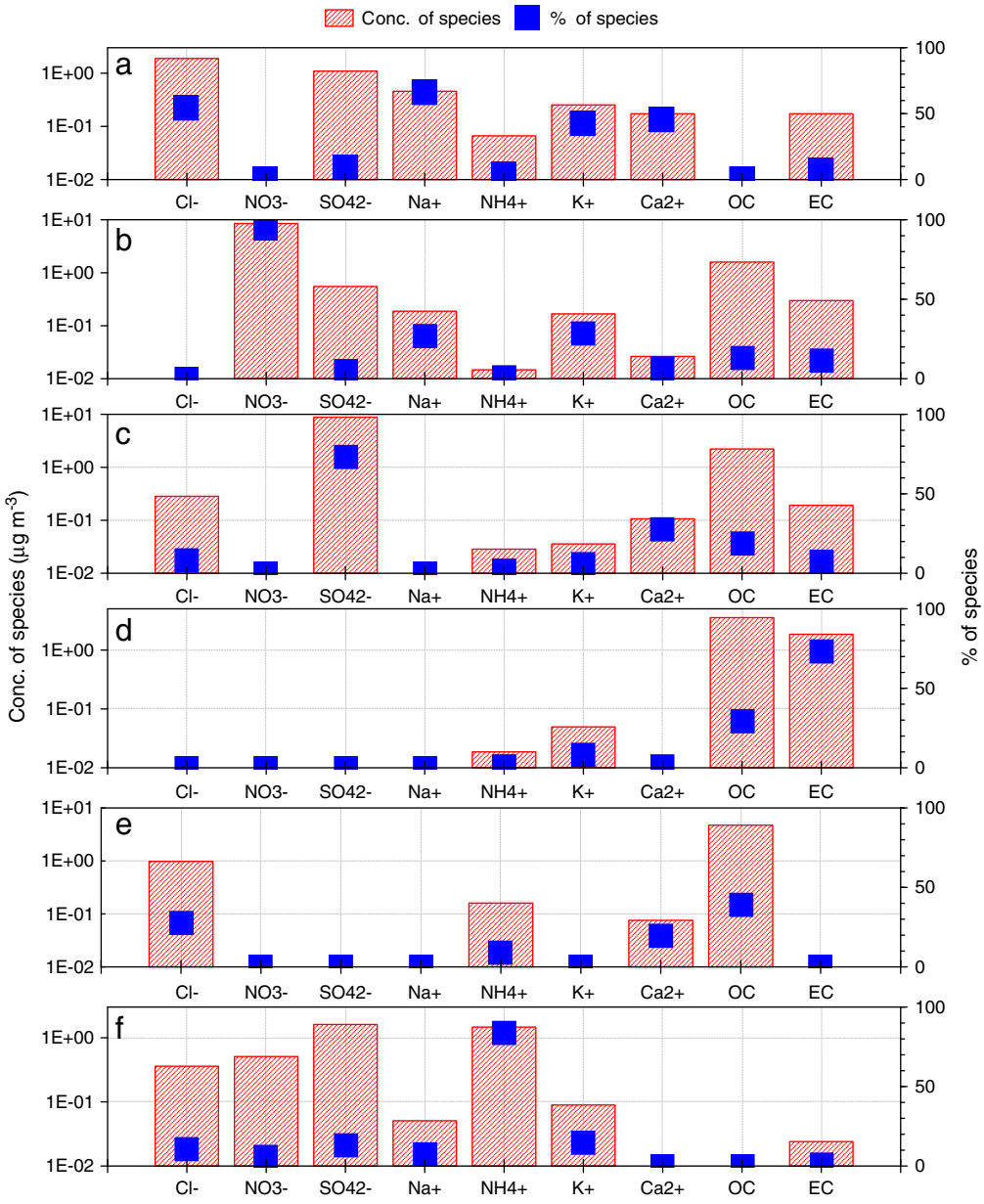

Fig. 5. The contributions of ions for the six sources identified by the PMF. (a) Marine/crustal aerosols, (b) secondary nitrate, (c) secondary sulfate, (d) direct vehicle exhaust, (e) coal/incinerator combustion and (f) local sewage emission.

and water availability. As shown in Fig. 6(f), the trends for the time series of this factor's contribution and derivatives of secondary nitrate were similar during the stagnant weather conditions before December 15. The correlation coefficient (R^2) of the hourly $PM_{2.5}$ concentrations between the secondary nitrate factor and this factor was 0.71 suggesting the local sewage provides the urban background ammonia emissions to be bound in particles as ammonium nitrate. The low concentrations of NH_4^+ may be due to inhibiting the micro-biological degradation and ammonia evaporation on cold surface, which caused the uncertainty after December 15.

3.4. Reconstructed $PM_{2.5}$ and light extinction coefficient

The $PM_{2.5}$ mass concentration that was reconstructed by PMF was correlated with the results from measurements. It has been observed that the average of the total ionic mass (sum of the concentrations of the cations and anions) concentration contributed 56.5% of $PM_{2.5}$ mass, whereas, total carbon (organic carbon + elemental carbon) account for 31.4% of $PM_{2.5}$ mass. The comparisons between the reconstructed and measured $PM_{2.5}$ mass concentrations showed that the resolved sources effectively reproduce the measured values and account for most of the variation in the $PM_{2.5}$ mass concentrations (Fig. 7). The difference is believed to be associated with the bias and uncertainties of factors, such as the sampling artifacts, species analysis, incorrectly assumed molecular forms, and sources unaccounted by the PMF analysis.

The hourly reconstructed mass of each source during the sampling period is illustrated in Fig. 6. As shown in Table 3, the average reconstructed mass concentrations of marine/crustal aerosols, secondary nitrate, secondary sulfate, direct vehicle exhaust, coal/incinerator combustion, and local sewage emission were 2.5, 3.8, 12.4, 2.2, 4.2, and 2.7 μg m^{-3}, respectively, during the transport weather conditions and 3.0, 5.1, 19.5, 10.1, 14.3, and 3.6 μg m^{-3}, respectively, during stagnant weather conditions.

Among the reconstructed sources, the secondary sulfate was the most abundant source of $PM_{2.5}$, and it has contributed 44.6 and 35.0% of the total reconstructed sources during the transport and stagnant

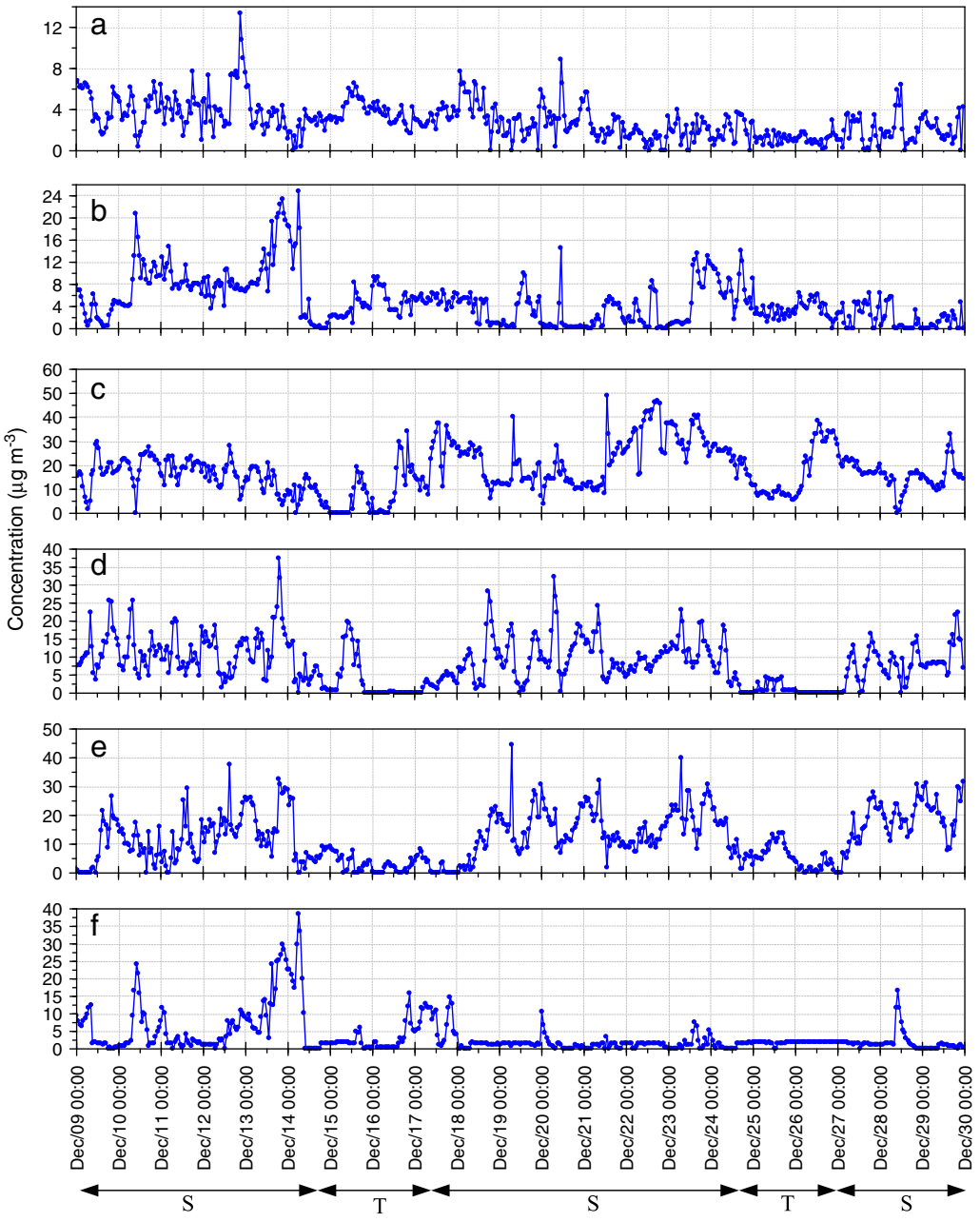

Fig. 6. The hourly variations of reconstructed concentrations of $PM_{2.5}$ for the six sources identified by the PMF. (a) marine/crustal aerosols, (b) secondary nitrate, (c) secondary sulfate, (d) direct vehicle exhaust, (e) coal/incinerator combustion and (f) local sewage emission. S: Stagnant weather condition; T: Transport weather condition.

weather conditions, respectively. The contributions of direct vehicle exhaust and coal/incinerator combustion during stagnant weather conditions were significantly higher than that during transport weather conditions, which was primarily a result of the accumulation of local pollutants during stagnant weather conditions. The contribution of marine/crustal aerosols source to $PM_{2.5}$ mass increased from 5.4% in stagnant weather conditions to 9.1% in transport weather conditions because of sea salt transport. The secondary nitrate source had a higher contribution (13.8%) of the $PM_{2.5}$ mass in transport weather conditions than that (9.2%) in stagnant weather conditions due to the low temperatures and high humidity that facilitate the formation of secondary nitrate particles in transport weather conditions (Choi et al., 2013).

In this work, a multivariate linear regression analysis (MLRA) was applied to derive the relative contribution of atmospheric extinction sources to b_{ext}, with b_{ext} used as the dependent variable and the reconstructed $PM_{2.5}$ concentrations used as independent variables. The MLRA algorithm is presented as follows:

$$b_{ext} = \sum_i^5 a_i * Cf_{RH} * [PM_{2.5}]_i \quad (3)$$

where b_{ext} is the measured extinction coefficient, $[PM_{2.5}]_i$ is the reconstructed $PM_{2.5}$ concentration of source i, Cf_{RH} is an RH-correction factor, and a_i is the fitted MLRA coefficient of source i. The reconstructed b_{ext} of the local sewage emission source was not discussed due to the insignificant result of the MLRA.

Fig. 8 shows the hourly variations of the measured b_{ext} and reconstructed b_{ext} during the sampling period. The correlation coefficient between the measured b_{ext} and reconstructed b_{ext} exhibited a moderate correlation, with an R^2 of 0.70 and slope of 0.88. The system discrepancy

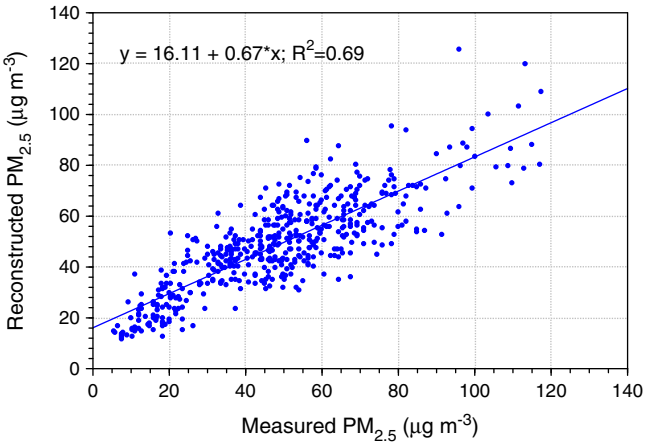

Fig. 7. The simple regression analysis between the measured $PM_{2.5}$ and reconstructed $PM_{2.5}$.

between single-point chemical measurements and long optical path measurements may be the primary reason for the residual variance of regression between the measured b_{ext} and reconstructed b_{ext}.

Table 4 compares the reconstructed light extinction coefficients and contributions of each source between the two weather conditions. The b_{ext} of the source of secondary sulfate, direct vehicle exhaust, and coal/incinerator combustion in stagnant weather conditions was about 1.4, 3.3, and 3.1 times that in transport weather conditions, respectively. In contrast, the b_{ext} is similar between two weather conditions for the sources of marine/crustal aerosols and secondary nitrate. The source of the secondary sulfate made the largest contribution to the b_{ext} and accounted for the similar contribution of b_{ext} between two weather conditions. For the sources of marine/crustal aerosols and secondary nitrate, the b_{ext} contributions had lower value in stagnant weather conditions than that in transport weather conditions. The b_{ext} contributions of direct vehicle exhaust and coal/incinerator combustion in stagnant weather conditions were 2.0 and 1.9 times higher than in transport weather conditions. Therefore, the extinction in Taichung was intensively influenced by anthropogenic sources, especially by direct vehicle exhaust and coal/incinerator combustion source in stagnant weather conditions.

4. Conclusions

The characteristics of ambient extinction coefficient and aerosol chemical compositions in the transport and stagnant weather conditions were presented. According to the classification of the weather conditions, the application of a PMF analysis provided a successful qualitative assessment of the hourly contributions to the $PM_{2.5}$ mass concentration of marine/crustal aerosol, secondary nitrate, secondary sulfate, direct vehicle exhaust, coal/incinerator combustion, and local sewage emission. A multivariate linear regression analysis of the reconstructed b_{ext} against the identified sources of PMF analysis was conducted between the two weather conditions. The secondary sulfate was the most abundant source of $PM_{2.5}$, which made the largest contribution to the b_{ext} during the sampling period. The contributions from direct vehicle exhaust and coal/incinerator combustion produced more of an

Table 3
The average concentrations and contributions of each source during the transport and stagnant weather conditions.

Sources	Transport weather condition		Stagnant weather condition	
	Concentration (μg m^{-3})	Contribution (%)	Concentration (μg m^{-3})	Contribution (%)
Marine/crustal aerosols	2.5	9.1	3.0	5.4
Secondary nitrate	3.8	13.8	5.1	9.2
Secondary sulfate	12.4	44.6	19.5	35.0
Vehicle exhaust	2.2	8.0	10.1	18.1
Coal and incinerator combustion	4.2	15.0	14.3	25.8
Local sewage emission	2.7	9.6	3.6	6.6

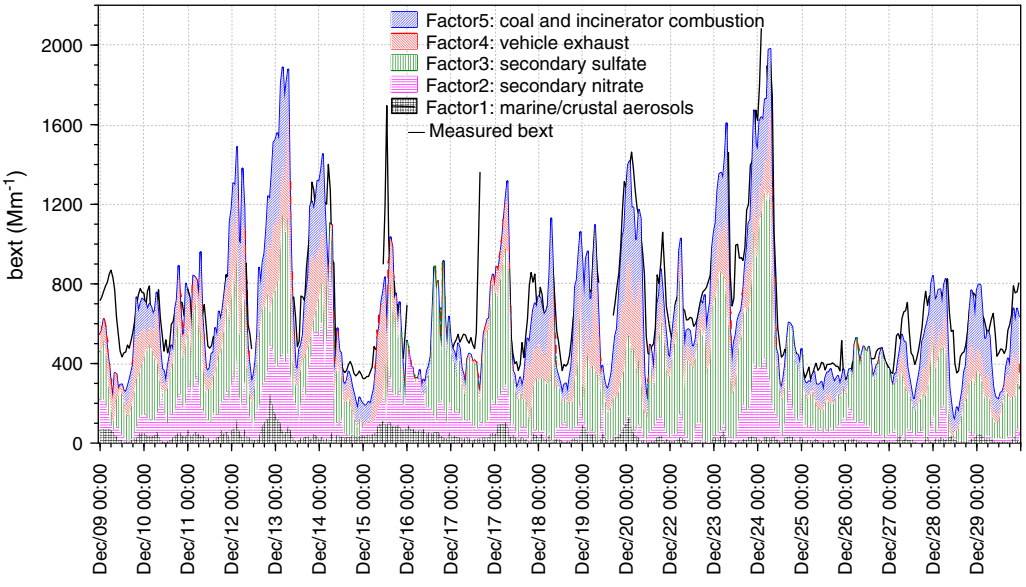

Fig. 8. The hourly variations of measured b_{ext} and reconstructed b_{ext} during the sampling period.

Table 4
The comparisons of the reconstructed light extinction and contribution.

Sources	Transport		Stagnant	
	b_{ext} (Mm^{-1})	Contribution (%)	b_{ext} (Mm^{-1})	Contribution (%)
Marine/crustal aerosols	36.0	8.4	32.4	4.6
Secondary nitrate	99.6	23.3	106.8	15.1
Secondary sulfate	207.5	48.6	298.3	42.2
Vehicle exhaust	40.4	9.5	133.1	18.8
Coal and incinerator combustion	43.4	10.2	136.3	19.3

impact on visibility degradation in stagnant weather conditions. Therefore, the reduction of the pollutants based on a reduction of direct vehicle exhaust and coal-incinerator combustion could effectively improve the visibility in metropolitan Taichung.

To the best of our knowledge, it is rare to reconstruct the real-time b_{ext} contributions of each pollutant source through the receptor model analysis of hourly ambient visibility and aerosol chemical compositions especially for Northeast Asia. The application of more time-resolved data can not only improve the efficiency of source apportionment, but also help to identify the influence of various sources by using time series analysis. The results of this work provided the useful method to determine the priority policy for improving the ambient visibility.

Acknowledgments

This work is supported by the Environmental Protection Bureau, Taichung City Government (No. 0990051279). The authors also gratefully acknowledge the Ministry of Science and Technology in Taiwan for financial support under project No. NSC99-2111-M-040-002-MY3.

References

Appel BR, Tokiwa Y, Hsu J, Kothny EI, Hahn E. Visibility as related to atmospheric aerosol constituents. Atmos Environ 1985;19:1525–34.
Bae MS, Schauer JJ, DeMinter JT, Turner JR, Smith D, Cary RA. Validation of a semi-continuous instrument for elemental, carbon and organic carbon using a thermal–optical method. Atmos Environ 2004;38:2885–93.
Bäumer D, Vogel B, Versick S, Rinke R, Möhler O, Schnaiter M. Relationship of visibility, aerosol optical thickness and aerosol size distribution in an ageing air mass over South-West Germany. Atmos Environ 2008;42:989–98.
Cass GR. The relationship between sulfate air quality and visibility at Los Angeles. Caltech Environmental Quality Laboratory Memorandum; 1976 [No. 18, Pasadena, California].
Chang SY, Lee CT, Chou CCK, Liu SC, Wen TX. The performance comparison of the In Situ IC instrument and the continuous field measurements of soluble aerosol compositions at the Taipei Aerosol Supersite, Taiwan. Atmos Environ 2007;41:1936–49.
Chen J, Qiu S, Shang J, Wilfrid OMF, Liu X, Tian H, et al. Impact of relative humidity and water soluble constituents of $PM_{2.5}$ on visibility impairment in Beijing, China. Aerosol Air Qual Res 2014;14:260–8.
Choi JK, Heo JB, Ban SJ, Yi SM, Zoh KD. Source apportionment of $PM_{2.5}$ at the coastal area in Korea. Sci Total Environ 2013;447:370–80.
Deng X, Tie X, Wu D, Zhou X, Bi X, Tan H, et al. Long-term trend of visibility and its characterizations in the Pearl River Delta (PRD) region, China. Atmos Environ 2008; 42:1424–35.
Eatough DJ, Farber R. Apportioning visibility degradation to sources of $PM_{2.5}$ using positive matrix factorization. J. Air Waste Manag. Assoc. 2009;59:1092–110.
EPA. Visibility monitoring guidance document. Emissions Monitoring and Analysis Division, Monitoring and Quality Assurance Group; 1999 [MD-14, Research Triangle Park, NC 27711].
Heo JB, Hopke PK, Yi SM. Source apportionment of $PM_{2.5}$ in Seoul, Korea. Atmos Chem Phys 2009;8:20427–61.
Huang W, Tan J, Kan H, Zhao N, Song W, Song G, et al. Visibility, air quality and daily mortality in Shanghai, China. Sci Total Environ 2009;407:3295–300.
IMPROVE. Spatial and seasonal patterns and temporal variability of haze and its constituents in the United States. Report V; 2006.
IMPROVE. Spatial and seasonal patterns and temporal variability of haze and its constituents in the United States. Report IV; 2010.
IPCC. Climate Change 2007. The physical science basis. Contribution of Working Group I to the Fourth Assessment Report of the Intergovernmental Panel on Climate Change. Cambridge, United Kingdom: Cambridge University Press; 2007.
Kang S, Hwang H, Park Y, Kim H, Roh CU. Chemical compositions of subway particles in Seoul, Korea determined by a quantitative single particle analysis. Environ Sci Tech 2008;42:9051–7.
Kim S, Shen S, Sioutas C, Zhu Y, Hinds WC. Size distribution and diurnal and seasonal trends of ultrafine particles in source and receptor sites of the Los Angeles basin. J Air Waste Manag 2002;52:297–307.
Kim YJ, Kim KW, Kim SD, Lee BK, Han JS. Fine particulate matter characteristics and its impact on visibility impairment at two urban sites in Korea: Seoul and Incheon. Atmos Environ 2006;40:593–605.
Kuo CY, Cheng FC, Chang SY, Lin CY, Chou CCK, Chou CH, et al. Analysis of the major factors affecting the visibility degradation in two stations. J Air Waste Manag 2013; 63:433–41.
Lai LY, Sequeira R. Visibility degradation across Hong Kong: its components and their relative contributions. Atmos Environ 2001;35:5861–72.
Liaw JJ, Lian SB, Huang YF, Chen RC. Using sharpness image with haar function for urban atmospheric visibility measurement. Aerosol Air Qual Res 2010;10:323–30.
Lin CY, Liu SC, Chou CCK, Liu TH, Lee CT. Long-range transport of Asian dust and air pollutants to Taiwan. TAO 2004;15:759–84.
Marmur A, Unal A, Mulholland JA, Russell AG. Optimization-based source apportionment of $PM_{2.5}$ incorporating gas-to-particle ratios. Environ Sci Tech 2005;39:3245–54.
NIOSH Method 5040In: Cassinelli ME, O'Connor PF, editors. NIOSH manual of analytical methods (NMAM), second supplementSupplement to DHHS (NIOSH) Publication No. 94–113, 4th ed.; 1998.
OPTEC. Model LPV-2 long path visibility transmissometer version 2: technical manual for theory of operation and operating procedures. 199 Smith Street Lowell, MI 49331, USA: OPTEC Inc.; 1996.
Paatero P. Least squares formulation of robust nonnegative factor analysis. Atmos Environ 1997;37:23–35.
Paatero P, Tapper U. Positive matrix factorization: a non-negative factor model with optimal utilization of error estimated of data values. Environmetrics 1994;5:111–26.
Pandis SN, Seinfeld JH, Pilinis C. Heterogeneous sulfate production in an urban fog. Atmos Environ 1992;26A:2509–22.
Pathak RK, Chan CK. Inter-particle and gas-particle interactions in sampling artifacts of $PM_{2.5}$ in filter-based samplers. Atmos Environ 2005;39:1597–607.
Polissar AV, Hopke PK, Malm WC, Sisler JF. Atmospheric aerosol over Alaska: 2. Elemental composition and sources. J Geophys Res 1998;103:19045–57.
Raja S, Biswas KF, Husain L, Hopke PK. Source apportionment of the atmospheric aerosol in Lahore, Pakistan. Water Air Soil Pollut 2010;208:43–57.
Sardar SB, Fine PM, Mayo PR, Sioutas C. Size-fractionated measurements of ambient ultrafine particle chemical composition in Los Angeles using the nanoMOUDI. Environ Sci Tech 2005;39:932–44.
Seinfeld JH, Pandis SN. Atmospheric chemistry and physics: from air pollution to climate change. 2nd ed. New York: Wiley; 2006.
Sharma SK, Mandal TK, Saxena M, Rohtash R, Sharma A, Gautam R. Source apportionment of PM_{10} by using positive matrix factorization at an urban site of Delhi, India. Urban climate; 2014 [in press, available online 21 November 2013].
Sun YL, Zhuang GS, Tang AH, Wang Y, An ZS. Chemical characteristics of $PM_{2.5}$ and PM_{10} in haze–fog episodes in Beijing. Environ Sci Technol 2006;40:3148–55.
Tan J, Duan J, He K, Ma Y, Duan F, Chen Y, et al. Chemical characteristics of $PM_{2.5}$ during a typical haze episode in Guangzhou. J Environ Sci China 2009;21:774–81.
USEPA. EPA positive matrix factorization (PMF) 3.0, fundamentals and user guide. USEPA Office of Research and Development; 2008.
Wang JL, Zhang YH, Shao M, Liu XL, Zeng LM, Cheng CL, et al. Quantitative relationship between visibility and mass concentration of $PM_{2.5}$ in Beijing. J Environ Sci China 2006; 18:475–81.
Wang X, Ding X, Fu X, He Q, Wang S, Bernard F, et al. Aerosol scattering coefficients and major chemical compositions of fine particles observed at a rural site in the central Pearl River Delta, South China. J Environ Sci China 2012;24:72–7.
Watson JG. Visibility: science and regulation. J Air Waste Manag 2002;52:628–713.
World Meteorological Organization. International meteorological vocabulary. WMO-No. 182, Geneva; 1992.
World Meteorological Organization. Manual on the global observing system. WMO-No. 544, Geneva; 2003.
Yuan CS, Lee CG, Liu SH, Yuan C, Yuan HY, Chen CTA. Developing strategies for improving urban visual air quality. Aerosol Air Qual Res 2002;2:9–22.

摘要

本計劃在 2014 年 2 月 28 日至 4 月 6 日於恆春海生館進行大氣污染物逐時觀測，以逐時 $PM_{2.5}$ 水溶性陰陽離子、含碳物質與氣膠垂直分佈等數據，配合氣象因子(溫濕度、風向與風速)、氣態污染物(O_3、SO_2、CO 與 NO_2)與粒狀污染物(PM_{10} 與 $PM_{2.5}$)濃度進行同步觀測，並使用逐時氣象因子與氣流軌跡模式(HYSPLIT)來區分不同傳輸事件。

本次觀測期間不同傳輸事件分別為高屏地區人為污染傳輸、陸風傳輸、西風傳輸、東北季風傳輸四種不同傳輸事件。首先，不同事件的氣象場特徵分別為日間海風(西北風)-夜間陸風(東北風)環流風、風速較弱的盛行西風、以及乾冷且風速大的盛行東北風。另外，本研究以來自於中南半島的生質燃燒污染物作為驗證下沖事件的指標物種，而下沖事件的辨別與驗證則以現址光達(LIDAR)的氣膠垂直分佈觀測與氣象模式的垂直風場剖面模擬判別出下沖氣流發生時間，同時在地面逐時生質燃燒指標污染濃度也可以觀測到峰值的出現。

本計畫不同大氣環境類別下氣膠污染特徵如下: 高屏地區人為污染傳輸的污染情況最嚴重的類型，由 NOR、NO_3^-/SO_4^{2-}與 NO_3^-/K^+當量濃度比的分析顯示污染源與西北方的高屏都會區污染排放及光化污染物有關，陸風傳輸污染物濃度迅速回復低值。在西風傳輸期間為空氣品質最佳的類型，且 Cl^-/Na^+質量濃度比(1.5)與海鹽比值(1.8)較為接近，顯示受到海洋氣流的影響。東北季風傳輸若氣流經大陸沿海污染地區，NH_4^+與 SO_4^{2-}濃度則會有上升的趨勢。下沖事件地面量測結果顯示生質燃燒指標污染物(K^+、EC 與 OC)與衍生性離子等濃度僅在下沖現象發生期間呈現較高趨勢，並且與鹿林山觀測結果比較顯示兩者生質燃燒污染來源相同，主要受到中南半島生質燃燒排放的影響。

關鍵字：中南半島、生質燃燒、下沖氣流、光化污染物

Abstract

Hourly measurements of meteorological parameters (temperature, relative humidity, wind direction and wind speed), particulate and gaseous pollutants (PM_{10}, $PM_{2.5}$, O_3, SO_2, CO and NO_2), chemical compositions of $PM_{2.5}$ (water soluble ions and carbonaceous materials), and vertical distribution of aerosols were made from February 28 to April 6 2014 at Hungchen in Taiwan. The HYSPLIT and hourly measurements of meteorological parameters were applied to distinguish the weather condition.

In this work, four types of air masses were identified as Anthropogenic emissions from Kaohsiung and Pingtung area, the land breeze, northeast monsoon and western sea wind. The four types of air masses can be directly characterized as daily variations with sea wind (northwest) in daytime and land wind (northeast) in nighttime, the prevailing northeaster with strong and cold wind, and the prevailing light breeze from west, respectively. The downwash processes were verified that the occurrence of peak in biomass burning tracer concentration was consistency with the period of downwash transport in the ground station. The vertical distribution of aerosols measured from the in situ LIDAR and the vertical wind section simulated from the meteorological model were used to define the period of the downwash transport. The biomass burning pollutants from the Indo-China Peninsula were regarded as the tracer to observe the downwash transport of the upper atmosphere.

The pollutant characteristics of each air mass were found in this study. Anthropogenic emissions from Kaohsiung and Pingtung area with primary photochemical pollutants led to the serious pollution at Hungchen. However, the concentrations of pollutants were quickly reduced when the wind was changed to the land wind. The pollution was related to the long range transport of polluted air from Asia in the prevailing northeasterly. During the westerly, the air quality was the best during the observed period. The ambient aerosols with the Cl^-/Na^+ ratio of 1.5 (similar to the ratio of 1.8 from sea salts) were characterized as the oceanic transport. The long-range transport of biomass burning from the Indo-China Peninsula affected the air quality at Hungchen through the downwash process. The aerosols were characterized as the high proportion of biomass pollutants. The comparison of Lulin station's results showed that they had same biomass burning source, mainly influenced by Indo-China Peninsula's biomass burning emissions.

Keywords: Indo-China Peninsula, biomass burning, downwash, photochemical pollutants

目錄

一、前言

近十年期間，已有研究探討中南半島生質燃燒對於台灣地區的影響，每年春季 3 至 4 月為中南半島生質燃燒活動頻繁期間，農業廢棄物與森林的大規模燃燒排放，造成大量的氣體與氣膠污染物。由於受到地形與天氣系統的抬升影響，將地表污染物傳輸至 2 至 5 公里的高度，並經由高層西風向東傳輸至台灣地區，自 2004 年起已於鹿林山高山背景測站進行東亞污染物傳輸的相關研究(黃希爾，2004)，在生質燃燒影響下，氣膠質量濃度較高，$PM_{2.5}$ 中的硫酸鹽、銨鹽、硝酸鹽與氣膠碳濃度明顯上升，且發現有較高濃度的鉀離子在細粒徑氣膠中，而在 $PM_{2.5\text{-}10}$ 中有較高濃度的塵土與海鹽成分。Yen et al. (2012)利用衛星火點觀測與氣象場觀測及模擬，發現受到大陸冷高壓南移過程的影響下，來自中南半島生質燃燒的污染物亦可能經由下沖氣流影響地表環境。上述研究顯示，在中南半島生質燃燒期間，台灣地區的高層大氣明確受到生質燃燒傳輸的影響，但在探討高層生質燃燒污染物可否經由下沖氣流影響平地空氣品質，因僅有氣象層面探討與環保署一般測站的觀測數據，欠缺氣膠在大氣中垂直傳輸與化學成分特徵的觀測，因此仍不足以說明下沉氣流對空氣品質的影響。

在已發表的文獻中，雖然已有相當多關於氣膠組成量測與其影響效應的研究，此類探討氣膠的文獻多數皆以批次式的濾紙採樣為主，即使用濾紙經長時間採樣收集大氣氣膠，再經過冗長繁瑣的實驗室程序分析氣膠化學組成。但氣膠上所進行的相關化學反應可能在數分鐘至一小時內即可完成，所獲得氣膠化學組成亦往往無法反應在空間與時間快速變異下的實際大氣氣膠特性，且樣品攜帶與保存過程亦容易受到污染。此外，在量測氣膠相的物質收集過程中，會受到氣相物質的干擾，樣本的誤差有主要兩個來源:1. 濾紙與氣膠樣本吸收氣相的酸性物質，進而使得氣膠量測濃度增加；2. 在濾紙上的氣膠樣本經由揮發損失導致氣膠濃度減少(Bao et al., 2012)，氣膠物種間的交互反應亦會造成組成改變。因此為了避免誤差，應用現址量測技術於空氣污染物的採樣，且增加氣相物質收集系統(denuder systems)提高分析氣相與氣膠相物種組成量測準確度是必要的(Pathak and Chan., 2005)。

台灣多數地區因都市化與地形限制，不易辨別本地排放與長程傳輸污染對於空氣品質的影響。恆春海生館位於台灣南部墾丁國家公園西北端，其鄰近地區無明顯污染源，且大氣環境深受盛行風向的影響，為一探討外來大氣污染傳輸對於本地空氣品質影響的極佳觀測地點。因此，本研究團隊已於 2013 年 2 月 26 日至 4 月 15 日在恆春海生館進行氣膠化學水溶性離子組成的逐時量測，下沉氣流所傳輸污染以西北風為主，但在日間的海風發生時恆春海生館西北部亦可能有高屏地區污染傳輸影響恆春地區空氣品質，若為長時間濾紙採樣，不僅無法解析短時間的下沉傳輸污染物質，且無法區分高屏地區的污染傳輸，因此對於中南半島生質燃燒下沉氣流的辨別需藉由氣膠組成即時量測、光達的氣膠光學量測、模式模擬大氣氣象的垂直風場與天氣型態分類的四者交互證明，在此次的研究期間共驗

證兩次中南半島生質燃燒下沖傳輸事件。本次結果中，中南半島生質燃燒經由下沖氣流對於恆春地區空氣品質的影響時間不長，但其污染傳輸量佔有相當的影響程度。但下沉氣流傳輸仍在驗證期間，需更多數據探討在中南半島生質燃燒的長程傳輸機制，以及對於恆春地區的影響。此外台灣位處中國大陸的東南外海，在受東北季風影響時，可能受到中國大陸污染物與沙塵長程輸送影響，導致空氣品質惡化。當東北季風轉弱時，空氣品質往往因大氣擴散不良時，而導致本地嚴重污染物累積並伴隨光化衍生氣膠污染。因此，春季在恆春地區的大氣觀測，可發現空氣品質主要受到中南半島生質燃燒經由下沖氣流傳輸、高屏地區人為污染傳輸與東北季風攜帶大陸污染傳輸的影響，但相關的污染事件驗證、氣膠特徵辨別與不同污染事件的交互影響仍有待更深入的研究。

二、研究目的

1.辨別高屏地區污染物對於恆春地區傳輸的氣膠組成特徵與污染源貢獻。

2.藉由衛星火點觀測、氣象模擬、氣膠垂質分佈與水溶性離子的逐時變化，驗證中南半島生質燃燒污染物經下沉氣流傳輸的現象。

3.對照恆春地區與鹿林山高山測站觀測結果，建立中南半島生質燃燒污染物經下沉氣流傳輸時的氣膠組成特徵與評估對於空氣品質的影響。

三、文獻回顧

本研究以了解中南半島生質燃燒下沉現象為出發點，探討本地污染與跨境傳輸間的交互作用，並利用已發表的文獻定義氣膠來源、氣膠年齡與污染物質傳輸的遠近，以下與本計畫有關的研究情況共分為(1) 氣膠來源的特徵與辨別; (2)中南半島生質燃燒氣膠傳輸至台灣的相關研究; (3)台灣本島污染與大陸污染傳輸; (4)大氣氣膠光學特性。

3.1 氣膠來源的特徵與辨別

「氣膠」(Aerosol)是懸浮在空氣中的液態或固態粒狀物質，也常被稱為「氣溶膠」或「懸浮微粒」。大氣懸浮氣膠依據來源大致可區分為自然與人為來源，氣膠因為其來源、形成條件及傳播途徑的不同，而具有不同的物理和化學性質。若依據氣膠在大氣中生成機制的差異，大致上可分為原生（primary）與二次衍生（secondary）氣膠。原生氣膠主要源自於污染源的直接排放，例如風蝕揚塵、海水飛沫、火山爆發所釋出的火山灰或燃煤電廠等大型燃燒器所排出的煙塵等，原生微粒的粒徑分佈較廣，但大部份分布在粒徑大於2.5μm的粗粒徑範圍內；二次衍生氣膠則主要由於氣態分子在大氣中經由物理及化學反應所衍生，這些氣態分子稱為二次氣膠的「前驅物」(precursor)，例如：酸鹼氣體的中和反應、膠凝與凝結反應等，二次衍生氣膠的粒徑分佈則主要分佈在細粒徑的範圍內。氣膠化學組成可提供探討氣膠來源及對於環境影響最直接的訊息，氣膠主要組成包括無機水溶性離子、有機碳與元素碳、金屬元素與水等物種。

許多的研究探討氣膠水溶性物種組成與氣膠來源特性的關係，氣膠水溶性物種的時間與空間分佈受到氣相污染物與大氣狀況的影響。農廢燃燒可產生大量的K^+與Cl^- (Park et al., 2004; Allen et al., 2004)以及有機物質的增加(Bae et al., 2014)。

都會區的二次氣膠含有大量的SO_4^{2-}、NO_3^-與NH_4^+（Grosjean, 1989），在高溫高濕、低風速與無降雨的大氣環境下，二次氣膠生成與氣相前驅物(SO_2、NO_x與NH_3)有關聯(Pio et al., 1996; Chow et al., 1998)。氣膠內的Mg^{2+}與Ca^{2+}主要來自地殼元素(Allen et al., 2004)，在沙塵影響期間，Ca^{2+}與PM_{10}有一致的濃度遽增變化，且Ca^{2+}對於氣膠物種組成的貢獻度增加(Hatakeyama et al., 2004；Topping et al., 2004)，Funasaka et al. (2003)以Ca^{2+}量測濃度高於月平均濃度的1.05倍定義沙塵影響時間。海鹽氣膠主要含有Na^+、Cl^-與Mg^{2+}，且其大氣濃度深受風速與風向的影響(Kocak et al., 2004)。而粗粒徑微粒中的succinic acid、Na^+及NO_3^-之間的相關性高，表示三者均與海洋氣膠有關，其中succinic acid為海洋所排放的不飽和脂肪酸經過光化分解後的產物(Hsieh et al., 2007)。氣膠NO_2^-可來自交通工具與生質能燃燒的直接排放，亦可來自二次污染物的生成，其反應為NOx在潮濕地表與氣膠表面經由異相反應生成HNO_2，HNO_2可在氣相與氣膠間快速達到平衡，氣膠可視為大氣中HNO_2的主要儲存場所。然而，HNO_2在日間因光解反應可快速生成OH・與NO，其濃度高值皆發生在夜間（Rondon and Sanhueza,1989; Kurtenbach et al., 2001; Rubio et al., 2002）。

Morgan et al. (2010)與Freney et al. (2011)利用CO/NO_x的比值判斷氣膠傳輸為新生氣膠或老化氣膠，當比值為5-10代表為都市來源，10-50為臨近污染源，比值>50則為遠離污染源。Henning et al. (2003)則使用NO_3^-/SO_4^{2-}當量比來判斷鄰近污染源與遠離污染源，如表3-1 所示，主要有兩個因素影響此比值的大小，NO_X相較於SO_2氧化的速率更快，在鄰近污染源時產生的NO_3^-濃度較高，所以比值較高；而遠離污染源，氣膠經長距離傳輸會造成硝酸銨的揮發，致使比值偏低。

表3-1. $[NO_3^-]/[SO_4^{2-}]$當量濃度比之相關文獻

類型	採樣地區	NO_3^-/SO_4^{2-}	參考文獻
鄰近污染源	瑞士-蘇黎世	0.7	Hueglin (2000)
鄰近污染源	義大利-米蘭	1.1	Putaud et al. (2002)
鄰近污染源	英國-韋伯恩	1.6	Yeatman et al. (2001a)
遠離污染源	阿爾卑斯山	0.3	Preunkert et al. (2002)
遠離污染源	喜馬拉雅山	0.2	Shrestha et al. (1997)
遠離污染源	冒納羅亞山	0.2	Galasyn et al. (1987)
遠離污染源	少女峰	0.2	Krivacsy et al. (2001a) Henning et al. (2003)

在特定地點的氣膠特性量測結果，可顯示氣膠的可能來源與所歷經的大氣物化反應，增進鄰近地區大氣污染物特性的了解，更有助於辨別外來污染物輸送與本地污染排放對於環境的影響。許多研究根據不同天氣系統與污染事件下單一採樣點的量測結果，以受體模式與統計方法配合氣流逆軌跡與大氣狀況模擬判斷該採樣區域的大氣污染物來源，此一方式雖常用於推估大氣污染源特性的研究，但對於外來污染物傳輸量與本地污染排放量的差異卻無法準確區分，尤其對於探討二次衍生氣膠來源的研究而言，本地二次硫酸鹽氣膠與外來傳輸硫酸鹽氣膠具有

相同化學組成與粒徑分佈的特性，此一原因往往限制評估本地二次硫酸鹽氣膠貢獻量與生成機制的研究。

3.2 中南半島生質燃燒氣膠傳輸至台灣的相關研究

每年春季(2 至 4 月)中南半島及亞洲地區生質燃燒事件發生頻率最高，先前的研究指出中南半島生質燃燒污染物會藉由熱浮力傳輸至高層西風帶，其生質燃燒所產生污染物會隨盛行季風與高層西風往東傳輸至東亞下風處，進而影響台灣地區的空氣品質與生態環境(Streets et al., 2003; Wang et al., 2012)。Lin et al. (2009)指出除了熱浮力的傳輸機制外，透過氣象模式的模擬結果指出在天氣條件適合下，中南半島地形的背風面會形成背風槽造成生質燃燒污染物上升至高層西風帶，為相當重要的傳輸機制之一。

在中南半島生質燃燒源區的研究顯示，Tsai et al. (2012) 在泰國清邁於生質燃燒期間進行 PM_{10} 的氣膠特性研究，結果發現當生質燃燒事件發生時，PM_{10} 濃度高達 140 μg m^{-3} 遠高於非生質燃燒事件，而事件發生時，其化學組成中 K^+ 與左旋葡萄糖(Levoglucosan)具有高度相關性，顯示此兩種物質來自相同的來源，且先前的文獻指出 K^+ 與左旋葡萄糖為生質燃燒的重要指標(Zhang et al., 2010)。Chuang et al. (2012)於 2010 年 3~4 月在鄰近東南亞生質燃燒源區的北印度及柬埔寨進行 $PM_{2.5}$ 與 PM_{10} 氣膠特性分析，其 $PM_{2.5}/PM_{10}$ 的比例達 0.73±0.09，顯示生質燃燒活動產生較多的 $PM_{2.5}$，其中 K^+ 離子佔 $PM_{2.5}$ 比例高達 2.51%，相較於其他生質燃燒研究有較高比例，而 $PM_{2.5}$ 中 OC 與 EC 的相關性分析顯示兩者具有高度相關(R^2=0.84)，代表此兩種物質皆由生質燃燒活動直接貢獻。

在中南半島生質燃燒傳輸的下風處研究結果則顯示， Chuang et al. (2012)分析七海計畫中東沙群島的量測結果，由於東沙群島環境周圍並無明顯污染源，因此適合觀測不同氣流的影響，藉由氣流軌跡模式回推氣流的來源，將觀測期間分成亞洲大陸氣流、菲律賓氣流及西太平洋氣流，結果發現亞洲大陸氣流與菲律賓氣流的 $PM_{2.5}$ 氣膠特性類似，可能與人為污染有關，而亞洲大陸氣流會挾帶亞洲沙塵暴，在沙塵暴影響期間 $PM_{2.5-10}$ 中 Ca^{2+} 也有較高的情形。但在東沙群島實驗中並無明顯觀測到中南半島生質燃燒的影響，可能與污染物為經高層大氣傳輸有關。

就生質燃燒的氣流軌跡而言，台灣的地理位置相對於東沙群島為更下風處，但台灣因有高海拔山脈可觀測生質污染物隨大氣高層西風帶的傳輸。鹿林山測站位於台灣中部山區，由於海拔高度(2,862 公尺)較高，受到本地污染的干擾較小，適合觀測長程傳輸污染物的氣膠特性。Lee et al. (2011)在鹿林山測站研究結果發現，$PM_{2.5}$ 平均濃度在中南半島生質燃燒影響期間為 17.5 μg m^{-3}，其中最大日平均值可達 40 μg m^{-3}，此時氣膠中 K^+ 濃度顯著高於平日時期的濃度，顯示來自於中南半島生質燃燒污染物可經由氣流傳輸影響鹿林山。Yen et al. (2012)在 2010 年 3 至 4 月分析恆春海生館密集觀測的數據，藉由氣象模式推論中南半島生質燃燒活動產生強烈的熱浮力，可將污染物往上抬至 850 hPa 以上的西風帶，經西風

將大量的生質燃燒污染物往東傳輸至台灣，當遇到大陸冷高壓南移過程中，可能經由下沉氣流影響地表環境的空氣品質。

3.3 台灣本島污染與大陸污染傳輸

台灣位處中國大陸東南外海，大氣環境深受陸地與海洋季風的影響，在每年秋季至春季，盛行季風自亞洲內陸地區向東南太平洋傳輸，同時亦將中國大陸的污染物向外傳輸至韓國、日本與台灣等地區(Chang et al., 2006a; 2006b; Bae et al., 2014)；當季風影響減弱時，台灣本地的污染排放往往是造成大氣污染的主要原因(Tsuang et al., 2003)。台灣地區空氣品質受天氣型態影響，秋末與冬季時期，中南部地區因位於中央山脈背風面，風速微弱且日照較強，清晨近地面極易形成逆溫層，不利於污染物的擴散，空氣品質較差(環保署, 2005)。

一般都會地區 PM_{10}、CO 及 NOx 多來自機動車輛，三種污染物濃度會因氣象條件變化而受到影響，彼此存有高度相關性(Smith et al., 2001)。然而 PM_{10} 污染除來自機動車輛的直接排放，張順欽和李崇德（2005）研究 1994 年至 2003 年台北市空氣品質監測結果，發現台北都會地區在高光化活性下，二次生成氣膠亦占 PM_{10} 重要比例。張順欽等(2005)分析環保署新莊超級測站資料顯示，強烈光化活性下二次氣膠增量相當顯著，二次氣膠高值發生時間約與 O_3 高值同時或落後 1 至 2 小時。在高臭氧污染事件日時，增加的二次氣膠濃度可佔 PM_{10} 的 38 %；或佔 $PM_{2.5}$ 的 48%。Chang et al. (2010)收集 2002-2008 年台灣北部微粒超級測站資料，利用每日 $O_{3,max}$ 來進行分層分析，當每日 $O_{3,max}$ 大於 100 ppb 相較於每日 $O_{3,max}$ 小於 40 ppb 的 $PM_{2.5}$、EC、OC、NO_3^- 及 SO_4^{2-}，其濃度增幅分別為 124%、78%、72%、130%及 127%，且 CO 濃度也增加 35%，此結果證明強烈的大氣光化學反應生成更多的衍生性氣膠。Park et al. (2013)利用 CO/NO_x 及氣流軌跡模式去判斷污染來源及氣流來源，將採樣期間分成兩種事件，事件一為南中國生質燃燒長程傳輸事件，其污染特性為高 CO/NO_x 及高濃度 K^+，且 OC 對於 EC 與 K^+ 間存在高度相關，顯示 K^+ 與含碳物質有相同的來源; 事件二則為本地污染事件，其污染特性為低 CO/NO_x，且觀察到 EC、OC 及 NO_3^- 的濃度變化趨勢相同。Cheng et al. (2013)在南京、蘇州、杭州、寧波與上海的長三角區域研究中，採樣期間發生的霧霾事件中所量測的結果為生質燃燒的貢獻。生質燃燒所排放的物質佔了 $PM_{2.5}$ 的 37%，在 OC 與 EC 中則分別佔了 70%及 61%，且氣膠中的非塵土 K^+ 與含碳物質銳增。且進一步利用逆軌跡與衛星火點圖探討生質燃燒污染來源，其來源除了當地燃燒排放的污染外，還包含了安徽、江蘇、浙江與其他區域，表示開放式的生質燃燒污染物會經由空氣的流通傳輸到其他地區。在 Bae et al. (2014)在韓國濟州島的冬季研究顯示，亞洲大陸的生質燃燒污染物質會經由冬季季風的長程傳輸影響韓國，使得污染物質中的 OC 與 EC 濃度增加。Yu et al.(2013)以 PMF (Positive Matrix Factorization)受體模式判斷北京 2010 年的空氣中微量元素的來源，其來源與對於 $PM_{2.5}$ 質量濃度的貢獻、比例與特徵元素分別為:二次硫化物(S)-13.8 μgm^{-3} (26.5%)、汽機車排放(Cu、 Zn、 Mn、 Br、 Pb 與 Ba) 8.9μgm^{-3} (17.1%)、

石化燃料燃燒過程(Cl, Se, V, Ni, As, and Pb)- 8.3 mgm^{-3}(16%)、道路揚塵(Si、 Fe、 Al、 Ca、 Cr、 Ni、 Cu、 Zn、 As、 Ba 與 Pb)- 6.6μgm^{-3} (12.7%)、生質燃燒(K)- 5.8 μgm^{-3} (11.2%)、塵土揚塵(Mg, Al, Si, Ti, Ca, and Fe)– 5.4μgm^{-3} (10.4%)與金屬加工過程(Fe, Mn, Al, V, and Cr)- 3.1 μgm^{-3} (6.0%)。而在春秋冬季的污染來源以"燃燒"所產生微量元素 K、Cl、 Se、 V、 Ni、 As 與 Pb 為主。

Fang et al.(2004)量測台中市郊與台中工業區的總懸浮微粒組成，主成分統計分析顯示工業製程與交通污染排放為工業區的主要微粒污染來源，土壤塵土與交通排放則為市郊地區的主要微粒污染來源。以模式探討台中地區污染物來源，粗粒徑微粒在事件日與非事件日下無顯著差異，約有 60-66%來自面源污染。當污染事件發生時，點源的污染排放為 $PM_{2.5}$ 微粒主要來源，約貢獻全部 $PM_{2.5}$ 微粒質量的 27%；但在非事件日時，$PM_{2.5}$ 微粒的主要污染源通常來自外來污染物經長距離的傳輸。此外，海陸風對流效應在事件日下增強，沿海電廠所排放的污染物經由對流效應對於都會區的危害將增大。在微粒粒徑分佈的分析結果顯示，Cl^-、NO_3^-、Na^+、Mg^{2+}、Ca^{2+}與 Fe 主要分佈在粗粒徑範圍，SO_4^{2-}、NH_4^+、Zn、Pb 與 Ni 則主要分佈在細粒徑範圍(Tsuang et al., 2003)，而日夜微粒的變化顯示 Cl^-與 Na^+在下午受到海風傳輸影響而濃度增加(Fang et al., 2002)。Cheng et al. (2009)在台中地區的研究發現農廢燃燒期間 $PM_{2.5}$ 與 $PM_{2.5\text{-}10}$ 濃度分別為 123.6 與 31.5 $\mu g\ m^{-3}$，且當農廢期間 $PM_{2.5}$ 中 Cl^-、K^+及 NO_3^-分別高於非農廢期間 11.0、6.7 and 5.5 倍，研究中以鉀離子在細粒徑中的濃度(FK)與鉀離子在粗粒徑中的濃度(CK)的比例來判斷生質燃燒的指標，結果顯示農廢期間與非農廢期間 FK/CK 分別為 10.7 與 3.9。Ryu et al. (2007)指出氣膠組成中 FK/CK 大於 9.2，表示有受到生質燃燒的影響。

2004 年 9-11 月台南郊區所做的研究中表示，非高污染時期平均混合層高度為 320.2±273.8m，而高污染時期平均混合層高度為 277.0±176.8 m，顯示在高污染時期大氣混合層轉低，導致區域性的污染物無法達到擴散而累積在當地。無論是高污染時期或非高污染時期，從各成分的濃度表現仍可看出一致的趨勢 SO_4^{2-} >NO_3^- >NH_4^+，在主要無機鹽 Na^+、NH_4^+、K^+、Mg^{2+}、Ca^{2+}、Cl^-、NO_3^-和 SO_4^{2-}成分都較高，乃因為台南地區靠海，沿岸有魚塭的存在，而氣膠 NH_4^+、K^+和 Cl^-濃度上升趨勢顯示，高污染時期的污染來源主要為農廢燃燒所引起，且二元酸的成分幾乎完全偏向較細微粒的粒徑範圍，因而在細微粒部分的濃度都有明顯的偏高(黃香儒, 2005；Hsieh et al., 2008)。探討台灣高雄屏東的城市/工業/農業綜合無機離子分佈，發現在懸浮微粒增加的事件當中以 0.1-1.0 μm 細微粒為主要增加對象。其中氣相的 NO_2 及 SO_2 分別為氣膠中硝酸鹽及硫酸鹽的前驅物質，並且轉換後以 0.1μm 超細粒徑的氣膠為主。Lin et al. (2012)研究屏東地區的露天農廢燃燒，發現 $PM_{2.5}/PM_{10}$ 在燃燒前、燃燒期間及燃燒後分別為 0.57、0.90 及 0.55，顯示燃燒活動產生較多的細粒徑微粒，而燃燒期間 OC 與 K^+為濃度增幅最大的物種，且此兩物種佔 $PM_{2.5}$ 分別為 70.5%與 2.28%，代表 OC 與 K^+為農廢燃燒的重要指標物種。Wang et al. (2008)利用 CMB 受體模式(Chemical mass balance, CMB)

分析屏東市(都市)與潮州鎮(鄉村)的污染貢獻源，結果顯示屏東市主要污染來源為移動污染源(49.3-62.4%)與衍生性鹽類(31.2-37.8%)，而潮州鎮則以農廢露天燃燒(25.3-50.4%)、衍生性鹽類(27.2-34.3%)及移動污染源(12.0-26.9%)為主要污染來源，代表不同的城市類型，污染來源也會有所不同。

亞洲大陸的污染傳輸事件的研究中，大陸污染可在 12 小時內經由長程傳輸影響台灣，在台灣北部持續可長達 36 小時，而由於天氣系統的變化，約 3-12 小時後測得台灣東部與西部地區污染濃度增加(Liu et al., 2006)。Chang et al. (2010)以台灣空氣品質監測站數據分析亞洲大陸的污染傳輸，數據包含 CO、氮氧化物(NO_X =NO+NO_2)、SO_2、O_3 、與微粒的質量濃度(PM_{10} and $PM_{2.5}$)，長時間數據分析中 2006 年 3 月發生高污染物件，利用逆軌跡來源辨別判定為長程傳輸事件，長程傳輸過程中，台灣測站的微粒濃度數據由北至南有依序增加的趨勢，且SO_2、O_3 與 CO 均隨東北季風傳輸影響台灣地區，NOx 在同段時間中沒有明顯增加，可能的原因為傳輸過程中已反應成硝酸鹽類。Lin et al. (2005)評估 2000-2001 年冬季季風影響下的空氣污染物來自於亞洲大陸，在長程傳輸的影響下 PM_{10} 濃度約增加了 30μgm^{-3}，CO 與 SO_2 的貢獻分別為 230 與 0.5ppb，以沿海地區受到的衝擊較都會地區高，其範圍包括台灣北部和東部地區，以及小部分的西部平原。

3.4 大氣氣膠光學特性

亞洲地區的污染物在 30°N~45°N 的邊界層(0~2 km)與 20°N~45°N 的低自由對流層(2~5 km)為傳輸活動最強烈的地區。台灣位於亞洲區域大氣污染傳輸的下風處，其主要大氣污染排放源區為中國、中南半島與東南亞等區域，污染物會隨著季節盛行氣團長程傳輸至台灣，而地面空品監測站雖然能夠提供地面及區域性的氣膠污染特性，但無法解釋氣膠垂直分佈的特性，因此利用大氣遙測技術(光達及太陽輻射儀)於長時間持續監測氣膠垂直分佈與光學的特性，提供污染物在垂直剖面上隨時間演變的資料便顯得重要。

Chen et al. (2007 a)與 Chen et al. (2007 b)指出亞洲沙塵暴期間在台北地區利用 Raman 光達觀察氣膠垂直分佈的特性，且搭配氣流軌跡模式(HYSPLT)證明氣流皆來自於中國西北方地區，觀測結果發現沙塵暴氣膠最常出現在在距地面 1~6 km 的自由大氣中。每年 2~4 月為高層西風盛行時，中南半島生質燃燒污染物會經高層西風傳輸影響台灣。Wang et al. (2012)在七海計畫中東沙群島的觀測結果發現源自於中南半島的高層氣流(3~4 km)，因生質燃燒污染物受熱上升至高層氣流，經盛行西風往東傳輸至東沙群島的高空，因此在光達觀測結果中可發現氣膠垂直分佈分成高層與低層的氣膠，其高層則為中南半島生質燃燒氣膠。

生質燃燒活動中以含碳物質氣膠(EC 與 OC)排放為主，其中 EC(元素碳)與 BC(黑碳)的污染特性相似(Salako et al.,2012)，BC 對太陽輻射的吸收能力較強，導致大氣環境的溫度加熱且減少太陽輻射進入地表，此影響會造生溫室效應產生，亦可能影響區域的大氣穩定度與水循環的變化，因此，BC 氣膠在氣候變遷上扮演相當重要的角色(Chou et al., 2005; Ramanathan and Carmichael, 2008)。

Yuan et al. (2006)研究中發現消光係數以氣膠散光係數(b_{sp})貢獻 72-78%及氣膠吸光係數(b_{ap})貢獻 17-23%為兩大主要因子，另外氣體的散光係數與吸光係數只貢獻約 5%，結果顯示消光係數受氣膠的影響程度較高。都市中氣膠的散射效應為主導消光係數的原因(Chan et al., 1999)，而影響散光係數的因子包括微粒粒徑大小、微粒濃度及化學組成份，其中以 $PM_{2.5}$ 為主要影響因子，且當 $PM_{2.5}$ 濃度越高，其所造成散光係數越高(Sloane et al., 1991)。有學者利用相關矩陣分析發現 $PM_{2.5}$ 中化學組成(NH_4^+、NO_3^-、SO_4^{2-}及 TC)對散光係數具有高度正相關，顯示大氣中以衍生性鹽類與含碳物質為主要影響散光係數的因子，(Lee et al., 2005; Yuan et al., 2006)。另外，不同型態污染事件對散光係數的影響也會有所不同，Chang et al. (2006) 發現在本土污染事件期間有最高之散光係數，與人為污染所生成的細微粒有關，而沙塵暴事件發生時，其散光係數值為最低，與沙塵暴事件以粗微粒為主有關。

3.5 二次衍生氣膠生成的影響因子

Galindo et al. (2008)在地中海西部沿海地區的量測結果顯示，夏季因太陽輻射強，SO_2 可快速被氧化形成硫酸鹽，使得硫酸鹽相較於其他季節在 PM_{10} 與 $PM_{2.5}$ 氣膠中皆佔有最大比例。但夏季時硝酸鹽僅在粗粒徑氣膠組成所佔比例略為增加，硝酸鹽在細粒徑氣膠中不管是濃度或是質量百分比組成皆偏低。Kumar et al. (1998)在美國 Fresno 地區的冬季氣膠量測結果顯示二次衍生硝酸銨為 $PM_{2.5}$ 氣膠質量組成中佔有最大比例的化學物種，在都會區 $PM_{2.5}$ 氣膠質量組成中通常含有超過 50%的二次衍生硝酸銨，在非都會區二次硝酸銨所佔比例甚至更高，在冬季因為充裕的氨氣與低溫有利於由氣相趨向固相反應，氣相的硝酸氣體約僅佔總硝酸鹽 10-20%的比例。有機碳與元素碳在都會區大約佔 $PM_{2.5}$ 氣膠質量組成的 20-40%，但在非都會區 $PM_{2.5}$ 氣膠中的有機碳與元素碳比例略低。$PM_{2.5}$ 氣膠中的其餘組成為硫酸銨與懸浮性塵土物質。在地表風速低、日照時數少、太陽仰角低與太陽輻射被雲與霧遮蔽下，雖然光化反應所產生的硝酸與臭氧反應速率較慢，但其所導致的二次衍生硝酸銨氣膠在廣達 64000 km^2 地區皆出現濃度均一的高污染事件。Watson 與 Chow (2002)在同一地區由每日變化的量測結果更進一步說明，冬季逆溫層可導致二次衍生氣膠高濃度的污染事件，此外，許多原生性氣膠在冬季夜間與清晨的污染排放呈現累積現象，當地表受太陽照射而溫度增加時，原生性污染物如黑炭與 PAH 的濃度將快速遞減，但須分析時間解析度為 5-10 分鐘的量測技術才足以觀測其變化。

Chu (2004)分析 2000-2002 Speciation Trends Network 的 $PM_{2.5}$ 污染事件，發現雖然 $PM_{2.5}$ 高污染事件在每一季節皆可能發生，但在夏季的污染事件中，酸性的硫酸鹽氣膠為主導高濃度 $PM_{2.5}$ 的主要組成，且其最高濃度並非發生在太陽輻射最強的時候。Wang et al. (2005)分析北京地區 2001-2003 三年的 $PM_{2.5}$ 逐日氣膠化學組成，多數離子分別在冬季與夏季有最高與最低大氣濃度，但與二次衍生氣膠相關的硫酸鹽與硝酸鹽在夏季與冬季皆有高值發生，其中發生夏季高值的原因

為潮濕與強太陽輻射使得二次衍生氣膠轉換生成增加，冬季高值的原因則是因大氣擴散不佳的情況下燃煤增加導致 SO_2 排放不易移除，此一結果顯示二次衍生氣膠中硫酸鹽與硝酸鹽氣膠分別受到溫度與銨鹽分布的影響。Calvert 與 Stockwell(1984)指出在氣體均相反應中，硫酸與硝酸的重要來源為 OH 與二氧化硫及二氧化氮的反應，其中 OH 的來源可能是都會環境下的臭氧與甲醛的光化反應所產生，DeMore et al. (1983)的研究結果顯示 OH 與二氧化氮反應速率為 OH 與二氧化硫反應速率的 10 倍，因此在氣相反應中，二氧化氮的轉化速率較二氧化硫為快。Stein 與 Lamb (2003)探討在光化反應下氮氧化物對於二次衍生硫酸鹽與硝酸鹽氣膠的生成影響，發現當大氣中氮氧化物濃度較低(通常為夏季期間)，此時自由基的生成速率較氮氧化物的排放速率高，氮氧化物可經由形成硝酸而自大氣中移除，大氣中所殘留超量的自由基可進一步形成過氧化物，高度氧化狀態的大氣環境有利於二次衍生硫酸鹽氣膠的生成。當大氣中氮氧化物濃度高(通常為冬季)，此時自由基的生成量不足以提供去除所有的氮氧化物，氮氧化物的累積導致大氣中過氧化物生成減少，二次衍生硫酸鹽氣膠因大氣環境氧化能力降低而不利於生成。其結果顯示氮氧化物的排放與太陽輻射通量的改變可影響大氣自由基的生成速率，進而影響後續二次衍生硫酸鹽反應途徑的進行。

四、研究方法

4.1 觀測時間

本計畫的觀測時間為 2014 年 2 月 28 日至 4 月 6 日，中南半島在每年 3~4 月易觀測到嚴重的生質燃燒排放，此一時期中南半島的氣流經由高層西風傳輸可到達台灣地區高空，此一時期亦常發生大陸冷高壓南移通過台灣地區。

4.2 觀測地點

本計畫觀測地點位於台灣南部屏東縣國立海洋生物博物館內的臨海空地(22.06N,120.70E, 7m)，海生館位居恆春半島上墾丁國家公園的西北端，東邊與北邊連接恆春縱谷平原與中央山脈，西邊鄰近台灣海峽，如圖所示。恆春半島於每年十月上旬至翌年四月下旬間，來自西伯利亞的季風順著高聳的中央山脈向南吹，到了恆春半島時由於山脈陡降，東北季風順著地形加速吹向海洋，形成了強勁的風勢，即為落山風。

2010 年東沙實驗曾在此地點進行密集觀測期間，推論特定氣候條件下，由高層西風帶長程傳輸的生質燃燒污染物被下沖氣流帶至地表，進而影響空氣品質，使得採樣點是一個觀測生質燃燒下沉氣流影響的最佳地點，且此採樣點附近並無明顯的重大污染源，因此受到本地污染干擾較小，適合觀測外來傳輸污染物對恆春地區氣膠的影響。

4.3 觀測設備與方法

本計畫觀測項目為大氣氣膠垂直分佈結構及大氣氣膠化學物種量測，採用中央研究院環境變遷中心陳韡鼎博士提供的光達系統(Lidar, Light Detection And Range)(如圖 4-1 所示)進行大氣氣膠的垂直分析結構分析，而使用現址式空氣組成量測設備(In-situ Air Composition Measuring Equipment, In-situ ACME)進行大氣氣膠化學物種量測，此套系統為串聯計畫主持人於 2003 年所發展現址式水溶性離子氣膠連續量測(Chang et al., 2007) 與 2013 年的氣膠水溶性有機物逐時量測，量測物質包含 F^-、Cl^-、NO_2^-、NO_3^-、SO_4^{2-}、Li^+、Na^+、NH_4^+、K^+、Mg^{2+}與 Ca^{2+}共 11 種水溶性離子及含碳物質的 20 分鐘濃度變化，In-situ ACME(如圖 4-2 所示)包含氣膠粒徑篩分單元、氣體捕捉單元(denuder)、濾紙收集單元、氣膠成長捕捉單元與氣膠化學物種分析單元。在入流口氣膠採樣流量為 16.7 lpm 下，可依據量測需求選擇氣膠採樣入流口的粒徑篩分器進行 $PM_{2.5}$ 或 PM_{10} 氣膠收集。經粒徑篩分後的採樣氣流加以分流，其中 10 lpm 採樣氣流先經由 denuder 收集氣相酸鹼物質，其餘 6.7 lpm 通入濾紙收集組中，可依照欲分析氣膠化學組成選擇合適材質的濾紙加以收集氣膠。10 lpm 採樣氣流通入氣膠成長捕捉器中，經由高溫吸濕成長與冷凝過飽和成長，以慣性衝擊方式將氣膠自空氣中移除，並通入 D.I.Water 將衝擊板上的氣膠沖洗帶出，氣態與粒狀樣品經由除泡過濾後注入離子層析儀(Chang et al., 2007)。此外，以氣膠成長捕捉單元所收集的樣品亦可與濕式氧化法有機碳分析儀(Aurora Model 1030W)分別分析氣膠中含碳物質的濃度。

另外本計畫中氣象、氣狀及粒狀污染物資料取自於環保署位於恆春海生館之移動監測站，主要為 PM_{10}、$PM_{2.5}$、O_3、SO_2、NO_2、CO、溫度、相對濕度、風速、風向、降雨等每日小時觀測值，以及使用 NOAA air Resources Laboratory 研發的 HYSPLIT 模式 (Hybrid Single Particle Lagrangian Integrated Trajectory Model) 進行逆溯氣流軌跡線繪製(Draxler and Rolph, 2010)。HYSPLIT 模式可直接利用個人電腦進形運作，只需選擇繪製軌跡線的區域經緯度、高度、時間等，即按照使用者的設定進行運算並繪製軌跡線。本研究以 HYSPLIT 模式模擬恆春海生館當地在不同高度的三天前氣流軌跡線來觀察氣流來源。

圖 4-1 光達(Lidar)

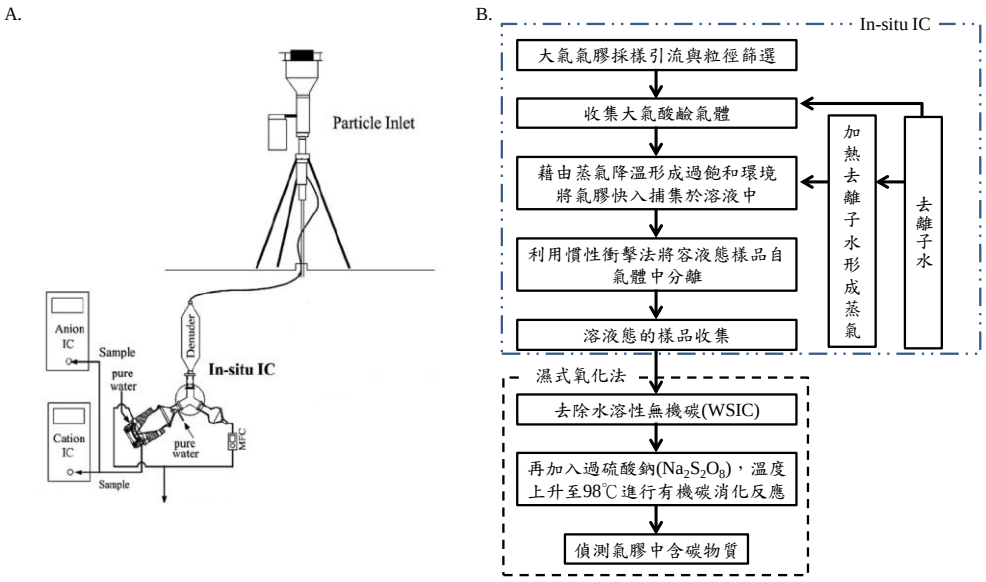

圖 4-2. A. In-situ IC 系統示意圖。B.為大氣組成量測系統(In-situ Air Composition Measuring Equipment, ACME)包含 In-situ IC 系統與水溶性有機物量測系統。

4.4 大氣環境類型判定

首先依據風速與風向將觀測期間分類成海陸風、西風、西北風及東北風等不同類型的氣象場，接著利用氣流軌跡模式分析不同氣流來源，將四種氣象場區分成鄰近地區污染與長程傳輸污染等傳輸類型，再來使用光達(Lidar)觀測氣膠垂直移動的變化，以用來判斷有無氣膠下沉傳輸現象。

海陸風氣象場的特徵為具有規律變化的日夜環流風場，盛行風場在中午過後轉為較高風速的西北風(海風)，傍晚至隔日中午前，盛行風場為低風速的東北風(陸風)，由於海風與陸風的污染物濃度變化差異極大，若將海風與陸風合併一起探討，會稀釋掉兩種氣流類型所表現出的污染特性，因此將海陸風傳輸畫分成海風與陸風等兩種傳輸類型。西風主要發生在溫和穩定的大氣環境下，平均溫度與平均相對溼度為較高，可持續一段長時間的微弱西風，且無日夜環流的風向變化，屬於溫暖且潮溼的氣流。西北風多發生在鋒面過境時，風速較強但持續時間短，伴隨鋒面移動，風向轉為東北風且風速增強。東北風主要受到大陸冷高壓的影響，平均溫度與相對溼度較低，屬於乾冷且風速大的氣象場。

4.5 污染物特徵比值計算

為了瞭解大氣中氮氧化物轉化成硝酸鹽與硫氧化物轉化成硫酸鹽效率，分別計算氮的氧化率（Nitrogen oxidation ratio, NOR)及硫的氧化率（Sulfur oxidation ratio, SOR)，當高 NOR 與 SOR 分別代表前驅氣體經大氣化學反應生成更多的 NO_3^- 與 SO_4^{2-}。其計算公式如下(Tao et al., 2012; Zhou et al., 2012):

1. Nitrogen oxidation ratio (NOR) =

NO_3^- (in μg m^{-3})/ [NO_3^- (in μg m^{-3}) + NO_2 (in μg m^{-3})]

2. Sulfur oxidation ratio (SOR) =

$nssSO_4^{2-}$ (in μg m^{-3})/ [$nssSO_4^{2-}$ (in μg m^{-3}) + SO_2 (in μg m^{-3})]

※$nssSO_4^{2-}$= SO_4^{2-} (in μg m^{-3}) — [0.252×Na^+ (in μg m^{-3})]

$nssSO_4^{2-}$指非海鹽的硫酸鹽，由所測得硫酸鹽扣除海鹽所貢獻的硫酸鹽。

4.6 統計軟體、方法及繪圖軟體

本計畫採用 STATISTICA 7 (windows release by Stat Soft, Inc., 2003)進行統計分析，而繪圖與表格製作以 Microsoft Excel 2007 與 STATISTICA 7 軟體繪製。

五、結果與討論

5.1 觀測期間監測數據分析

5.1.1 逐時氣象資料與污染物濃度

本計畫於2014年2月28日至4月6日期間在恆春海生館進行大氣採樣觀測，圖 5-1 為觀測期間氣象資料與污染物濃度的時間變化，其中圖 5-1(a)與(b)為大氣溫度、相對溼度、風速及風向的時間趨勢變化，本次觀測期間平均大氣溫度、相對溼度及風速分別為 23.2±2.7℃、74.5±9.5%及 7.4±3.9 ms^{-1}，與本研究團隊在 2013 年研究觀測結果相似，其值分別為 23.8±2.5℃、72.6±9.3%及 7.7±4.6 ms^{-1}。

圖 5-1(c)為觀測期間 PM_{10} 及 $PM_{2.5}$ 逐時趨勢變化，由圖 5-2 顯示兩者時間趨勢變化一致，觀測期間的平均濃度分別為 39.2±18.9 μgm^{-3} 及 13.7±10.4 μgm^{-3}，也可以由圖 5-3 得知 PM_{10} 與 $PM_{2.5}$ 的相關性高達 0.85，表示 $PM_{2.5}$ 影響 PM_{10} 濃度變化的主要粒徑微粒。

圖 5-1(d)及(e)為觀測期間 O_3、SO_2、NO_2 及 CO 逐時趨勢變化，觀測期間平均濃度分別為 48.3±15.7ppb、1.4±0.7ppb、3.0±2.7ppb 及 0.2±0.1ppm。由於觀測地點周遭區域沒有重大固定的人為排放污染源，因此 SO_2 的逐時濃度都在 9 ppb 以下，且觀測地點較遠離交通量大區域及都會區，所以交通排放污染物 NO_2 及 CO 的逐時濃度都較低，而 O_3 的逐時濃度介於 20 至 100ppb 之間呈現大氣背景測站的趨勢變化，由觀測結果可以發現 O_3 的濃度規律地在中午過後有較高峰值出現，此時 SO_2、NO_2 及 $PM_{2.5}$ 濃度也會出現較高峰值，此現象也有出現在 2013 的研究觀測結果。

圖 5-2 為觀測期間 $PM_{2.5}$ 中水溶性離子逐時趨勢變化，從圖 5-2(a)與(b)表示 SO_4^{2-} 與 $PM_{2.5}$ 的逐時趨勢變化相似，而 NO_3^- 與 NH_4^+ 在 $PM_{2.5}$ 低濃度時，兩者的逐時濃度會維持在低值，並且無明顯的濃度變化趨勢，當 $PM_{2.5}$ 濃度升高時，NO_3^- 與 NH_4^+ 的濃度也會升高且增加幅度很大，圖 5-4 為觀測期間水溶性離子在 $PM_{2.5}$ 中的百分比，其中 SO_4^{2-}、NO_3^- 與 NH_4^+ 三種離子佔 $PM_{2.5}$ 質量濃度的比例較大，三者比例總和高達 54%且在表 5-1 顯示三者與 $PM_{2.5}$ 的逐時變異的相關性較高，表示 SO_4^{2-}、NO_3^- 與 NH_4^+ 為影響 $PM_{2.5}$ 逐時變異的主要物種組成。另外從圖 5-2(c)、(d)與(e)顯示當 K^+ 濃度明顯升高的時候，$PM_{2.5}$ 濃度也會明顯增加。Na^+ 及 Cl^- 的逐時趨勢變化相似，兩者多在海風及西北風時期出現高值，表示與海鹽飛沫的貢獻有關，而塵土元素 Mg^{2+} 及 Ca^{2+} 在觀測期間出現較少及濃度大致維持在穩定的低濃度，兩者逐時趨勢變化相似且高值常發生在風向轉換後風速大的東北風期間。

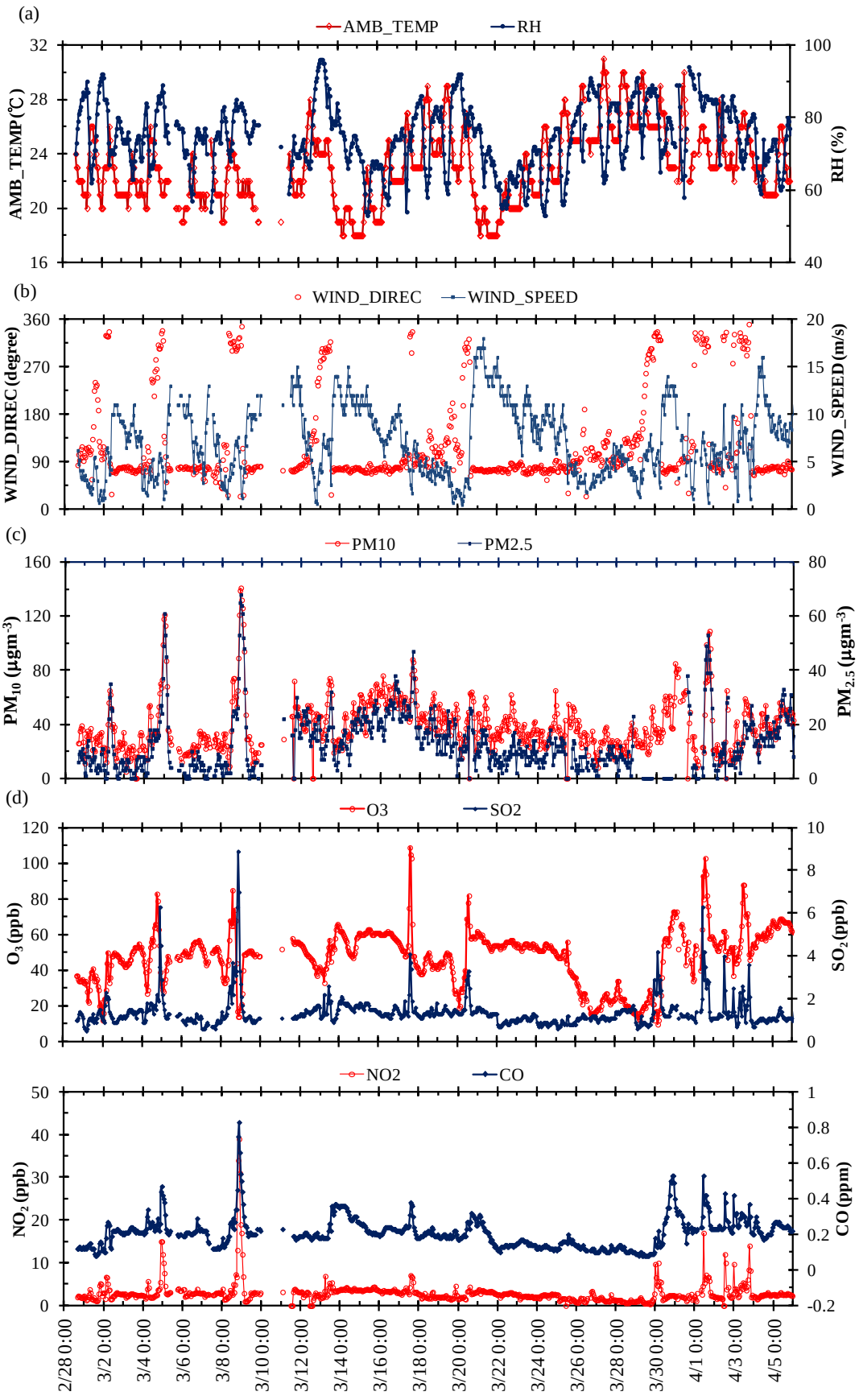

圖 5-1 計劃觀測期間逐時氣象與污染物監測結果

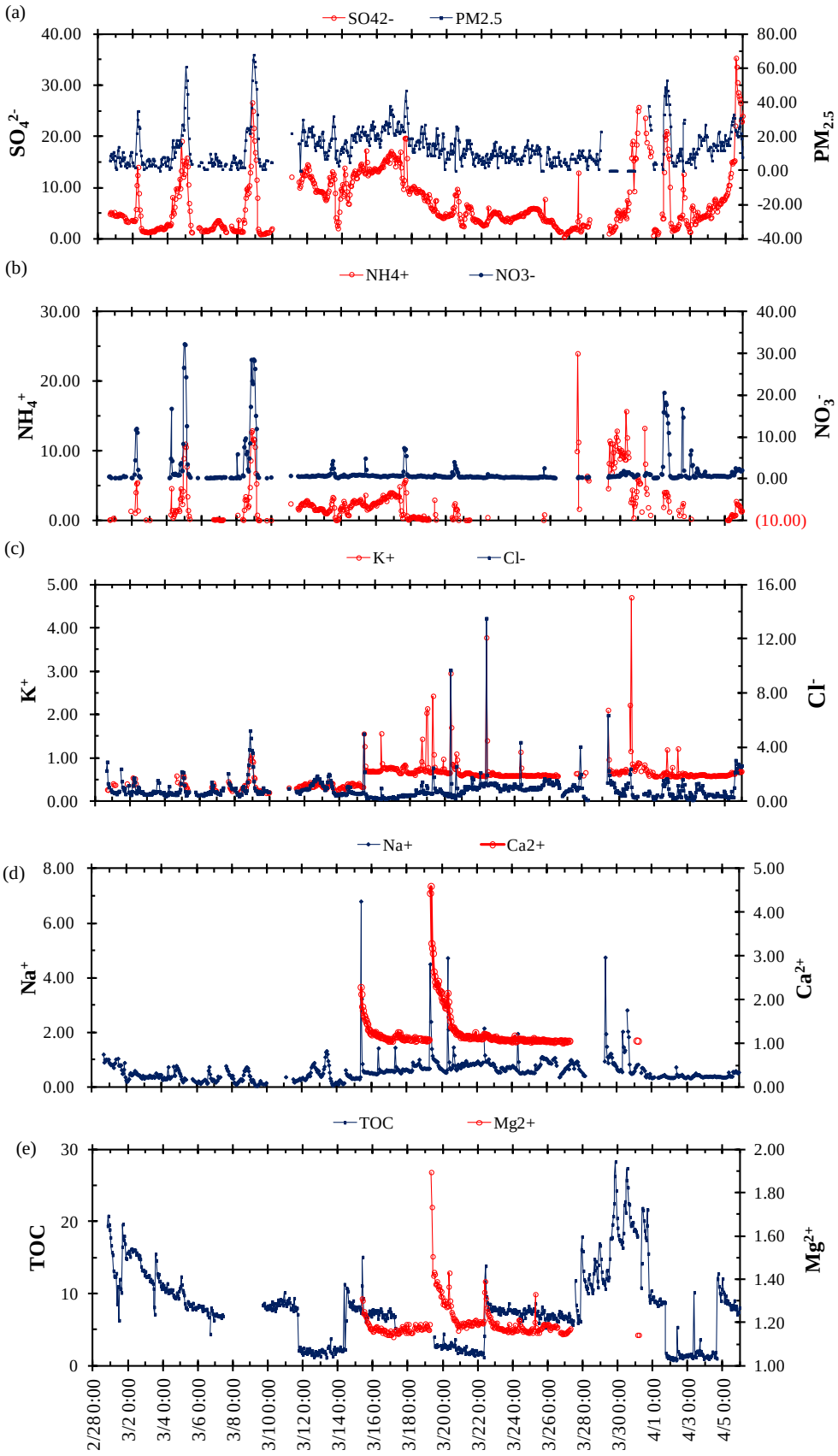

圖 5-2 計劃觀測期間 $PM_{2.5}$ 中逐時水溶性離子(μgm^{-3})及含碳物質(μgCm^{-3})監測結果

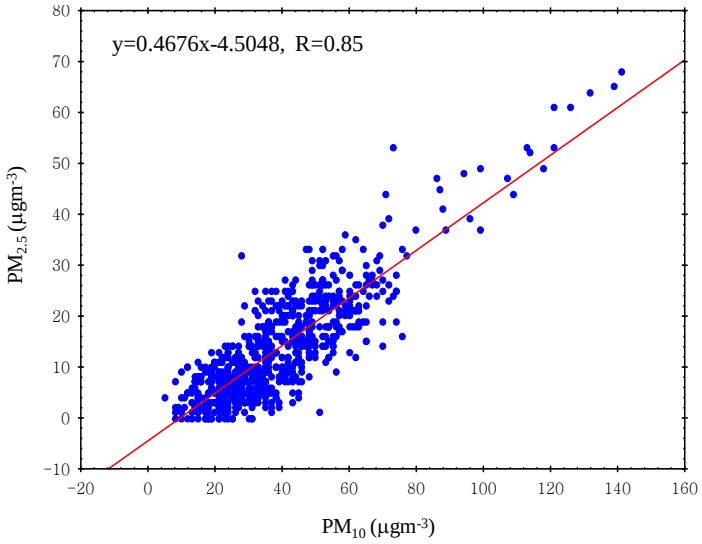

圖 5-3 觀測期間 $PM_{2.5}$ 與 PM_{10} 的相關性比較

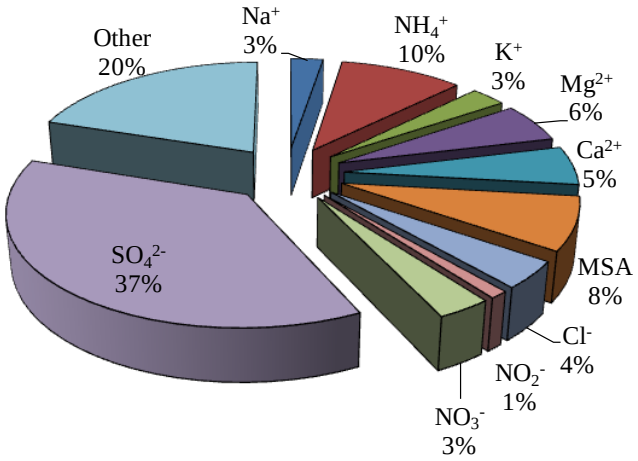

圖 5-4 $PM_{2.5}$ 中化學組成的百分比比較

表 5-1 $PM_{2.5}$ 與化學組成份相關性比較

	$PM_{2.5}$	Na^+	NH_4^+	K^+	Mg^{2+}	Ca^{2+}	MSA	Cl^-	NO_2^-	NO_3^-	SO_4^{2-}
$PM_{2.5}$	1.00										
Na^+	0.03	1.00									
NH_4^+	**0.58**	**0.18**	1.00								
K^+	**0.13**	**0.63**	**0.14**	1.00							
Mg^{2+}	-0.06	**0.54**	-0.14	**0.42**	1.00						
Ca^{2+}	0.08	**0.46**	-0.07	**0.30**	**0.92**	1.00					
MSA	-0.26	**0.66**	-0.24	**0.34**	0.78	0.81	1.00				
Cl^-	**0.18**	**0.59**	**0.16**	**0.47**	**0.25**	0.09	**0.43**	1.00			
NO_2^-	**0.54**	0.07	**0.67**	**0.18**	0.02	0.05	-0.11	**0.26**	1.00		
NO_3^-	**0.68**	-0.03	**0.41**	0.07	0.07	0.11	**0.69**	**0.32**	**0.35**	1.00	
SO_4^{2-}	**0.78**	0.03	**0.14**	**0.13**	-0.10	0.04	0.26	**0.15**	0.07	**0.37**	1.00

Bold numbers are significant at $p<0.05$

5.1.2 不同傳輸類型氣象因子與污染物濃度比較

本計畫主要分為東北季風、西北風、海風、陸風、西風五種不同大氣環境類型，西北風及海風類型的風向皆以西北方向為主，兩者合併一起用來探討高屏地區人為污染傳輸事件，以東北季風類型探討東北季風攜帶大陸污染傳輸，陸風傳輸類型主要用來探討恆春本地污染，而西風傳輸類型主要探討受海洋氣流影響的事件。

(1) 東北季風攜帶大陸污染傳輸

不同傳輸事件下氣象因子及污染物濃度比較如表 5-2 所示，在平均溫度方面以東北季風傳輸影響期間的溫度最低(21.7℃)，其平均風速為所有事件最高(10.2 m/s)，表示東北季風傳輸期間受大陸冷高壓影響導致溫度低且風速高的現象，而各氣相(NO_x、NO_2、NO、SO_2、O_3及 CO)及粒狀污染物(PM_{10}及 $PM_{2.5}$)在所有事件中皆為次高，但在本計畫中受東北季風影響的時間佔觀測期間中最大部分，因此恆春地區主要受東北季風影響為主，而水溶性離子佔 $PM_{2.5}$ 比例為 80%，其中 SO_4^{2-}及 NH_4^+比例較高分別為 37%及 10%且與 $PM_{2.5}$ 相關性高達 0.8 及 0.65，顯示 SO_4^{2-}及 NH_4^+為東北季風期間影響 $PM_{2.5}$ 逐時變異的主要物種組成。

(2) 高屏地區人為污染傳輸

高屏地區人為污染主要由西北風向的海風及西北風傳輸至觀測地點，由表 5-2 可知在氣象因子平均溫度及風速皆為所有事件中次高，分別為 25.1℃及 5.4 m/s，而在氣相及粒狀污染物方面為所有事件中濃度最高，其中 O_3 濃度高達 58.8 ppb，以及水溶性離子 SO_4^{2-}、NO_3^-及 NH_4^+的濃度亦較所有事件最高且。Fang et al. (2011)指出高濃度 O_3 事件會造成衍生性離子濃度增加的情形，與光化學反應生成有關，高屏都會區排放的污染物可經由盛行的西北風傳輸至恆春地區，前驅氣體在高 O_3 環境下傳輸可進一步因光化反應生成更多的衍生性污染物。海風及西北風傳輸類型中受到混合著原生性與衍生性污染來源的貢獻，造成污染物濃度偏高的現象，導致恆春地區空氣品質的加劇惡化。

(3) 陸風及西風傳輸事件

陸風傳輸則因夜晚的盛行風向為東北風，而恆春地區東北方無明顯污染源貢獻，污染物濃度相較於高屏地區人為污染傳輸則明顯較低。當發生西風傳輸時，來自於海洋氣流所攜帶各項污染濃度皆不高，唯有海洋離子(Na^+)為最高。

表 5-2 不同傳輸事件下氣象因子及污染物濃度比較

		東北季風			西風			陸風			高屏地區		
	單位	N=485		WSIs/$PM_{2.5}$	N=6		WSIs/$PM_{2.5}$	N=69		WSIs/$PM_{2.5}$	N=65		WSIs/$PM_{2.5}$
PM_{10}	μgm^{-3}	427	39.1		6	26.5		69	30.7		63	48.7	
$PM_{2.5}$	μgm^{-3}	409	13.4		6	5.5		69	10.3		63	19.2	
Na^+	μgm^{-3}	412	0.4	3%	6	0.5	9%	65	0.4	4%	65	0.4	2%
NH_4^+	μgm^{-3}	198	1.3	10%				27	0.4	4%	41	1.5	8%
K^+	μgm^{-3}	338	0.4	3%				47	0.4	4%	62	0.4	2%
Mg^{2+}	μgm^{-3}	168	0.8	6%				16	0.7	7%	12	0.8	4%
Ca^{2+}	μgm^{-3}	167	0.7	6%				15	0.7	7%	12	1.0	5%
MSA	μgm^{-3}	10	1.0	8%									
Cl^-	μgm^{-3}	404	0.5	4%	6	0.8	15%	62	0.4	4%	65	0.7	4%
NO_2^-	μgm^{-3}	200	0.1	1%	1	0.1	2%	37	0.2	2%	59	0.2	1%
NO_3^-	μgm^{-3}	344	0.4	3%	3	0.4	7%	52	0.4	4%	64	2.6	14%
SO_4^{2-}	μgm^{-3}	404	5.0	37%	6	2.4	43%	61	3.6	35%	65	5.6	29%
Other				20%			25%			30%			31%
$PM_{2.5}/PM_{10}$			0.3	80%		0.2	75%		0.3	70%		0.4	69%
SO_2	ppb	429	1.2		6	1.1		69	1.2		64	2.1	
CO	ppm	430	0.2		6	0.1		69	0.2		64	0.3	
O_3	ppb	430	55.5		6	36.2		68	41.1		64	58.8	
NOx	ppb	431	3.7		6	2.0		69	3.6		62	6.0	
NO	ppb	432	0.9		6	0.6		69	1.1		64	1.3	
NO_2	ppb	429	2.8		6	1.3		69	2.4		62	4.7	
AMB_TEMP	℃	434	21.7		6	25.2		69	23.1		65	25.1	
RH	%	434	69.9		6	69.3		69	81.3		65	82.7	

5.1.3 不同事件污染物特徵比值探討

不同傳輸事件下污染物特徵比值如表 5-3 所示，其中 NOR 與 SOR 分別代表氮化物與硫化物在微粒中相對於整體大氣的分佈，可用於評估 NO_2 與 SO_2 前驅氣體經大氣反應生成 NO_3^-與 SO_4^{2-}的狀態，由結果顯示 SOR 在各類型事件中變動的幅度不如 NOR 來得明顯，可能原因為測站附近無硫化物的排放源，且硫化物在大氣中有較長的生命週期，故區域背景硫化物的貢獻大於本地排放的影響且主導硫化物的大氣反應機制，造成 SOR 在各類型事件中變異不大。而在各類型事件中以高屏地區人為污染傳輸事件的 NOR(0.19)最高，由於在此事件期間具有高濃度 O_3 的日間，此時光化作用劇烈，大氣中的 NO_2 可被大量氧化成 NO_3^-，故在此事件中可發現 NOR 高值。

不同傳輸事件下 Cl^-/Na^+質量濃度比如表-3 所示，由於採樣地點位於鄰海空地，故海洋飛沫的影響極為重要，因此，本計畫採用 Cl^-/Na^+質量濃度比，為瞭解不同傳輸事件中受海洋飛沫影響的程度，Emanuelsson et al. (1954)與 Chuang et al. (2012)指出受到海洋影響時，其 Cl^-/Na^+的比值為 1.8。東北季風攜帶大陸污染傳輸、高屏地區人為污染傳輸、陸風傳輸及西風傳輸的 Cl^-/Na^+質量濃度比值分別為 1.86、1.91、1.06 及 1.5，結果各傳輸事件與文獻值接近表示各類型傳輸事件均會受到海洋飛沫影響，其中東北季風攜帶大陸污染傳輸及高屏地區人為污染傳輸 Cl^-/Na^+質量濃度比值大於文獻值，表示除了海洋飛沫影響外，仍有受到其他污染源影響。

表-3 為不同傳輸類型下 NO_3^-/SO_4^{2-}當量濃度比，本計畫採用利用 NO_3^-/SO_4^{2-}當量濃度比用來判斷污染源的遠近。在所有事件中，以高屏地區人為污染傳輸的比值最高，與 NOR 比值有相同的結果，Park et al. (2013)指出本地來源可能多來自於 NO_3^-所貢獻，表示在高屏地區人為污染傳輸距離本地人為污染來源較近，所受到 NO_3^-的影響程度較高，而東北季風攜帶大陸污染傳輸由於氣膠經長距離傳輸會造成 NO_3NH_4 的揮發有關，致使比值較低。

本計畫採用 NO_3^-/K^+當量濃度比值來區別污染來源類別，如表 5-3 所示，此比值的分母為生質燃燒指標污染物(K^+)，分子則為本地來源指標污染物(NO_3^-)，生質燃燒排放與移動源排放的衍生物皆為 NO_3^-的來源，但 NO_3^-在大氣中的生命週期短，可能經由揮發與沉降等機制自大氣中移除，故其濃度隨傳輸距離而遞減，本研究用以判斷是否受到鄰近都會區的污染影響。另搭配表 5-4 中不同傳輸類型下生質燃燒指標污染物(K^+)與衍生性離子(NH_4^+、NO_3^-、SO_4^{2-})的相關性比較，來判斷是否來自相同污染來源。而所有事件中以高屏地區人為污染傳輸 NO_3^-/K^+當量濃度比值最高(0.65)，且 K^+與 NH_4^+、NO_3^-、SO_4^{2-}相關性分別為 0.98、0.93 及 0.93 呈現高度相關性，由以上結果表示高屏地區人為污染傳輸期間受到本地污染來源的影響大於生質燃燒來源的影響，並且生質燃燒指標污染物(K^+)與衍生性離子皆來自相同污染來源，雖然在表 K^+在 $PM_{2.5}$ 的百分比及質量濃度並不高，但經由以上比值與相關性的結果可得知在高屏地區人為污染傳輸期間均會受到本地污染及生質燃燒的影響，但受本地污染影響更為嚴重，而其他傳輸事件 NO_3^-/K^+

當量濃度比值及 K^+與衍生性離子相關性皆不高，但都以受本地污染來源的影響為主且 K^+與衍生性離子來自不同污染來源，其中西風傳輸事件主要受到海洋飛沫影響，各項污染物濃度皆不高也因低於檢量線濃度導致有無值的現象，因此無法計算比值與相關性。

表 5-3 不同傳輸類型下相關比值得比較

	東北季風	西風	陸風	高屏地區
NOR	0.08	N.D.	0.07	0.19
SOR	0.54	0.46	0.51	0.49
Cl^-/Na^+	1.86	1.50	1.06	1.91
NO_3^-/SO_4^{2-}	0.05	0.07	0.06	0.18
NO_3^-/K^+	1.28	N.D.	1.14	6.54

NOR(Nitrogen oxidation ratio);SOR(Sulfur oxidation ratio);

Cl^-/Na^+質量濃度比 (Emanuelsson et al., 1954)

NO_3^-/SO_4^{2-}當量濃度比 (Henning et al., 2003)

NO_3^-/K^+當量濃度比 (周俊宏,2013)

N.D.為低於偵測極限

表 5-4 不同傳輸類型下 K^+與衍生性離子的相關性比較

與K^+相關性	東北季風	西風	陸風	高屏地區
NH_4^+	**0.19**	**0.45**	N.D.	**0.98**
NO_3^-	**0.14**	0.22	N.D.	**0.93**
SO_4^{2-}	**0.21**	**0.31**	N.D.	**0.93**

Bold numbers are significant at p <0.05

N.D.為低於偵測極限

5.2 下沖事件探討

先前的文獻指出大氣高層西風遇到大陸冷高壓南移，因冷空氣擠壓所產生的下沖氣流，可將高層氣流向下帶至地表(Yen et al., 2012; Lin et al., 2013)。為瞭解高層大氣污染物是否亦經由此一下沖傳輸機制影響地面空氣品質，本計畫以中南半島生質燃燒指標污染物為大氣高層西風傳輸的追蹤劑，透過現址光達觀測氣膠垂直分佈，並搭配氣象模式模擬垂直風場剖面，以確認下沖氣流傳輸現象的起迄時間，同時利用氣流軌跡模式與衛星火點圖判別下沉氣流發生時的高層大氣是否攜帶中南半島生質燃燒排放的指標物質，最後配合地面的逐時污染物觀測數據，以生質燃燒指標污染物高濃度起迄時間與下沖現象發生時間的符合度以證明高層氣團挾帶生質燃燒污染物經下沖氣流傳輸至地表環境。

而本計劃觀測期間並無發生明顯的下沖事件，故以本研究團隊於 2013 年 2 月 26 日至 4 月 15 日期間所發生的下沖事件做為探討。觀測期間共發現現兩次下沖傳輸事件，分別為 3 月 24 日 23:00 至 3 月 25 日 05:00 與 3 月 29 日 10:00 至 20:00，本研究透過氣膠垂直分佈圖(圖 5-5)、垂直風場剖面圖(圖 5-6)及氣流軌跡模式(圖 5-7)，並且搭配污染物的逐時變化(圖 5-8 至 5-11)，發現下沖氣流發生的過程中，在生質燃燒指標污染物都有明顯的變化，顯示下沖氣流有夾帶生質燃燒污染。

中南半島的生質燃燒活動會直接排放大量的氣狀與粒狀污染物，以及生質燃燒氣膠(K^+、NO_3^-與 SO_4^{2-})，就生質燃燒污染物傳輸機制來說，污染物長時間在高空傳輸，可能會造成污染物濃度遞減或是衍生成其他污染物的狀況，進而造成經傳輸過的氣膠與污染源的氣膠特徵會有所差異。CO、EC、SO_4^{2-}等較穩定的污染物，在整個氣流傳輸過程中，較容易保持一致的濃度；相反地，SO_2、NO_x、NH_3 等反應性的前驅氣體在氣流傳輸過程中，受到光化學反應影響生成衍生性污染物，增加 NH_4^+、NO_3^-、SO_4^{2-}以及 O_3 的濃度。另外，半揮發性污染物如 NO_3^-，經長距離傳輸會造成硝酸銨的揮發，造成濃度偏低。

中南半島生質燃燒活動中包括許多不同類型生質材料的燃燒，每種類型的生質燃燒活動，所造成的污染特性也有所不同，而生質燃燒污染物在傳輸過程中，也會受到污染源區燃燒排放強度大小或傳輸過程中大氣狀況的影響，因而造成台灣地區所偵測到的污染特徵也會有所差異。

Park et al. (2013)利用 EC-OC 與 K^+-OC 的相關性比較用來判斷是否來自於生質燃燒的來源。因此本研究利用兩次下沖傳輸事件中 EC 與 OC 的相關性比較用來判斷是否來自於相同的污染源，如表 5-5 所示，由結果得知兩次事件的相關性分別為 0.99 與 0.95，顯示 EC 與 OC 來自於相同的來源，但從斜率來看，第一次事件與第二次事件分別為 3.02 與 4.34，顯示兩次事件所受到的污染強度不同。因此再利用 K^+當作生質燃燒指標污染物，與 OC 進行相關性比較如表 5-5 所示，結果顯示第一次下沖傳輸事件的 K^+-OC 相關性為 0.92，而第二次下沖傳輸事件的 K^+-OC 相關性為 0.37，代表第一次下沖傳輸事件來自於生質燃燒來源，然而第二次下沖傳輸事件的相關性差且斜率很高(9.00)，此結果可能受到其他污染貢獻有關。

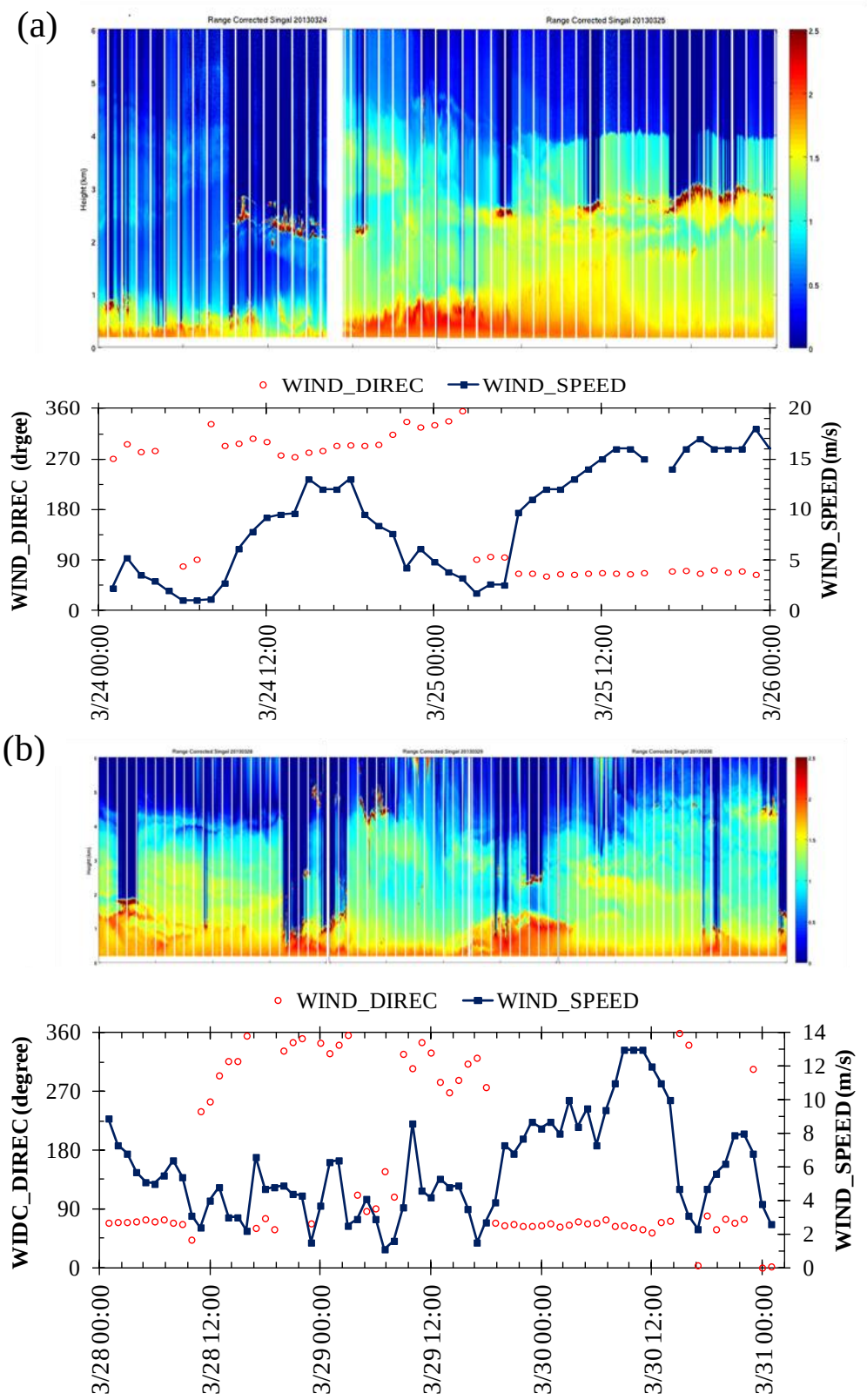

圖 5-5 不同下沖事件的風速風向與氣膠垂直分布圖。
(a)第一次下沖事件 (b)第二次下沖事件

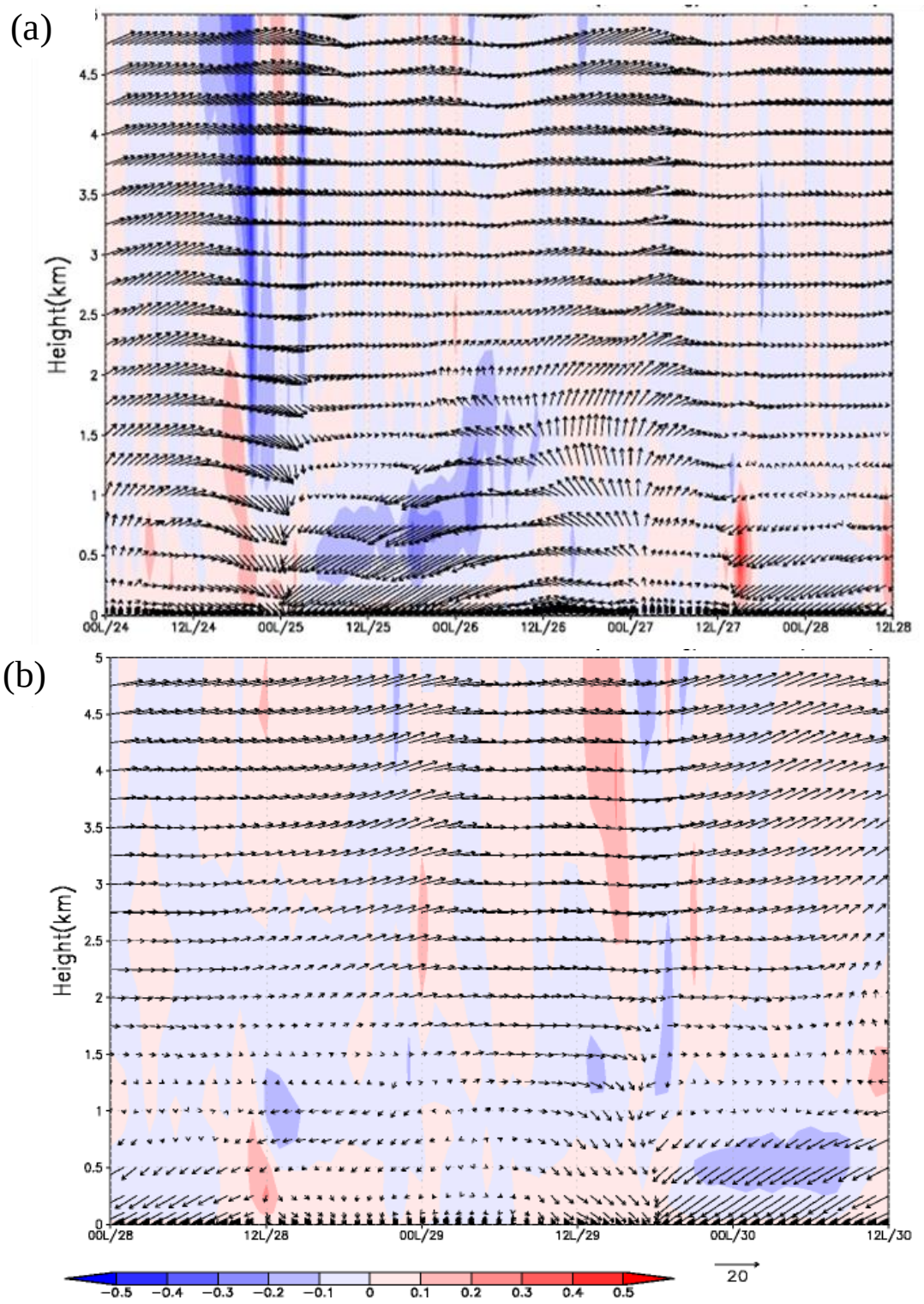

圖 5-6 不同下沖事件的垂直風場剖面圖。(a)第一次下沖事件 (b)第二次下沖事件

(a)

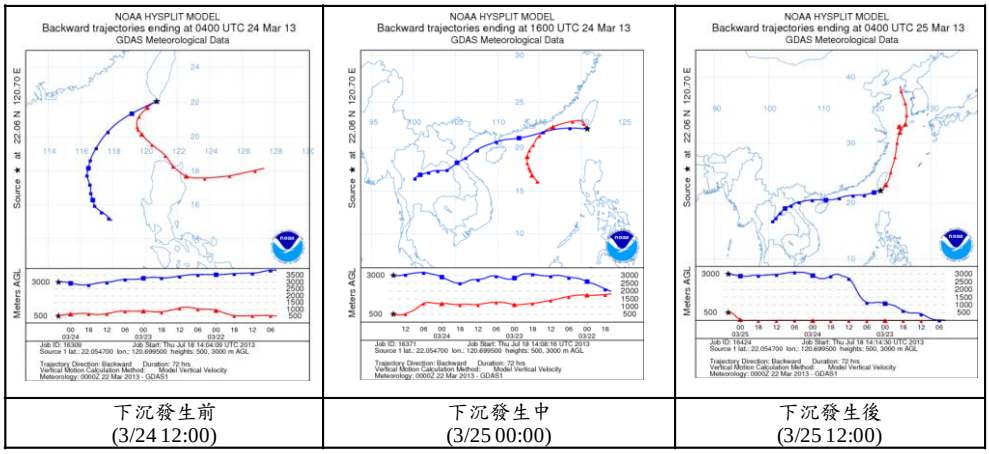

下沉發生前 (3/24 12:00)	下沉發生中 (3/25 00:00)	下沉發生後 (3/25 12:00)

(b)

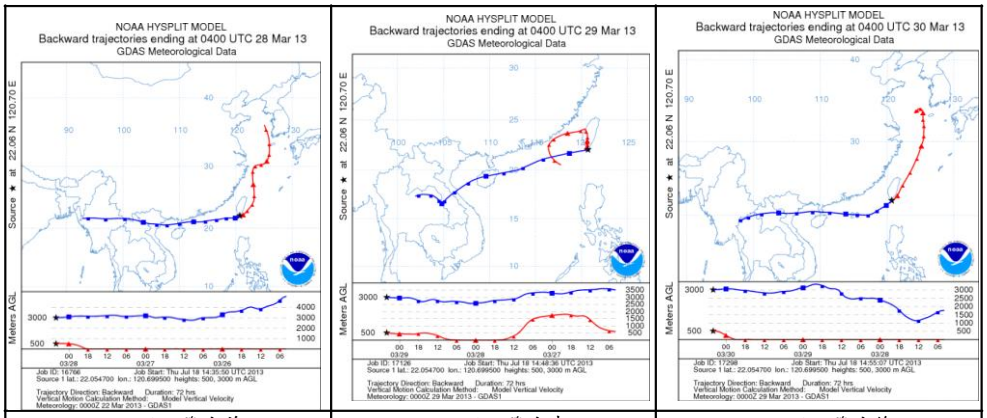

下沉發生前 (3/28 12:00)	下沉發生中 (3/29 12:00)	下沉發生後 (3/30 12:00)

圖 5-7 不同下沖事件的氣流軌跡圖。(a)第一次下沖事件 (b)第二次下沖事件

表 5-5 不同下沖傳輸事件中指標污染物相關性比較

	第一次下沉傳輸事件	第二次下沉傳輸事件
EC-OC	y=3.02x+0.04 r=0.99	y=4.34x+1.06 r=0.95
K-OC	y=3.26x+0.59 r=0.92	y=9.00x+0.71 r=0.37

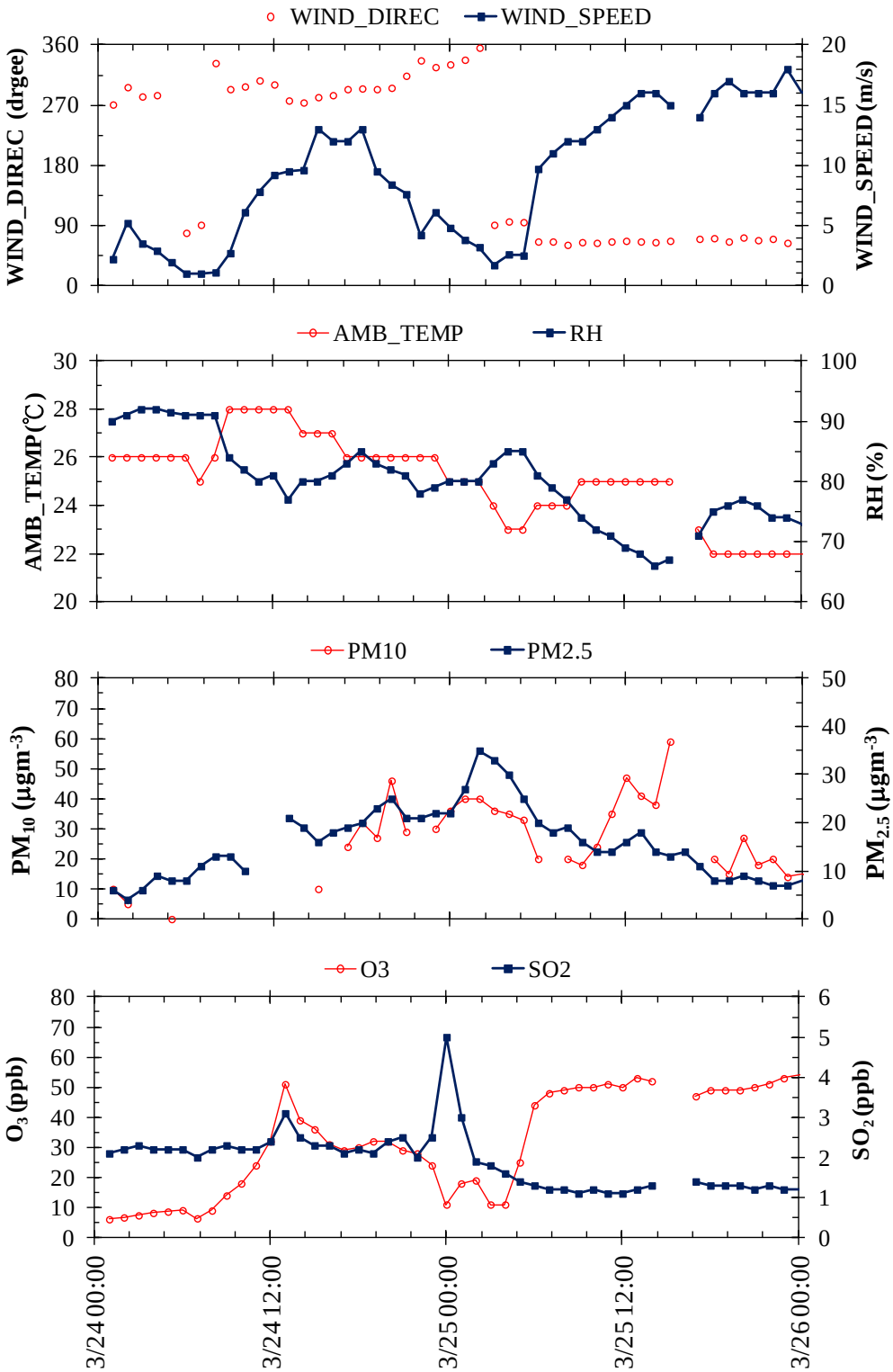

圖 5-8 第一次下沖事件的氣象及污染物濃度監測結果

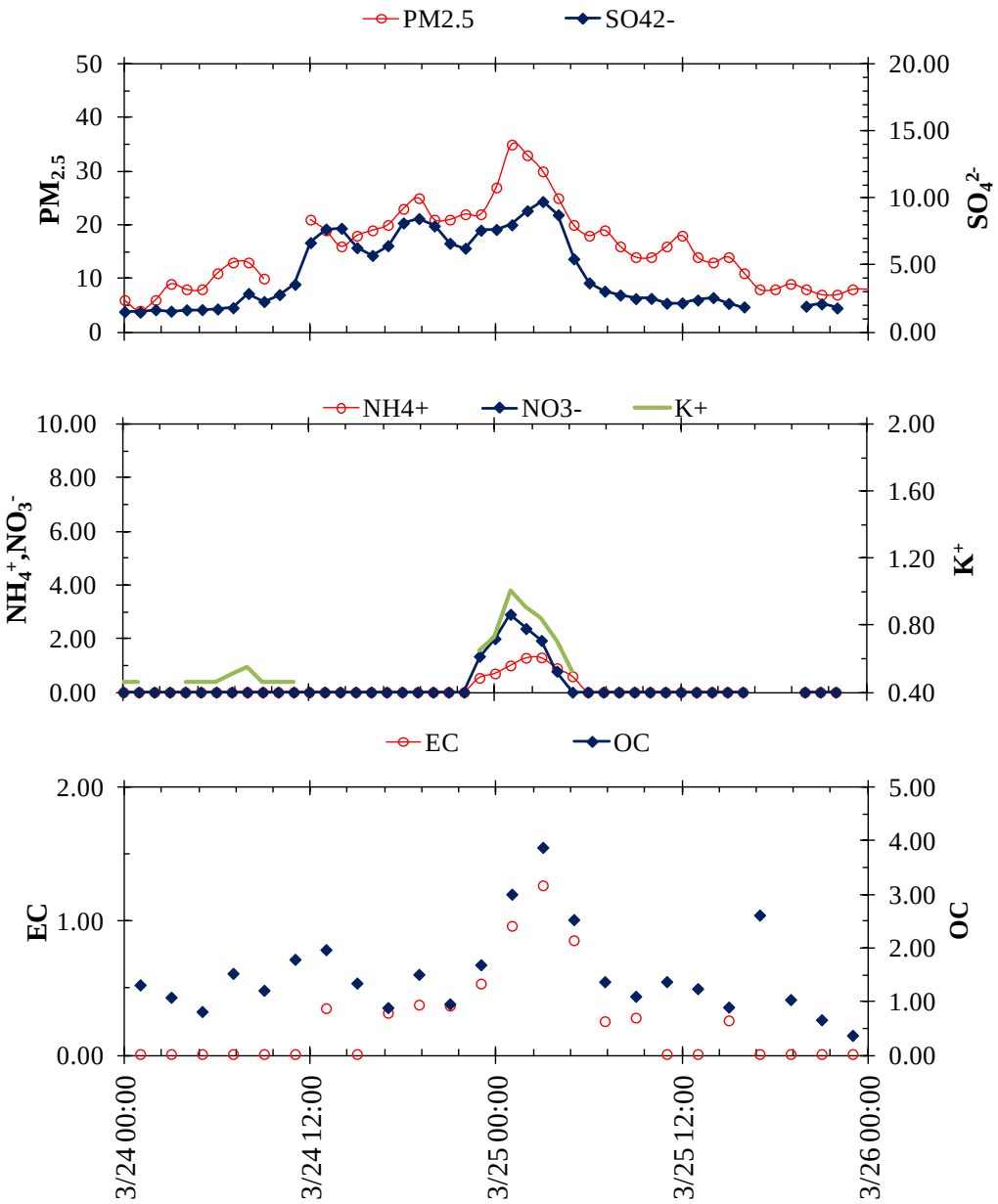

圖 5-9 第一次下沖事件 $PM_{2.5}$ 中化學組成濃度變化(μgm^{-3})

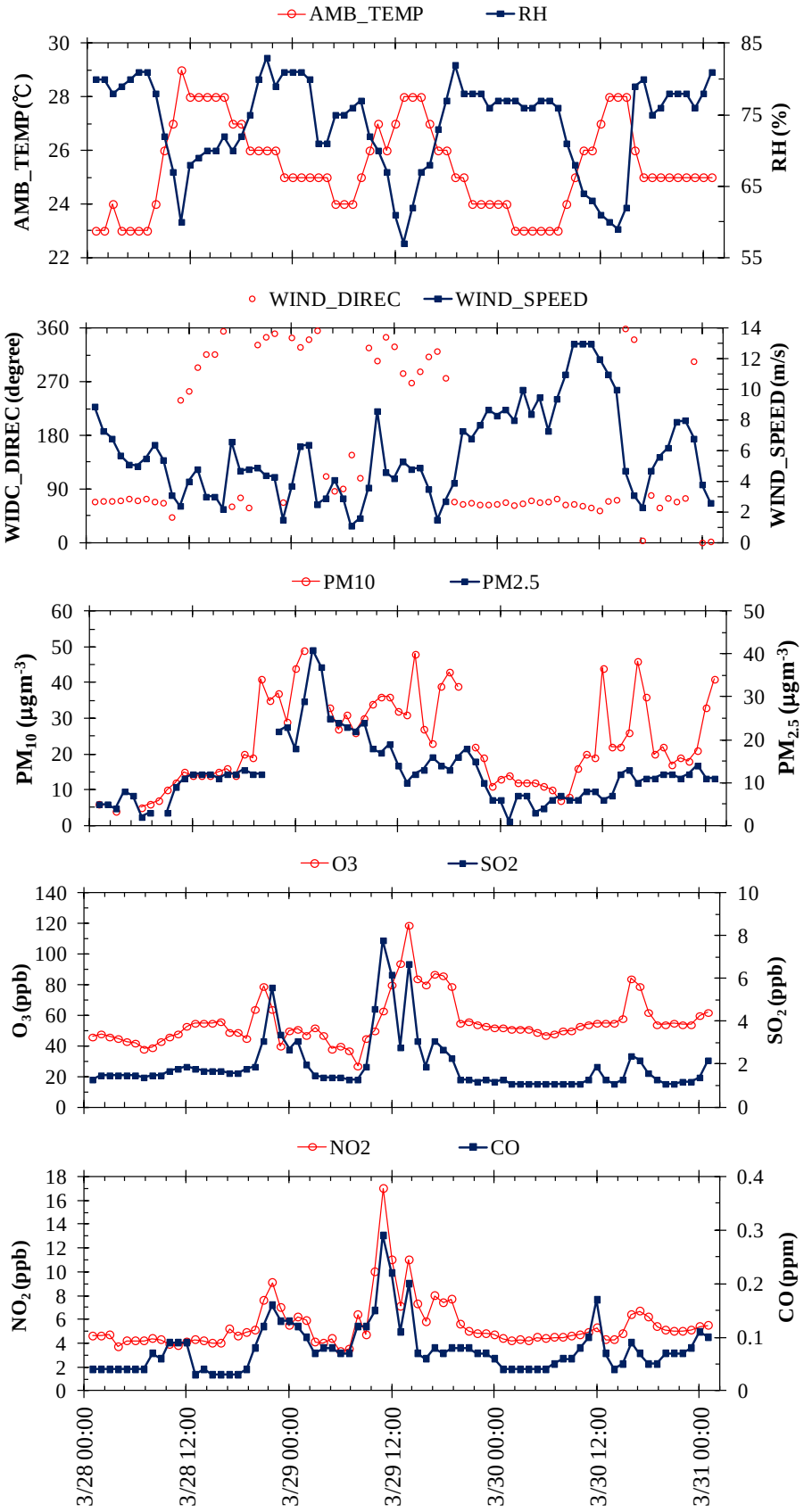

圖 5-10 第二次下沖事件的氣象及污染物濃度監測結果

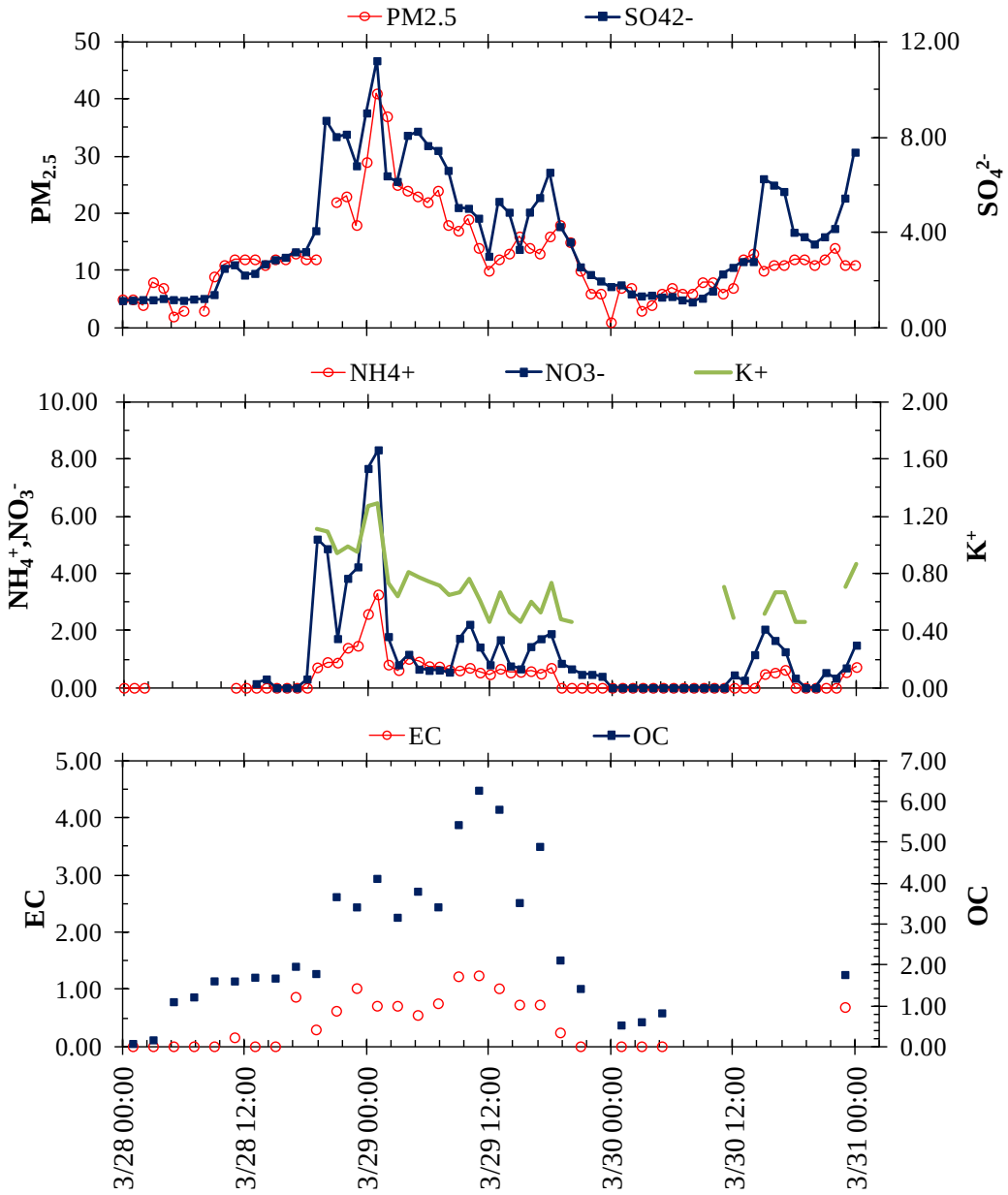

圖 5-11 第二次下沖事件 $PM_{2.5}$ 中化學組成濃度變化(μgm^{-3})

5.3 恆春海生館與鹿林山高山測站觀測結果比較

本節主要探討 2013 年恆春與鹿林生質燃燒傳輸事件(蔡茗宇，2014)觀測結果比較探討，在恆春地區觀測期間發現兩次下沖事件分別為 3 月 24 日 23:00 至 3 月 25 日 05:00 與 3 月 29 日 10:00 至 20:00，而鹿林山則發現五次下沖事件分別為 3 月 3 日 17:00 至 3 月 4 日 15:00，3 月 14 日 19:00 至 3 月 15 日 00:00，3 月 18 日 01:00 至 3 月 21 日 01:00，3 月 24 日 19:00 至 3 月 26 日 19:00 與 3 月 27 日 22:00 至 3 月 30 日 09:00，鹿林山測站海拔高度較高，受本地污染較小，比較容易觀測到由大氣高層西風帶傳輸的中南半島生質燃燒污染物，因而比恆春平地測站觀測到生質燃燒傳輸現象的次數較多，當中第四次及第五次生質燃燒傳輸期間恆春測站同時因下沖現象而觀測到生質燃燒污染物質，因此可以驗證在恆春地區觀測到的兩次下沖事件與鹿林山觀測到的生質燃燒污染來源相同，皆來自中南半島的生質燃燒。

六、計畫成果

本計劃在 2014 年 2 月 28 日至 4 月 6 日於恆春海生館進行大氣污染物逐時觀測，以逐時 $PM_{2.5}$ 水溶性離子與含碳物質數據配合氣象因子、氣態污染物與粒狀污染物的同步觀測，本計畫以逐時風速風向變化區分四種傳輸類型事件作為探討，分別為東北季風攜帶大陸污染傳輸、高屏地區人為污染傳輸、陸風傳輸及西風傳輸事件， 在觀測期間東北季風攜帶大陸污染傳輸事件發生次數較多，發生期間受到大陸冷高壓所影響使平均溫度較低且平均風速較大，污染物逐時濃度因風速較大、大氣混合度高而稀釋，以 SO_4^{2-} 及 NH_4^+ 為東北季風期間影響 $PM_{2.5}$ 逐時變異的主要物種組成，而受高屏地區人為污染傳輸為污染情況最為嚴重的類型，觀測期間以人為污染物($PM_{2.5}$、O_3、SO_4^{2-}、NO_3^- 及 NH_4^+)濃度較高，並由 NOR、NO_3^-/SO_4^{2-} 與 NO_3^-/K^+ 污染物特徵比值分析顯示污染源與西北方的高屏都會區污染排放及光化衍生污染物有關，陸風傳輸因恆春地區東北方無明顯污染源貢獻，污染物濃度比高屏地區人為污染傳輸較低，西風傳輸主要來自於海洋氣流，其所攜帶各項污染濃度皆不高，唯有海洋離子(Na^+)為最高且 Cl^-/Na^+ 質量濃度比與文獻值接近。

本計劃觀測期間較無出現明顯的下沖事件，故以 2013 年觀測結果作為探討，主要受到中南半島生質燃燒排放的影響，生質燃燒指標污染物(K^+、EC 與 OC)與衍生性離子在逐時變化趨勢中皆有上升的現象，兩次下沖傳輸事件中 EC 與 OC 的相關性分別為 0.99 與 0.95，顯示 EC 與 OC 來自於相同的來源，但從斜率來看，第一次事件與第二次事件分別為 3.02 與 4.34，顯示兩次事件所受到的污染強度不同。而使用 K^+ 當作生質燃燒指標污染物與 OC 進行相關性比較，結果顯示兩次下沖傳輸事件的 K^+-OC 相關性分別為 0.92 與 0.37，代表第一次下沖傳輸事件來自於生質燃燒來源，然而第二次下沖傳輸事件的相關性差且斜率很高(9.00)，此結果可能受到其他污染貢獻有關，本計畫將恆春海生館與鹿林山高山測站觀測結果比較，結果顯示當鹿林山觀測到生質燃燒現象期間，恆春測站同時

也有觀測到下沖現象，因而驗證兩者觀測到的生質燃燒污染來源相同皆來自中南半島的生質燃燒。

七、致謝

承蒙科技部提供計畫經費補助(計畫編號：NSC　102－2111－M－040 －002)，使本研究得以順利進行，謹致由衷謝忱。

八、參考文獻

Allen, G.A., Cardoso, A.A., Rocha, G.O. da, (2004) Influence of sugar cane burning on aerosol soluble ion composition in Southeastern Brazil. Atmospheric Environment 38, 5025-5038.

Bao, L., Matsumoto, M., Kubota, T., Wang, S.Q., Sakamoto, K., (2012) Gas/particle partitioning of low-molecular-weight dicarboxylic acids at a suburban site in Saitama, Japan. Atmospheric Environment 47, 546–553.

Calvert, J.G., Stockwell, W.R., (1984) The mechanism and rates of the gas-phase oxidations of sulfur dioxide and the nitrogen oxides in the atmosphere. In: Calvert, J.G. (ED.), Acid Precipitation: SO_2, NO and NO_2 Oxidation Mechanisms Atmospheric Considerations. Ann Arbor Science Publishers, Ann Arbor, MI, 1-62.

Chang, S.C., Chou, C.C.K., Chan, C.C., Lee, C.T., (2010) Temporal characteristics from continuous measurements of $PM_{2.5}$ and speciation at the Taipei Aerosol Supersite from 2002 to 2008. Atmospheric Environment 44, 1088-1096.

Chang, S.Y., Fang, G.C., Chou, C.C.K., Chen, W.N., (2006) Chemical compositions and radiative properties of dust and anthropogenic air masses study in Taipei Basin, Taiwan, during spring of 2004. Atmospheric Environment 40, 7796-7809.

Chang, S.Y., Lee, C.T., Chou, C.C.K., Liu, S.C., Wen, T.X., (2007) The performance comparison of the In Situ IC instrument and the continuous field measurements of soluble aerosol compositions at the Taipei Aerosol Supersite, Taiwan. Atmospheric Environment 41, 1936-1949.

Chen, W.N., Chang, S.Y., Chou, C.C.K., Chen, Y.W., Chen, J.P., (2007a) Study of relationship between water-soluble Ca^{2+} and lidar depolarization ratio for spring aerosol in the boundary layer. Atmospheric Environment 41, 1440-1455.

Chen, W.N., Tsai, F.J., Chou, C.C.K., Chang, S.Y., Chen, Y.W., Chen, J.P., (2007b) Optical properties of Asian dusts in the free atmosphere measured by Raman lidar at Taipei, Taiwan. Atmospheric Environment 41, 7698-7714.

Cheng, M.T., Horng, C.L., Su, Y.R., Lin, L.K., Lin, Y.C., Chou, C.C., (2009) Particulate matter characteristics during agricultural waste burning in Taichung City, Taiwan. Journal of *Hazardous* Materials 165, 187-192.

Cheng, Z., Wang, S., Fu, X., Watson, J.G., Jiang,J., Fu, Q., Chen, C., Xu, B., Yu, J., Chow, J.C., Hao, J., (2013) Impact of biomass burning on haze pollution in the Yangtze River Delta, China: a case study in summer 2011. Atmos. Chem. Phys.

Discuss., 13, 30687–30720

Chou, C.C.K., Chen, W.N., Chang, S.Y., Chen, T.K., Huang, S.H., (2005) Specific absorption cross-section and elemental carbon content of urban aerosols. Geophysical Research Letters 32, L21808.

Chow, J.C., Watson, J.G., Lowenthal, D.H., Egami, R.T., Solomon, P.A., Thuillier, R.H., Magliano, K., Ranzieri, A., (1998) Spatial and temporal variations of particulate precursor gases and photochemical reaction products during SJVAQS/AUSPEX ozone episodes. Atmospheric Environment 32, 2835-2844.

Chu, S.H., (2004) $PM_{2.5}$ episodes as observed in the speciation trends network. Atmospheric Environment 38, 5237-5246.

Chuang, M.T., Chang, S.C., Lin, N.H., Wang, J.L., Sheu, G.R., Chang, Y.J., Lee, C.T., (2012a) Aerosol chemical properties and related pollutants measured in Dongsha Island in the northern South China Sea during 7-SEAS/Dongsha Experiment. Atmospheric Environment.

Chuang, M.T., Chou, C.C.K., Sopajareepom, K., Lin, N.H., Wang, J.L., Sheu, G.R., Chang, Y.J., Lee, C.T., (2012b) Characterization of aerosol chemical properties from near-source biomass burning in the northern Indochina during 7-SEAS/Dongsha experiment. Atmospheric Environment.

DeMore, W.B., Molina, M.J., Watson, R.T., Golden, D.M., Hampson, R.F., Kurylo, M.J., Howard, C.J., Ravishankara, A.R., (1983) Chemical kinetics and photochemical data for use in stratospheric modeling: Evaluation nu,ber 6, JPL Publ., 83-62.

Draxler, R.R. and Rolph, G.D., (2010) HYSPLIT (Hybrid Single-Particle Lagrangian Integrated Trajectory) Model access via NOAA ARL READY Website. NOAA Air Resources Laboratory, Silver Spring, MD. http://ready.arl.noaa.gov/HYSPLIT.php.

Emanuelsson, A., Eriksson, E., Egner, H., (1954) Composition of atmospheric precipitation in Sweden. Tellus 3, 261-267.

Fang, G.C., Chang, C.N., Wu, Y.S., Chen, M.H., Ho, T.T., Huang, S.H., (2004) A study of metallic elements at suburban and industrial regions in central Taiwan during 2002–2003. Atmospheric Research 70, 131-142.

Fang, G.C., Chang, C.N., Wu, Y.S., Fu, P.P.C., Yang, C.J., Chen, C.D., Chang, S.C., (2002). Ambient suspended particulate matters and related chemical species study in central Taiwan, Taichung during 1998–2001. Atmospheric Environment 36, 1921-1928.

Fang, G.C., Lin, S.C., Chang, S.Y., Lin, C.Y., Chou, C.C., Wu, Y.J., Chen, Y.C., Chen, W.T., Wu, T.L., (2011) Characteristics of major secondary ions in typical polluted atmospheric aerosols during autumn in central Taiwan. Journal of

Environmental Management 92, 1520-1527.

Freney, E.J., Sellegri, K., Canonaco, F., Boulon, J., Hervo, M., Weigel, R., Pichon, J.M., Colomb, A., Prévôt, A.S.H., Laj, P., (2011) Seasonal variations in aerosol particle composition at the puy-de-Dôme research station in France. Atmospheric Chemistry and Physics 11, 13047-13059.

Funasaka, K., Sakai, M., Shinya, M., Miyazaki, T., Kamiura, T., Kaneco, S., Ohta, K., Fujita, T., (2003) Size distributions and characteristics of atmospheric inorganic particles by regional comparative study in Urban Osaka, Japan. Atmospheric Environment 37, 4957-4605.

Galasyn, J. F., Tschudy, K. L., Huebert, B. J., (1987) Seasonal and diurnal variability of nitric-acid vapor and ionic aerosol species in the remote free troposphere at Mauna-Loa, Hawaii. Journal of Geophysical Research 92(D3), 3105-3113.

Galindo, N., Nicolás, J. F., Yubero, E., Caballero, S., Pastor, C., Crespo, J., (2008) Factors affecting levels of aerosol sulfate and nitrate on the Western Mediterranean Coast. Atmospheric Research 88, 305–313.

Hatakeyama, S., Takami, A., Sakamaki, F., Mukai, H., Sugimoto, N., Shimizu, A., (2004) Aerial measurement of air pollutants and aerosols during 20-22 March 2001 over the East China Sea. Journal of Geophysical Research 109, D13304, doi:10.1029/2003JD004271.

Henning, S., (2003) Seasonal variation of water-soluble ions of the aerosol at the high-alpine site Jungfraujoch (3580 m asl). Journal of Geophysical Research 108.

Hsieh, L.Y., Chen, C.L., Wan, M.W., Tsai, C.H., Tsai, Y.I., (2008) Speciation and temporal characterization of dicarboxylic acids in PM2.5 during a PM episode and a period of non-episodic pollution. Atmospheric Environment 42, 6836–6850.

Hsieh, L.-Y., Kuo, S.-C., Chen, C.-L., Tsai, Y.I., (2007) Origin of low-molecular-weight dicarboxylic acids and their concentration and size distribution variation in suburban aerosol. Atmospheric Environment 41, 6648-6661.

Hueglin, C., (2000) Anteil des Strassenverkehrs an den PM_{10}- und $PM_{2.5}$-Immissionen. EDMZ, Bern, 173.

Kocak, M., kubilay, N., Mihalopoulos, N., (2004) Ionic composition of lower tropospheric aerosols at a Northeastern Mediterranean site: implications regarding sources and long-range transport. Atmospheric Environment 38, 2067-2077.

Krivacsy, Z., et al., (2001) Study on the chemical character of water soluble organic compounds in the fine atmospheric aerosol at the Jungfraujoch. Journal of Atmospheric Chemistry 39(3), 235-259.

Kumar,N.K., Lurmann,F.W.,Pandis,S.N., (1998) Analysis of Atmospheric Chemistry

during 1995 Integrated Monitoring Study. Report No. STI-997214-1791-DFR. Prepared for California Air Resources Board, Sacrame nto, CA, by Sonoma Technology Inc., Santa Rosa, CA.

Kurtenbach, R., Becker, K.H., Gomes, J.A.G., Kleffmann, J., Lorzer, J.C., Spittler, M., Wiesen, P., Ackermann, R.,Gyer, A., Platt, U., (2001) Investigation of emissions and heterogeneous formation of HNO_2 in a road traffic tunnel. Atmospheric Environment 35, 3385-3394.

Lee, C.G., Yuan, C.S., Chang, J.C., Yuan, C., (2005) Effects of aerosol species on atmospheric visibility in Kaohsiung City, Taiwan. Journal of the *Air & Waste Management Association* 55, 1031-1041.

Lee, C.T., Chuang, M.T., Lin, N.H., Wang, J.L., Sheu, G.R., Chang, S.C., Wang, S.H., Huang, H., Chen, H.W., Liu, Y.L., Weng, G.H., Lai, H.Y., Hsu, S.P., (2011) The enhancement of $PM_{2.5}$ mass and water-soluble ions of biosmoke transported from Southeast Asia over the Mountain Lulin site in Taiwan. Atmospheric Environment 45, 5784-5794.

Lin, C.C., Huang, K.L., Tsai, J.H., Lee, W.J., Chen, S.J., Lin, S.K., (2012) Characteristics of water-soluble ions and carbon in fine and coarse particles collected near an open burning site. Atmospheric Environment 51, 39-45.

Lin, C.Y., Hsu, H.M, Lee, Y.H., Kuo, C.H., Sheng, Y.F., Chu, D.A., (2009) A new transport mechanism of biomass burning from Indochina as identified by modeling studies. Atmospheric Chemistry and Physics 9, 7901-7911.

Lin, N.H., Tsay, S.C., Maring, H.B., Yen, M.C., Sheu, G.R., Wang, S.H., Chi, K.H., Chuang, M.T., OuYang, C.F., Fu, J.S., Reid, J.S., Lee, C.T., Wang, L.C., Wang, J.L., Hsu, C.N., Sayer, A.M., Holben, B.N., Chu, Y.C., Nguyen, X.A., Sopajaree, K., Chen, S.J., Cheng, M.T., Tsuang, B.J., Tsai, C.J., Peng, C.M., Schnell, R.C., Conway, T., Chang, C.T., Lin, K.S., Tsai, Y.I., Lee, W.J., Chang, S.C., Liu, J.J., Chiang, W.L., Huang, S.J., Lin, T.H., Liu, G.R., (2013) An overview of regional experiments on biomass burning aerosols and related pollutants in Southeast Asia: From BASE-ASIA and the Dongsha Experiment to 7-SEAS. Atmospheric Environment.

Lin,C.Y., Liu,S.C., Choua, C.K., Huang, S.J., Liu, C.M., Kuo, C.H., Young, C.Y., (2005) Long-range transport of aerosols and their impact on the air quality of Taiwan. Atmospheric Environment 39, 6066-6076.

Liu, C.M., Young, C.Y., Lee, Y.C., (2006) Influence of Asian dust storms on air quality in Taiwan. Science of the Total Environment 368, 884–897

Morgan, W.T., Allan, J.D., Bower, K.N., Highwood, E.J., Liu, D., McMeeking, G.R., Northway, M.J., Williams, P.I., Krejci, R., Coe, H., (2010) Airborne measurements of the spatial distribution of aerosol chemical composition across Europe and

evolution of the organic fraction. Atmospheric Chemistry and Physics 10, 4065-4083..

Park, S.S., Hong, S.B., Jung, Y.G., Lee, J.H., (2004) Measurements of PM_{10} aerosol and gas-phase nitrous acid during fall season in a semi-urban atmosphere. Atmospheric Environment 38, 293-304.

Park, S.S., Jung, S.A., Gong, B.J., Cho, S.Y., Lee, S.J., (2013) Characteristics of $PM_{2.5}$ haze episodes revealed by highly time-resolved measurements at an air pollution monitoring supersite in Korea. Aerosol and Air Quality Research 13, 957-976.

Pathak, R.K., Chan, C.K., (2005) Inter-particle and gas-particle interactions in sampling artifacts of $PM_{2.5}$ in filter-based samplers. Atmospheric Environment 39, 1597–1607.

Pio, C.A., Castro, L.M., Cerqueirz, M.A., Santos, I.M., Belchior, F., Salgueiro, M.L., (1996) Source assessment of particulate air pollutants measured at the Southwest European coast. Atmospheric Environment 30, 3309-3320.

Preunkert, S., Wagenbach, D., Legrand, M., (2002) Improvement and characterization of an automatic aerosol sampler for remote (glacier) sites. Atmospheric Environment 36, 1221-1232.

Putaud, J. P., Dingenen, R.V., Raes, F., (2002) Submicron aerosol mass balance at urban and semi-rural sites in the Milan area (Italy). Journal of Geophysical Research 107(D22), 8198.

Ramanathan, V., Carmichael, G., (2008) Global and regional climate changes due to black carbon. Nature Geoscience 1, 221-227.

Rondon, A., Sanhueza, E., (1989) High HNO_2 atmospheric concentrations during vegetation burning in the tropical savannah. Tellus 41B, 474-477.

Rubio, M.A., Lissi, E., Villena, G., (2002) Nitrite in rain and dew in Santiage city, Chile. Its possible impact on the early morning start of the photochemical smog. Atmospheric Environment 36, 293-297.

Ryu, S.Y., Kwon, B.G., Kim, Y.J., Kim, H.H., Chun, K.J., (2007) Characteristics of biomass burning aerosol and its impact on regional air quality in the summer of 2003 at Gwangju, Korea. Atmospheric Research 84, 362-373.

Salako, G.O., (2012) Exploring the variation between EC and BC in a variety of locations. Aerosol and Air Quality Research 12, 1-7.

Shrestha, A. B., Wake, C. P., Dibb, J. E., (1997) Chemical composition of aerosol and snow in the high Himalaya during the summer monsoon season. Atmospheric Environment 31, 2815-2826.

Smith, S., Stribley, F.T., Milligan, P., Barratt, B., (2001) Factors influencing measurements of PM_{10} during 1995–1997 in London. Atmospheric Environment

35, 4651-4662.

Stein, A.F., Lamb, D., (2003) Empirical evidence for the low- and high-NOx photochemical regimes of sulfate and nitrate formation. Atmospheric Environment 37, 3615-3625.

Streets, D.G., Yarber, K.F., Woo, J.H., Carmichael, G.R., (2003) Biomass burning in Asia: Annual and seasonal estimates and atmospheric emissions. Global Biogeochemical Cycles 17, 1099.

Tao, J., Shen, Z., Zhu, C., Yue, J., Cao, J., Liu, S., Zhu, L., Zhang, R., (2012) Seasonal variations and chemical characteristics of sub-micrometer particles (PM1) in Guangzhou, China. Atmospheric Research 118, 222-231.

Topping, D., Coe, H., McFiggans, G., Burgess, R., Allan, J., Alfarra, M.R., Bower, K., Choularton, T.W., Decesari, S., Facchini, M.C., (2004) Aerosol chemical characteristics from sampling conductedon the Island of Jeju, Korea during ACE Asia. Atmospheric Environment 38, 2111-2123.

Tsai, Y.I., Sopajaree, K., Chotruksa, A., Wu, H.C., Kuo, S.C., (2012) Source indicators of biomass burning associated with inorganic salts and carboxylates in dry season ambient aerosol in Chiang Mai Basin, Thailand. Atmospheric Environment.

Tsuang, B.J., Chen, C.L., Lin, C.H., Cheng, M.T., Tsai, Y.I., Chio, C.P., Pan, R.C., Kuo, P.H., (2003) Quantification on the source/receptor relationship of primary pollutants and secondary aerosols by a Gaussian plume trajectory model: Part II. Case study. Atmospheric Environment 37, 3993-4006.

Wang, S.H., Tsay, S.C., Lin, N.H., Chang, S.C., Li, C., Welton, E.J., Holben, B.N., Hsu, N.C., Lau, W.K.M., Lolli, S., Kuo, C.C., Chia, H.P., Chiu, C.Y., Lin, C.C., Bell, S.W., Ji, Q., Hansell, R.A., Sheu, G.R., Chi, K.H., Peng, C.M., (2012) Origin, transport, and vertical distribution of atmospheric pollutants over the northern South China Sea during the 7-SEAS/Dongsha Experiment. Atmospheric Environment.

Wang, S.H., Tsay, S.C., Lin, N.H., Chang, S.C., Li, C., Welton, E.J., Holben, B.N., Hsu, N.C., Lau, W.K.M., Lolli, S., Kuo, C.C., Chia, H.P., Chiu, C.Y., Lin, C.C., Bell, S.W., Ji, Q., Hansell, R.A., Sheu, G.R., Chi, K.H., Peng, C.M., (2012) Origin, transport, and vertical distribution of atmospheric pollutants over the northern South China Sea during the 7-SEAS/Dongsha Experiment. Atmospheric Environment.

Wang, W.C., Chen, K.S., Chen, S.J., Lin, C.C., Tsai, J.H., Lai, C.H., Wang, S.K., (2008) Characteristics and receptor modeling of atmospheric $PM_{2.5}$ at urban and rural sites in Pingtung, Taiwan. Aerosol and Air Quality Research 8, 112-129.

Wang, Y., Zhuang, G., Tang, A., Yuan, H., Sun, Y., Chen ,S., Zheng, A., (2005) The

ions chemistry and the source of $PM_{2.5}$ aerosol in Beijing. Atmospheric Environment 39, 3771-3784.

Watson, J.G., Chow, J.C., (2002) A wintertime $PM_{2.5}$ episode at the Fresno, CA, supersite. Atmospheric Environment 36, 465-475.

Yeatman, S. G., Spokes, L. J., Dennis, P. F., Jickells, T. D., (2001) Comparisons of aerosol nitrogen isotopic composition at two polluted coastal sites. Atmospheric Environment 35, 1307-1320.

Yen, M.C., Peng, C.M., Chen, T.C., Chen, C.S., Lin, N.H., Tzeng, R.Y., Lee, Y.A., Lin, C.C., (2012) Climate and weather characteristics in association with the active fires in northern Southeast Asian and spring air pollution in Taiwan during 2012 7-SEAS/Dongsha Experiment. Atmospheric Environment 78, 35-50.

Yen, M.C., Peng, C.M., Chen, T.C., Chen, C.S., Lin, N.H., Tzeng, R.Y., Lee, Y.A., Lin, C.C., (2012) Climate and weather characteristics in association with the active fires in northern Southeast Asia and spring air pollution in Taiwan during 2010 7-SEAS/Dongsha Experiment. Atmospheric Environment.

Yuan, C.S., Lee, C.G., Liu, S.H., Chang, J.C., Yuan, C., Yang, H.Y., (2006) Correlation of atmospheric visibility with chemical composition of Kaohsiung aerosols. Atmospheric Research 82, 663-679.

Zhang, Z., Engling, G., Lin, C.Y., Chou, C.C.K., Lung, S.C.C., Chang, S.Y., Fan, S., Chan, C.Y., Zhang, Y.H., (2010) Chemical speciation, transport and contribution of biomass burning smoke to ambient aerosol in Guangzhou, a mega city of China. Atmospheric Environment 44, 3187-3195.

Zhou, J., Zhang, R., Cao, J., Chow, J.C., Watson, J.G., (2012) Carbonaceous and ionic components of atmospheric fine particles in Beijing and their impact on atmospheric visibility. Aerosol and Air Quality Research 12, 492-502.

周俊宏，2013。亞洲季風影響下大氣污染物傳輸對於恆春地區氣膠特性的探討。中山醫學大學公共衛生所碩士論文。

張順欽、李崇德；2005。台北都會區二次氣膠增量推估之研究。2005 年第十二屆國際氣膠科技研討會，1-10。

張順欽、黃薇如、李崇德；2005。光化學反應生成二次氣膠個案研究。2005 年第十二屆國際氣膠科技研討會，626-635。

黃希爾，2004。東亞生質燃燒對台灣高山氣膠特性的影響。國立中央大學環境工程研究所碩士論文。

黃香儒，2005。秋冬季節之大氣氣膠無機鹽類及二元酸之組成及粒徑變異研究。嘉南藥理科技大學環境工程與科學系碩士論文。

蔡茗宇，2014。2013 年春季鹿林山和夏季龍潭氣膠水溶性離子短時間動態變化特性。國立中央大學環境工程研究所碩士論文。

環保署，2005。全球資訊網，http://www.epa.gov.tw/

附件五

科技部補助專題研究計畫出席國際學術會議心得報告

日期：103 年 08 月 30 日

計畫編號	MOST 102-2111-M-040-002		
計畫名稱	氣體與微粒酸度對於二次衍生性水溶性氣膠的大氣流佈及其光學特性的影響		
出國人員姓名	陳瑀婕 鄭忠豪	服務機構及職稱	中山醫學大學公共衛生學系博士生 中山醫學大學公共衛生學系碩士生
會議時間	103 年 7 月 28 日至 103 年 8 月 1 日	會議地點	日本 札幌
會議名稱	(中文) 第 11 屆亞洲大洋洲地球科學學會年會 (英文)11 th Annual Meeting Asia Oceaning Geosciences Society (AOGS11)		
發表題目	(英文) 1. Impact of Secondary Pollutant Increases on Visibility Degradation in Taichung, Taiwan. (oral) 2. Pollutant Effect on the Ambient Visibility Between the Transport and Stagnant Weather Conditions During the Dry Period in Taichung. (poster) 3. The Impact of Atmospheric Transport on Aerosol Characteristics Under the Asian Monsoon in Hungchen Area. (poster)		

一、參加會議經過

本次跟隨中研院 陳韓鼐博士一同參與 2014 AOGS 研討會，以搭地鐵前往研討會現場，除了參與研討會外，也參觀周邊的觀光景點，在日本，馬路上鮮少可以看到摩托車，街道非常乾淨，是值得我們學習的地方，當地的人也很有禮貌且熱情的幫助我們，整個參與研討會的過程是很享受也很有收穫。

二、與會心得

前次為參與 AWMA 研討會並上台發表論文，非常感謝老師以及科技部的補助與支持，使得有機會可以再次出國看看不同的報告環境，本次參加 2014 第 11 屆 AOGS 研討會，為博士生陳瑀婕以英文口頭報告，口頭報告題目為「Impact of Secondary Pollutant Increases on Visibility Degradation in Taichung, Taiwan」，因為這次是第二次使用英文做口頭報告，報告過程雖然有點緊張但有了老師的細心指導以及之前不斷的反覆練習使得報告順利結束，其中回答問題時有遇到問題時感謝中研院 陳韓鼐博士協助幫忙可以很快解答提問者的疑問，以及碩士生鄭忠豪第一次以海報方式做研究結果的呈現，海報題目為「Pollutant Effect on the Ambient Visibility Between the Transport and Stagnant Weather Conditions During the Dry Period in Taichung」與「The Impact of Atmospheric Transport on Aerosol Characteristics Under the Asian Monsoon in Hungchen Area」，以此機會學習如何做出合適海報樣式與如何在一張海報當中將自己要表達的內容呈現出來，以及也學習到如何用英文回答詢問者的問題，此外本次也特別注意現場有各式各樣海報張貼方式，其中有不少的學者將自己的海報縮印成 A4 大小供人拿取，並也留下清楚的聯絡方式，之後可參考此次所學習到的經驗，做出一眼明瞭的海報，以最佳的方式呈現出自己的研究成果。

此次研討會與先前參與研討會較特別之處，是在會場的中間排了一排的桌子，上面陳列的是一桶一桶的啤酒，到了海報發表時間，可以看到每位學者的手上都有一杯酒的有趣畫面，更有趣的是有些學者甚至喝到整張臉紅通通的，整體來說，會場的氣氛是很悠閒自在的，也讓我沒那麼緊張。在參與的過程中，收穫最多的部分在海報時間，除了考驗臨場反應，也訓練自己如何在短短幾分鐘內介紹海報的主要內容，讓其他學者瞭解。

最後，真的很感謝老師及科技部的支持與協助，也謝謝陪伴我們參與這次研討會的陳韓鼐博士，感謝在研討會中給我們問題、建議與聆聽我們報告的學者夥伴們，也感謝在 AOGS 研討會的主辦單位、工作人員，有了這些人的幫忙與協助讓我們有了滿滿的收穫及往後對學習研究的態度與熱忱，也讓我們有了無法忘懷的回憶。

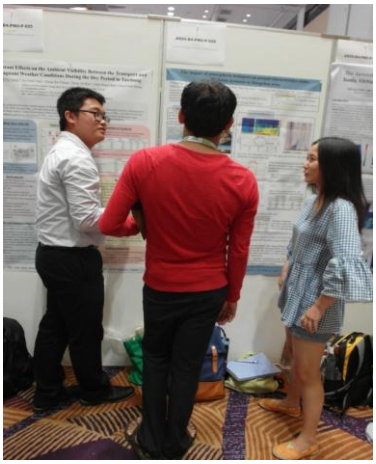

三、發表論文全文或摘要

詳見附錄一。

四、建議

無。

五、攜回資料名稱及內容

此會議的摘要以網路資源呈現，並帶回紙本的會議目次。

六、其他

摘要接受函

AOGS 2014 Abstract Notification (2613)

AOGS Secretariat 2014/3/18 相片, 電子報

收件者： sychang@csmu.edu.tw, with19801227@hotmail.com, u02615@hotmail.com, kcy@csmu.edu.tw, a7839141@hotn

Tuesday, March 18, 2014

Dear Authors,

Congratulations! Your abstract has been accepted for presentation at the AOGS 11th Annual Meeting (AOGS2014) taking place from 28 July to 01 August, 2014 at the Royton Sapporo Hotel in Sapporo, Hokkaido (Japan). The review report is as shown. This and other meeting details - your presentation schedule, meeting registration, invoice, receipts, etc. will be posted as they become available on your personal page on MARS.

AS55-A023 Pollutant effects on the ambient visibility between the transport and stagnant weather conditions during the dry period in Taichung

Shih-Yu CHANG, *Chung Shan Medical University, Taiwan*, Yu-Chieh CHEN, *Chung Shan Medical University, Taiwan*, Chung-Hao CHENG, *Chung Shan Medical University, Taiwan*, Chung-Yih KUO, *Chung Shan Medical University, Taiwan*, Chun-Hung CHOU, *Chung Shan Medical University, Taiwan*, Chun-Chieh HUANG, *Chung Shan Medical University, Taiwan*

Review Decision	Accepted
Comments	NIL

Please register and make payment by 27 May 2014. Failure to do so may result in the Abstract not being included in the conference program and any other publications printed for distribution at the conference.

Registration and Payment

Please check registration fee table at http://www.asiaoceania.org/aogs2014/public.asp?page=register.htm and note that discounted rate is only applicable for fees paid by **27 May 2014**. Regular fees apply after this date.

AOGS 2014 Abstract Notification (2590)

AOGS Secretariat 2014/3/18 相片, 電子報

收件者： with19801227@hotmail.com, sychang@csmu.edu.tw, u02615@hotmail.com, kcy@csmu.edu.tw, a783914:

Tuesday, March 18, 2014

Dear Authors,

Congratulations! Your abstract has been accepted for presentation at the AOGS 11th Annual Meeting (AOGS2014) taking place from 28 July to 01 August, 2014 at the Royton Sapporo Hotel in Sapporo, Hokkaido (Japan). The review report is as shown. This and other meeting details - your presentation schedule, meeting registration, invoice, receipts, etc. will be posted as they become available on your personal page on MARS.

AS55-A022 Impacts of secondary pollutant increases on visibility degradation in Taichung, Taiwan.

Yu-Chieh CHEN, *Chung Shan Medical University, Taiwan*, Shih-Yu CHANG, *Chung Shan Medical University, Taiwan*, Chung-Hao CHENG, *Chung Shan Medical University, Taiwan*, Chung-Yih KUO, *Chung Shan Medical University, Taiwan*, Chun-Hung CHOU, *Chung Shan Medical University, Taiwan*, CHIA-HSING YANG, *Chung Shan Medical University, Taiwan*, Chun-Chieh HUANG, *Chung Shan Medical University, Taiwan*

Review Decision	Accepted
Comments	NIL

Please register and make payment by 27 May 2014. Failure to do so may result in the Abstract not being included in the conference program and any other publications printed for distribution at the conference.

Registration and Payment

Please check registration fee table at http://www.asiaoceania.org/aogs2014/public.asp?page=register.htm and note that discounted rate is only applicable for fees paid by **27 May 2014**. Regular fees apply after this date.

AOGS 2014 Abstract Notification (2649)

AOGS Secretariat 2014/3/18 相片, 電子報
收件者： u02615@hotmail.com, a7839141@hotmail.com, with19801227@hotmail.com, wnchen@rcec.sinica.edu.tw,

Tuesday, March 18, 2014

Dear Authors,

Congratulations! Your abstract has been accepted for presentation at the AOGS 11th Annual Meeting (AOGS2014) taking place from 28 July to 01 August, 2014 at the Royton Sapporo Hotel in Sapporo, Hokkaido (Japan). The review report is as shown. This and other meeting details - your presentation schedule, meeting registration, invoice, receipts, etc. will be posted as they become available on your personal page on MARS.

AS55-A024 The impact of atmospheric transport on aerosol characteristics under the Asian monsoon in Hungchen area.

Chung-Hao CHENG, *Chung Shan Medical University, Taiwan*, Chun-Hung CHOU, *Chung Shan Medical University, Taiwan*, Yu-Chieh CHEN, *Chung Shan Medical University, Taiwan*, Wei-Nai CHEN, *Academia Sinica, Taiwan*, Chuan-Yao LIN, *Academia Sinica, Taiwan*, Neng-Huei LIN, *National Central University, Taiwan*, Fung-Chi KO, *National Dong Hwa University, Taiwan, Taiwan*, Shih-Yu CHANG, *Chung Shan Medical University, Taiwan*, Yu-Chen TSAI, *Chung Shan Medical University, Taiwan*

Review Decision	Accepted
Comments	NIL

Please register and make payment by 27 May 2014. Failure to do so may result in the Abstract not being included in the conference program and any other publications printed for distribution at the conference.

Registration and Payment

Please check registration fee table at http://www.asiaoceania.org/aogs2014/public.asp?page=register.htm and note that

附錄一　發表論文摘要與張貼海報

Impacts of secondary pollutant increases on visibility degradation in Taichung, Taiwan.

Yu-Chieh Chen[1], Chung-Yih Kuo[1,2], Chun-Hung Chou[1], Chung-Hao Cheng[1], Chun-Chieh Huang[1], Shih-Yu Chang[1,2*], Wen-Lin Shang[3]

[1]School of Public Health, Chung Shan Medical University, Taichung 402, Taiwan
[2]Department of Family and Community Medicine, Chung Shan Medical University Hospital, Taichung 402, Taiwan
[3]Bureau of Environmental Protection, Taichung City, Taiwan

*Corresponding author
No.110, Sec. 1, Jianguo N. Rd., South Dist., Taichung City 402, Taiwan (R.O.C.),
Tel: +886 4 24730022ext.12184, Fax: +886 4 23248179,
E-mail: sychang@csmu.edu.tw

Abstract

Atmospheric visibility which is a direct index for perceiving an air quality can be influenced by air pollution and meteorological conditions as the traveling process of visible light in the air is affected by the scatter and absorption effects. The hourly variations of gaseous pollutants (SO_2, O_3, CO, NO, NO_2), particulate matter (PM_{10}, $PM_{2.5}$), soluble ions (Cl^-, NO_2^-, NO_3^-, SO_4^{2-}, Na^+, NH_4^+, K^+, Mg^{2+} and Ca^{2+}) in fine particles, atmospheric visibility and meteorological parameter were measured in summer in Taichung, Taiwan. According to the two-tailed t-tests method, atmospheric visibility was significantly different at RH<70% (low RH) and RH>85% (high RH). The contributions of air pollutants to visibility degradation in the low and high RH atmosphere were discussed in this study. The primary results indicated that $PM_{2.5}$, NO_2, SO_2 and O_3 were significantly correlated with visibility in the low RH atmosphere. However, $PM_{2.5}$, $PM_{2.5-10}$, NO_2, O_3 and CO were significantly correlated with visibility in the high RH atmosphere. Multiple regression revealed that the $PM_{2.5}$ was the major light extinction contributor accounting for 62.8% and 74.3% of visibility degradation in the low and high RH respectively. About 8% mass fraction increase of nitrate an indicator of mobile source was observed in the high RH atmosphere. In contrast, mass fraction of other species were not significantly different in low and high RH atmosphere. The pollutant sources of soluble ions in $PM_{2.5}$ can be identified as the biomass burning, the secondary aerosol from anthropogenic emissions, crustal elements and sea salts. The secondary aerosol from anthropogenic emissions can explain more than half of $PM_{2.5}$ variations. The enhancement of secondary aerosol formation especially for secondary nitrate have vital impact of visibility degradation.

Keywords: Relative humidity, Soluble ion, Anthropogenic emission,

Pollutant effects on the ambient visibility between the transport and stagnant weather conditions during the dry period in Taichung

Shih-Yu Chang[1,2*], Yu-Chieh Chen[1], Chung-Yih Kuo[1,2], Chun-Hung Chou[1], Chung-Hao Cheng[1], Chun-Chieh Huang[1], Wen-Lin Shang[3]

[1]School of Public Health, Chung Shan Medical University, Taichung 402, Taiwan
[2]Department of Family and Community Medicine, Chung Shan Medical University Hospital, Taichung 402, Taiwan
[3]Bureau of Environmental Protection, Taichung City, Taiwan

*Corresponding author
No.110, Sec. 1, Jianguo N. Rd., South Dist., Taichung City 402, Taiwan (R.O.C.),
Tel: +886 4 24730022ext.12184, Fax: +886 4 23248179,
E-mail: sychang@csmu.edu.tw

Abstract

The air quality deterioration and ambient visibility degradation are serious environmental problems in Taichung due to the weak washout effect (less precipitation) during the dry period. The hourly measurements of soluble ions and light extinction coefficient (b_{ext}) were measured by the in-situ air composition measuring equipment (ACME) and the long-path visibility transmissometer (LPV-3), respectively. Depending on the meteorological analysis, the transport weather condition with prevailing northeaster monsoon and the stagnant weather condition with daily sea/land breeze circulation were identified during the observed period. The average percent contributions to b_{ext} by NO_2, $PM_{2.5}$, and $PM_{2.5-10}$ were calculated with the total variance explanation of 63% in the stagnant weather condition and 83% in the transport weather condition. Since $PM_{2.5}$ was significantly correlated with b_{ext} and had much higher contribution to b_{ext}, this study assessed the contribution of visibility degradation by relating b_{ext} to $PM_{2.5}$ pollution sources. The positive matrix factorization (PMF) method was applied to identify five sources of $PM_{2.5}$: secondary sulfate, coal/municipal waste combustion, a mixed source of sea salt and crustal element, motor vehicles exhaust, and local urban sewage emissions. The multiple linear regression was applied to calculated the b_{ext} contributions of each pollutant source based on the hourly $PM_{2.5}$ concentrations of each source estimated from PMF. The primary results indicated that the b_{ext} contributions of secondary sulfate, coal/municipal waste combustion, a mixed source of sea salt and crustal element, motor vehicles exhaust, and local urban sewage emissions were 22.0%, 16.0%, 42.9%, 15.9, and 3.2% in the transport weather condition and 20.7%, 17.8%, 33.4%, 24.9%, and 3.3% in the stagnant weather condition, respectively. Due to the great increasing of b_{ext} contribution, the motor vehicles exhaust played a leading role in visibility degradation in Taichung in the stagnant weather condition.

Keywords: Visual range, Soluble ion, Vehicle emission, $PM_{2.5}$, PMF, extinction coefficient

The impact of atmospheric transport on aerosol characteristics under the Asian monsoon in Hungchen area.

Chung-Hao Cheng[1], Yu-Chieh Chen[1], Chun-Hung Chou[1], Wei-Nai Chen[3], Chuan-Yao Lin[3], Neng-Huei Lin[4], Fung-Chi Ko[5], Shih-Yu Chang[1,2*], Yu-Chen Tsai[1]

[1]School of Public Health, Chung Shan Medical University, Taichung 402, Taiwan
[2]Department of Family and Community Medicine, Chung Shan Medical University Hospital, Taichung 402, Taiwan
[3]Research Center for Environmental Changes, Academia Sinica, Taipei, Taiwan
[4]Department of Atomspheric Sciences, College of Earth Sciences, National Central University, Jhongli, Taiwan
[5]National Dong Hwa University, Taiwan, Taiwan,

*Corresponding author
No.110, Sec. 1, Jianguo N. Rd., South Dist., Taichung City 402, Taiwan (R.O.C.),
Tel: +886 4 24730022ext.12184, Fax: +886 4 23248179,
E-mail: sychang@csmu.edu.tw

Abstract

Hourly measurements of meteorological parameters, particulate and gaseous pollutants, chemical compositions of $PM_{2.5}$, and aerosol vertical distribution were made from February 26 to April 15 2013 at Hungchen in Taiwan. The HYSPLIT and WRF models were applied to distinguish the weather condition.

In this work, four types of air masses were identified as the sea/land breeze circulation, northeast monsoon, western sea wind, and downwash. The first three air masses can be directly characterized as daily variations with sea wind in daytime and land wind in nighttime, the prevailing northeaster with strong and cold wind, and the prevailing light breeze from west, respectively. The biomass burning pollutants from the Indo-China Peninsula transported to Taiwan through the upper atmospheric winds. The downwash processes were verified that the occurrence of peak in biomass burning tracer concentration was consistency with the period of downwash transport which was defined by the vertical distribution of aerosols measured from the in-situ LIDAR and the vertical wind section simulated from the meteorological model.

The pollutant characteristics of each air mass were found in this study. The sea wind with primary photochemical pollutants led to the serious pollution at Hungchen. However, the concentrations of pollutants were quickly reduced when the wind was changed to the land wind. The pollution was related to the long range transport of polluted air from Asia in the prevailing northeasterly. During the westerly, the air quality was the best during the observed period, which was characterized as the oceanic transport. The long-range transport of biomass burning from the Indo-China Peninsula affected the air quality at Hungchen through the downwash process. The aerosols were characterized as the high proportion of biomass pollutants, low ratios of NO_3^-/K^+ and NO_3^-/SO_4^{2-}, and a trace of crustal and sea salts species.

Keywords: Downwash, Biomass burning, Long-range transport, LIDAR

Pollutant Effects on the Ambient Visibility Between the Transport and Stagnant Weather Conditions During the Dry Period in Taichung

Shih-Yu Chang[1,#], Yu-Chieh Chen[1], Chung-Hao Cheng[1], Chung-Yih Kuo[1], Chun-Hung Chou[1], Chun-Chieh Huang[1]

[1]School of Public Health, Chung Shan Medical University, Taichung 402, Taiwan
[#]Corresponding author
No.110, Sec. 1, Jianguo N. Rd., South Dist., Taichung City 402, Taiwan (R.O.C.),
Tel: +886 4 24730022ext.12184, Fax: +886 4 23248179, E-mail: sychang@csmu.edu.tw

Abstract

This study conducted the hourly measurements of atmospheric visibility, $PM_{2.5}$ soluble ions and organic/elemental carbon in Taichung from December 9-29, 2010. Because $PM_{2.5}$ was identified as the predominant species of light extinction, the sources of $PM_{2.5}$ were determined and investigated using a positive matrix factorization (PMF) analysis. The light extinction (b_{ext}) was reconstructed using a multivariate linear regression analysis with hourly-reconstructed $PM_{2.5}$ mass concentrations to determine the contributions of each source to b_{ext}.

Sampling time and site

- Air pollutants and ambient visibility were observed from December 9-29, 2010.
- The sampling sites were located in the Taichung urban area in central Taiwan.

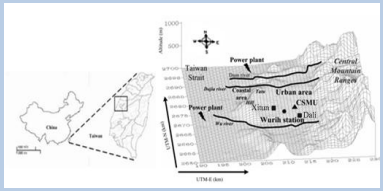

Figure 1. Geographical location of Taichung city and sampling sites. The LPV-3 light path is between Wurih station (round) and CSMU(triangular).

Instruments

- The in situ Air Composition Measuring Equipment (ACME) system:
  - The hourly measurements of $PM_{2.5}$ soluble ions.
- OCEC Carbon Aerosol Analyzer
  - The measurements of the EC and OC.
- Long-Path Visibility transmissometer 3 (LPV-3)
  - The hourly measurements of atmospheric visibility.
- Taiwan EPA measurement data
  - The aerosol mass concentrations, gas concentrations and meteorological parameters.

Model and Statistical Methods

- Positive Matrix Factorization (PMF) analysis (PMF v3.0; USEPA 2008)
  - The qualitative assessment of the hourly contributions to the $PM_{2.5}$ mass concentration of marine/crustal aerosol, secondary nitrate, secondary sulfate, direct vehicle exhaust, coal/incinerator combustion, and local sewage emission.
- Multivariate Linear Regression Analysis (MLRA)
  - The relative contribution of atmospheric extinction sources to b_{ext}.

$$b_{ext} = \sum_i^5 a_i * Cf_{RH} * [PM_{2.5}]_i \quad \text{..... eq.(1)}$$

Sources Analysis

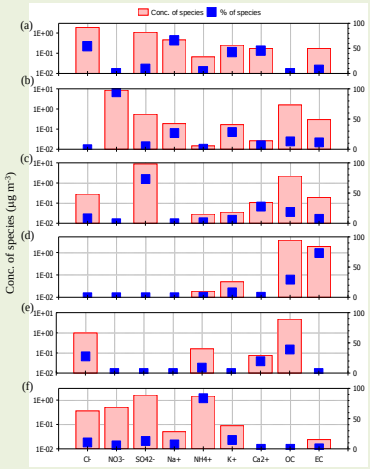

Figure 2. Six sources were identified by the PMF. (a) marine /crustal aerosols (b) secondary nitrate (c) secondary sulfate (d) direct vehicle exhaust (e) coal/incinerator combustion (f) local sewage emission.

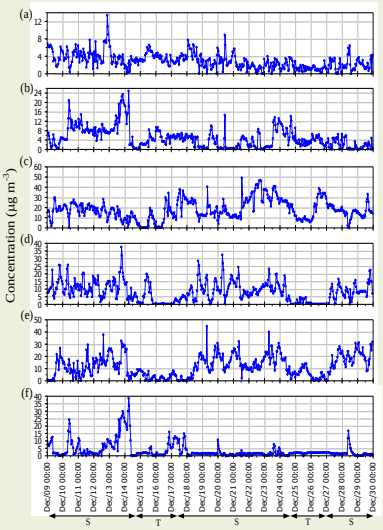

Figure 3. The hourly variations of reconstructed concentrations of $PM_{2.5}$ for the six sources. (a) marine/crustal aerosols (b) secondary nitrate (c) secondary sulfate (d) direct vehicle exhaust (e) coal/incinerator combustion (f) local sewage emission. S: Stagnant weather condition; T: Transport weather condition.

Statistical Analysis

Table 1. The contributions of major NO_2 and particulate matter with and without the RH-correction to the light extinction.

Weather condition	RH-correction	Number	Total variation	Fractional variation		
				NO_2	$PM_{2.5}$	$PM_{2.5-10}$
Transport	Without	104	0.65	0.17.	0.45	0.03
	With	104	0.67	0.02.	0.65	N.S.
Stagnant	Without	339	0.43	N.S.	0.43	N.S.
	With	339	0.76	N.S.	0.76	N.S.

N.S.: Non-Significant

Table 2. The comparisons of the reconstructed light extinction and contribution.

Sources	Transport		Stagnant	
	b_{ext} (Mm^{-1})	Contribution (%)	b_{ext} (Mm^{-1})	Contribution (%)
Marine/crustal aerosols	36.0	8.4	32.4	4.6
Secondary nitrate	99.6	23.3	106.8	15.1
Secondary sulfate	207.5	48.6	298.3	42.2
Vehicle exhaust	40.4	9.5	133.1	18.8
Coal and Incinerator combustion	43.4	10.2	136.3	19.3

Results

1. Table 1 showed that the RH-correction increased the variation of $PM_{2.5-10}$ and $PM_{2.5}$ to b_{ext}. The R^2 of $PM_{2.5}$ with the RH-correction was higher than that of $PM_{2.5-10}$ and NO_2 during the transport and stagnant weather conditions. It indicated $PM_{2.5}$ played an important role in light extinction.
2. The six source factor profiles were identified by PMF in Figure 2. Figure 3 illustrated a time series of the estimated hourly $PM_{2.5}$ mass concentrations of each source.
3. Table 2 indicated that secondary sulfate was the most abundant source of $PM_{2.5}$, which made the largest contribution to the b_{ext} during the sampling period .
4. The contributions from direct vehicle exhaust and coal/incinerator combustion produced more of an impact on visibility degradation in stagnant weather conditions. Therefore, the reduction of the pollutants based on a reduction of direct vehicle exhaust and coal-incinerator combustion could effectively improve the visibility in metropolitan Taichung.

Acknowledgments

This work is support by Environmental Protection Bureau, Taichung City Government.

The authors also gratefully acknowledge the National Science Council of the R.O.C (Taiwan) for financial support under project No. NSC99-2111-M-040-002-MY3.

The impact of atmospheric transport on aerosol characteristics under the Asian monsoon in Hungchen area.

Chung-Hao Cheng[1], Yu-Chieh Chen[1], Chun-Hung Chou[1], Wei-Nai Chen[3], Chuan-Yao Lin[3], Neng-Huei Lin[4], Fung-Chi Ko[5], Shih-Yu Chang[1,2*], **Yu-Chen Tsai[1]**

[1]School of Public Health, Chung Shan Medical University, Taichung 402, Taiwan
[2]Department of Family and Community Medicine, Chung Shan Medical University Hospital, Taichung 402, Taiwan
[3]Research Center for Environmental Changes, Academia Sinica, Taipei, Taiwan
[4]Department of Atomspheric Sciences, College of Earth Sciences, National Central University, Jhongli, Taiwan
[5]Graduate Institute of Marine Biodiversity and Evolutionary Biology, National Dong Hwa University, Pingtung, Taiwan

***Corresponding author**
No.110, Sec. 1, Jianguo N. Rd., South Dist., Taichung City 402, Taiwan (R.O.C.),
Tel: +886 4 24730022ext.12184, Fax: +886 4 23248179,
E-mail: sychang@csmu.edu.tw

Abstract

In this study, our purposes are how to identify downwash event and the effect on air quality. Hourly measurements of meteorological parameters, particulate mass and gaseous pollutants, chemical compositions of $PM_{2.5}$, and aerosol optical parameters were made from February 26 to April 15 2013 at Hungchen in Taiwan.

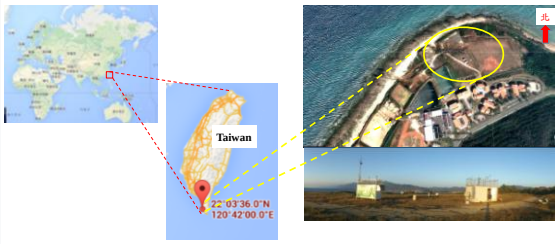

Instruments

➢Measurement Projects:
• Meteorological parameters
• Particulate mass and gaseous pollutants

Fig1. Mobile Stations of Hengchun NMMBA

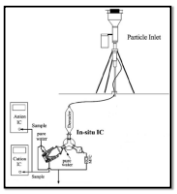

➢Measurement Projects:
• $PM_{2.5}$ ---water-soluble ions
① Cation : Na^+、K^+、NH_4^+、Mg^{2+}、Ca^{2+}
② Anion: Cl^-、SO_4^{2-}、NO_3^-

Fig2. In-situ Air Composition Measuring Equipment (ACME)

➢Measurement Projects:
• $PM_{2.5}$ --- Organic carbon (OC) and inorganic carbon (EC) concentration analysis

Fig3. Model-4 semi-continuous OC-EC field analyzer

➢Measurement Projects:
• Aerosol scattering coefficient

Fig4.Aerosol astigmatism meter (M9003)

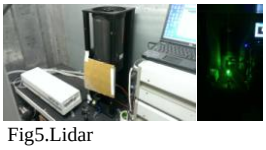

➢Measurement Projects:
• Rayleigh and Mie scattering light of air and suspended particles
• Raman scattered light of nitrogen molecule
•Depolarization rate of particles

Fig5.Lidar

Results and Discussions

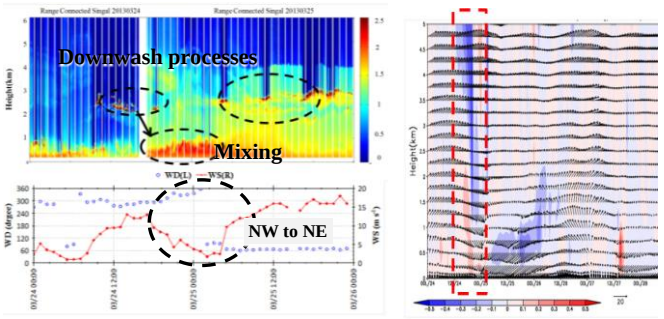

Fig 6.The first downwash event of wind speed and direction and vertical distribution of aerosols height map.

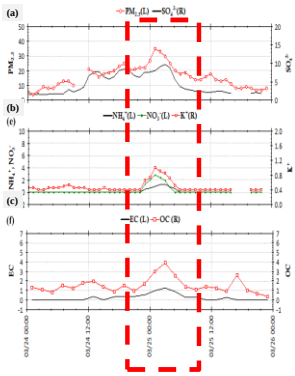

Fig 5.The variation of the chemical composition concentration in $PM_{2.5}$ at the first downwash transport event

➢The downwash processes were verified that the occurrence of peak in biomass burning tracer concentration was consistency

Table 1.The correlation between indicator pollutants of different downwash events

	First downwash event	Second downwash event
EC-OC	y=3.02x+0.04 **r=0.99**	y=4.34x+1.06 r=0.95
K-OC	y=3.26x+0.59 **r=0.92**	y=9.00x+0.71 r=0.37

Table 2. The correlation between K^+ and secondary ions of different transmission types

	Nearby pollution		Long-range transport	
	Sea breeze	West wind	Downwash	Northeast monsoon
NH_4^+	**-0.22**	**0.40**	**0.83**	**0.36**
NO_3^-	**0.30**	**0.31**	**0.85**	**0.35**
SO_4^{2-}	**-0.34**	-0.03	**0.82**	**0.44**

Bold numbers are significant at p <0.05

Table 3. The related ratios between different weather types

	Nearby pollution		Long-range transport	
	Sea breeze	West wind	Downwash	Northeast monsoon
NOR	0.27	0.03	**0.08**	0.03
SOR	0.50	0.45	**0.46**	0.50
Cl^-/Na^+	8.71	2.27	**8.80**	7.36
NO_3^-/SO_4^{2-}	0.46	0.04	**0.19**	0.05
NO_3^-/K^+	5.88	0.88	**1.32**	4.59

➢Biomass pollutants: Low ratios of NO_3^-/K^+ and NO_3^-/SO_4^{2-}, and a trace of crustal and sea salts species.

Conclusions

➢The downwash event occurred when the frontal passed, which is sustained continues for few hours.

➢Under atmosphere of downwash transfer type, finger pollutants of biomass burning(K^+、EC、OC) and second ions increased during hourly variation. Dust (Mg^{2+} and Ca^{2+}) and sea salt (Na^+ and Cl^-) concentrations were the lowest of all transport types which was related to air flow which came from height attitude downwash transmission.

➢By low levels NO_3^-/K^+ equivalent concentration ratio and the better correlation between K^+ and second ions showed that pollution characteristics were related to long-range transport of biomass burning.

The authors also gratefully acknowledge the National Science Council of the R.O.C (Taiwan) for financial support under project No. NSC 102-2111-M-040-002

科技部補助計畫衍生研發成果推廣資料表

日期:2014/10/03

科技部補助計畫	計畫名稱: 氣體與微粒酸度對於二次衍生水溶性氣膠的大氣流佈及其光學特性的影響
	計畫主持人: 張士昱
	計畫編號: 102-2111-M-040-002- 學門領域: 大氣化學

無研發成果推廣資料

102 年度專題研究計畫研究成果彙整表

計畫主持人：張士昱	計畫編號：102-2111-M-040-002-
計畫名稱：氣體與微粒酸度對於二次衍生水溶性氣膠的大氣流佈及其光學特性的影響	

成果項目			量化			單位	備註（質化說明：如數個計畫共同成果、成果列為該期刊之封面故事...等）
			實際已達成數（被接受或已發表）	預期總達成數(含實際已達成數)	本計畫實際貢獻百分比		
國內	論文著作	期刊論文	0	0	100%	篇	
		研究報告/技術報告	0	0	100%		
		研討會論文	1	1	200%		
		專書	0	0	100%		
	專利	申請中件數	0	0	100%	件	
		已獲得件數	0	0	100%		
	技術移轉	件數	0	0	100%	件	
		權利金	0	0	100%	千元	
	參與計畫人力（本國籍）	碩士生	2	2	100%	人次	
		博士生	1	1	100%		
		博士後研究員	0	0	100%		
		專任助理	0	0	100%		
國外	論文著作	期刊論文	1	1	100%	篇	
		研究報告/技術報告	0	0	100%		
		研討會論文	3	1	300%		
		專書	0	0	100%	章/本	
	專利	申請中件數	0	0	100%	件	
		已獲得件數	0	0	100%		
	技術移轉	件數	0	0	100%	件	
		權利金	0	0	100%	千元	
	參與計畫人力（外國籍）	碩士生	0	0	100%	人次	
		博士生	0	0	100%		
		博士後研究員	0	0	100%		
		專任助理	0	0	100%		

其他成果 (無法以量化表達之成果如辦理學術活動、獲得獎項、重要國際合作、研究成果國際影響力及其他協助產業技術發展之具體效益事項等，請以文字敘述填列。)	無

	成果項目	量化	名稱或內容性質簡述
科教處計畫加填項目	測驗工具(含質性與量性)	0	
	課程/模組	0	
	電腦及網路系統或工具	0	
	教材	0	
	舉辦之活動/競賽	0	
	研討會/工作坊	0	
	電子報、網站	0	
	計畫成果推廣之參與（閱聽）人數	0	

科技部補助專題研究計畫成果報告自評表

請就研究內容與原計畫相符程度、達成預期目標情況、研究成果之學術或應用價值（簡要敘述成果所代表之意義、價值、影響或進一步發展之可能性）、是否適合在學術期刊發表或申請專利、主要發現或其他有關價值等，作一綜合評估。

1. 請就研究內容與原計畫相符程度、達成預期目標情況作一綜合評估

■達成目標

□未達成目標（請說明，以 100 字為限）

□實驗失敗

□因故實驗中斷

□其他原因

說明：

2. 研究成果在學術期刊發表或申請專利等情形：

論文：■已發表 □未發表之文稿 □撰寫中 □無

專利：■已獲得 □申請中 □無

技轉：□已技轉 ■洽談中 □無

其他：(以 100 字為限)

本研究期間以產出一篇國際期刊，及兩項專利申請

3. 請依學術成就、技術創新、社會影響等方面，評估研究成果之學術或應用價值（簡要敘述成果所代表之意義、價值、影響或進一步發展之可能性）(以 500 字為限）

本計劃觀測期間較無出現明顯的下沖事件，故以 2013 年觀測結果作為探討，主要受到中南半島生質燃燒排放的影響，生質燃燒指標污染物(K+、EC 與 OC)與衍生性離子在逐時變化趨勢中皆有上升的現象，兩次下沖傳輸事件中 EC 與 OC 的相關性分別為 0.99 與 0.95，顯示 EC 與 OC 來自於相同的來源，但從斜率來看，第一次事件與第二次事件分別為 3.02 與 4.34，顯示兩次事件所受到的污染強度不同。而使用 K+當作生質燃燒指標污染物與 OC 進行相關性比較，結果顯示兩次下沖傳輸事件的 K+-OC 相關性分別為 0.92 與 0.37，代表第一次下沖傳輸事件來自於生質燃燒來源，然而第二次下沖傳輸事件的相關性差且斜率很高(9.00)，此結果可能受到其他污染貢獻有關，本計畫將恆春海生館與鹿林山高山測站觀測結果比較，結果顯示當鹿林山觀測到生質燃燒現象期間，恆春測站同時也有觀測到下沖現象，因而驗證兩者觀測到的生質燃燒污染來源相同皆來自中南半島的生質燃燒。